1968

Ammonation reactions of selected platinum(II) complexes and the cis-effect

Ronald George Gunther
Iowa State University

AMMONATION REACTIONS OF SELECTED PLATINUM(II) COMPLEXES AND THE CIS-EFFECT

by

Ronald George Gunther

A Dissertation Submitted to the
Graduate Faculty in Partial Fulfillment of
The Requirements for the Degree of
DOCTOR OF PHILOSOPHY

Major Subject: Physical Chemistry

Approved:

Signature was redacted for privacy.

In Charge of Major Work

Signature was redacted for privacy.

Head of Major Department

Signature was redacted for privacy.

Dean of Graduate College

Iowa State University
Ames, Iowa

1968

TABLE OF CONTENTS

	Page
INTRODUCTION	1
Factors Influencing Reaction Rates	5
Charge on the complex	5
Nature of leaving group	6
Ionic strength	7
Steric hindrance	7
Solvent	8
Nature of entering group	10
Concentration of reactants	11
Mechanism of Reactions	13
Formulas Correlating Reaction Rates	17
Trans-effect	20
Cis-effect	31
EXPERIMENTAL	33
Materials	33
Platinum	33
Chloro complexes of platinum	33
Trans-dichlorodiammineplatinum(II)	35
Trans-dichlorobis(triethylphosphine)platinum(II)	36
Trans-dichloroammine(triethylphosphine)platinum(II)	40
Additional platinum complexes	55
Other chemicals	56
Solutions	58
Instruments	60
Procedures	64
Conductivity measurements	64
Spectrophotometric measurements	69
RESULTS	71
Trans-dichloroammine(triethylphosphine)platinum(II)	83

	Page
Trans-dichlorodiammineplatinum(II)	103
Trans-dichlorobis(triethylphosphine)platinum(II)	111
DISCUSSION	152
SUMMARY	164
LITERATURE CITED	167
ACKNOWLEDGEMENTS AND DEDICATION	174
APPENDIX A	175
APPENDIX B	180
APPENDIX C	187

INTRODUCTION

A great deal of effort has been expended at various laboratories in Russia, Italy, England, and the United States to elucidate the characteristics of square-planar platinum(II) complexes and of their substitution reactions. The present research was undertaken as a systematic study of one of the characteristics of platinum(II) substitution reactions, the cis-effect.

Despite the great amount of research that has been conducted with platinum(II) complexes over the past twelve years, the nature of such an important phenomenon as the trans-effect remains in a state of conjecture. The cis-effect remains even more in the state of limbo because the evidence for the very existence of such an effect has been fragmentary. In an attempt to ascertain whether there is evidence for such an effect, the reaction of ammonia (NH_3) with three platinum(II) complexes in methanol (MeOH) solutions was studied. The three complexes studied were trans-dichlorodiammineplatinum(II), t-$[Pt(NH_3)_2Cl_2]$, trans-dichloroammine(triethylphosphine)platinum(II), t-$[Pt(NH_3)(PEt_3)Cl_2]$, and trans-dichlorobis(triethylphosphine)platinum(II), t-$[Pt(PEt_3)_2Cl_2]$. The reasons for the selection of these complexes will become apparent as the discussion of the factors involved in determining the

rates of reaction of platinum(II) complexes is presented.

Historically, t-$[Pt(NH_3)_2Cl_2]$ has the distinction of sharing in the advent of modern coordination chemistry, for it was one of the complexes Werner considered in his treatment of coordination compounds (1). Reiset had prepared this complex some fifty years previously (2), but some confusion arose when Peyrone synthesized a complex of similar empirical formula with different properties (3). Werner, using only chemical evidence, resolved this difficulty by proposing cis and trans isomers of a square-planar complex as the complexes found by Peyrone and Reiset respectively.

Reiset also reported the reaction of t-$[Pt(NH_3)_2Cl_2]$ with NH_3 (4) to form $[Pt(NH_3)_4]Cl_2$ in aqueous solutions, but it was not until more than a century later that any kinetics studies were made of this reaction (5). It should be noted, however, that all of the kinetics studies conducted on the reactions of t-$[Pt(NH_3)_2Cl_2]$ have been in aqueous solutions, while the present study is in methanol solutions.

The second of the complexes in this investigation, t-$[Pt(PEt_3)_2Cl_2]$, is also a centenarian, having first been reported by Hofmann in 1857 (6). The existence of isomeric forms of this complex was noted soon afterwards (7). Finally, an isomerization between the cis and trans forms of the complex was found by Cahours and Gal (8).

In 1952 Chatt and Wilkins became interested in the cis-

trans equilibrium of $[Pt(PEt_3)_2Cl_2]$ as part of their studies on the nature of the trans-effect, and they published a series of papers on the isomerization reaction (9,10,11). They found that the equilibrium reaction is quenched by the addition of traces of the dimeric $Pt_2(PEt_3)_2Cl_4$ (12). Cahours and Gal had already determined that this reaction was catalyzed by traces of PEt_3 (8). Further elaboration upon this isomerization was given by Haake and Hylton, who reported that in methanol solutions at ambient temperatures without any catalyst or inhibitor present, there was less than 10% completion of the isomerization reaction after 10 weeks when the solutions were in the dark. In the presence of sunlight, however, identical solutions attained steady state in approximately two hours (13). The composition of the steady-state solutions were markedly different for the photo-induced isomerization, and for the thermodynamic equilibrium (66% trans isomer and 92% trans isomer at equilibrium, respectively). In addition, the steady state position was very much dependent upon the nature of the solvent (13).

The reaction of t-$[Pt(PEt_3)_2Cl_2]$ with NH_3 has been reported by several authors, with each finding that the reaction yielded the cis configuration in the product (14,15). These papers did not deal with the kinetics of the reaction, however.

The complexes of formula [Pt(PR_3) am Cl_2], where R is an alkyl or aryl group and am is an amine or ammonia, were first reported by Chatt and Venanzi in 1955 as part of a study of the trans-effect (16). As yet, there have been no published studies of the reactions of these complexes. The particular complex of interest herein, t-[Pt(PEt_3)(NH_3)Cl_2], was first prepared as part of this study, so perforce there is nothing in the literature specifically about it.

Upon examining the formulas of the three complexes used in this study, it will be noted that in each case there are two chloride ligands trans to each other, and that the ligands in the positions cis to the chlorides have been systematically changed from two phosphines to an ammine and a phosphine to two ammines. Because of the inertness of both the ammine and phosphine ligands in platinum(II) complexes, it was expected that these three complexes would react with ammonia to replace the chloride ligands which they contain. Thus, the reaction site and ligand trans to the reaction site would be the same in each complex, with only the positions cis to the reaction site varying.

Factors Influencing Reaction Rates

Although the study of platinum complexes dates back into the nineteenth century, as is apparent from the preceding material, concerted efforts to obtain quantitative information concerning these complexes and their chemical reactions have been limited to the past decade. Of late, studies have tended to concentrate on discerning what factors in the total reaction system influence the reactions. The factors considered have been: the charge on the complex, the nature of the leaving group, ionic strength, steric hindrance, the solvent, the nature of the entering group, the concentrations of the reactants, and the other ligands present in the complex.

Charge on the complex

Martin and co-workers have found that in reactions of platinum(II) complexes with solvent H_2O the reaction rates were relatively insensitive to the charge on the complex (cf. Table 1). This insensitivity to charge remains as one of the strongest bits of evidence that association is the rate determinant in the reactions of these complexes. The neutral entering ligand - in these examples, the solvent - is significant for any argument against a dissociative step being rate determining, because electrostatic effects between a neutral entering group and the substrate are thereby

Table 1. Acid hydrolysis rate constants of the chloroammine complexes of platinum(II) at 25°C and 0.318 ionic strength

Complex		$10^5 \times k_1$ sec^{-1}	$10^5 \times k/n^a$ sec^{-1}	Reference
$[PtCl_4]^{2-}$		3.9	0.98	(17)
$[Pt(NH_3)Cl_3]^-$	cis	-5.6	2.8	(18)
	trans	-0.62	0.62	(18)
cis-$[Pt(NH_3)_2Cl_2]$		2.5	1.3	(19)
trans-$[Pt(NH_3)Cl_2]$		9.8	4.9	(20)
$[Pt(NH_3)_3Cl]^+$		2.6	2.6	(21)

[a]Acid hydrolysis rate constant k, divided by the number of equivalent chlorides n for the hydrolysis reaction.

minimized.

Nature of leaving group

Experiments conducted to determine the effect of the leaving group upon the reaction rate have shown that there is a parallel between the increasing rate of reaction, and the decreasing bond strength between the leaving ligand and the platinum (22,23). Attempts to correlate the leaving group rates with the trans-effect have faced the same difficulty that attempts to correlate trans-effect and bond stability have faced: NH_3 and OH^- do not fit nicely into any such schemata.

Ionic strength

A recent study concerning the effect of ionic strength upon reaction rates of Pt(II) compounds gave evidence for a dependence of the form:

$$k_2 = A + B\mu^{\frac{1}{2}}$$

where k_2 is the rate constant for the second order reaction which is dependent on the concentration of both the complex and the incoming ligand, A and B are constants for a given reaction at constant temperature, and μ is the ionic strength of the solution (24). The similarity of the second term in this relationship to the Debye - Hückel limiting law is rather apparent; and, indeed, this ionic strength dependence was found to disappear when either of the reactants was neutral (24). This is the type of behavior that would be expected for an associative mechanism.

Steric hindrance

The effect of steric hindrance on the reactions of platinum(II) complexes was determined in several studies (25,26,27, p.32). These studies found that complexes containing ligands which blocked the tetragonal axis of the square-planar complex had a marked decrease in reaction rate for substitution reactions. Also, they found that a blocking group trans to the reaction site had a more pronounced retardation of the reaction rate than when such a

group was cis to the reaction site (26). This diminution in reaction rate is significant in determining the reaction mechanism, because complexes which have dissociation as the rate determining step have an increase of reaction rate with the introduction of hindering groups (28, p. 85). Thus, steric hindrance gives an additional indication that an associative mechanism is rate determining in these platinum(II) reactions.

Solvent

An aspect of the platinum(II) complex reaction systems which has received extensive study of late is the influence of solvent (25,29,30,31,32,33,34,35). The reason for such concentration upon the solvent becomes evident when one report emphasizes that the coordinating properties of the solvent are the only important considerations (25), while another says that the solvating properties have been very much underrated in their importance (35). The following observations about the influence of the solvent have been reported. The reactivity of the incoming ligand is dependent upon its degree of solvation: Small anions which have high charge density show a large variation in reactivity in different solvents, depending on the solvating ability of the solvent, whereas large, polarizable anions exhibit a reactivity which is independent of the solvent (29,31). Solvation of the leaving group appears to have no kinetic

significance in these reactions (34). In systems that have a solvation path as well as a path involving direct ligand attack upon the substrate, the coordinating ability of the solvent can enhance the solvation rate (25), but the solvation of the incoming ligand can also be of great moment in determining the overall reaction rate (35). The solvation of the substrate seems to be of a similar nature: the greater the degree of solvation of the complex, the greater the retardation of the reaction rate (although the retardation is not of large magnitude) (31). In general, it is difficult to sort which of these factors are at play in any given reaction, and whether it is the solvating or donor properties of the solvent which are operative (35).

One last detail which emerged from research on reactions involving a complex with a single positive charge and an incoming ligand of single negative charge was a negative entropy of activation. If an associative step is rate determining, the entropy of activation would be expected to be positive for the neutral transition state. The negative entropy of activation has been explained in terms of bond polarization between platinum and the ligands in the transition state for those ligands which are highly solvated, and low overall solvation for the remaining cases. In both cases, the ordering introduced by formation of the transition state yields the negative entropy (36).

Nature of entering group

In considering the entering group contribution to reaction rates, one observation becomes paramount - the polarizability of the incoming group is the main factor, while basicity is relatively unimportant (30,31,34,36,37, 38,39,40). This emphasis upon polarizability is the outgrowth of work done by Edwards and Pearson on the factors influencing nucleophilic reactivity (41,42,43). Edwards first formulated a double basicity scale involving the basicity of a nucleophile towards a proton, and the oxidation potential of the nucleophile (41). Edwards and Pearson then introduced a threefold relationship involving the basicity, the polarizability, and the mesomeric effect of groups in the α-position of the nucleophilic site (42). The final development in the early phases of this approach to nucleophilicity was the hard and soft acids and bases theory of Pearson (43). In this last development, the hardness signifies nonpolarizability, and the softness signifies polarizability. As a further refinement, it was postulated that soft acids preferred to react with soft bases and hard acids with hard bases. By considering nucleophilic displacement reactions of platinum(II) complexes as a particular form of acid-base reaction, and noting that these complexes were soft (polarizable), Pearson stated that the polarizability of the nucleophile should be the determinant

in the entering groups influence upon the reaction rate. Since that time, everyone who has studied platinum(II) complex reactions in that light has reported a corroboration of Pearson's contention. Basicity seems to be of little significance in these reactions, and, indeed, a strong base such as OH^- is a poor nucleophile for platinum(II) complexes. Previous to this correlation of experimental data according to acid-base theory, some efforts at entering group classification were based on approximate parallelism with the trans-effect (5,44). Account was also taken of possible reaction intermediate stabilization (44), but no throughgoing analysis of entering ligand effects was attempted prior to the polarizability postulate.

Concentration of reactants

The reactions of platinum(II) complexes have long been recognized as first order in the complex concentration, with many reactions also exhibiting first order dependence upon the entering ligand concentration. In 1960, a refinement was proposed for the rate equations of the reactions which were found to be first order in both complex and reagent (i.e., an overall second order reaction) (22):

$$\text{rate} = k_1[\text{complex}] + k_2[\text{complex}]\,[Y], \qquad 91.1)$$

where k_1 is a first order rate constant, k_2 is a second order rate constant, [complex] is the concentration of the

complex, and [Y] is the concentration of the reagent. The validity of this equation has received general acceptance, and innumerable studies have shown its applicability to ligand substitution reactions of platinum(II) complexes. The existence of both a first order and second order dependence in what was to all appearances a single reaction required some explanation. The denouement of this problem occurred with the observation that the k_1 which resulted from this formula was identical to the reaction of the complex with the solvent. It was proffered that what was occurring was a reaction with two paths. The first order path was a replacement reaction of the complex with the solvent to form a labile solvent-complex intermediate, which then reacted rapidly with the entering ligand Y to form the final product. The second order path was a direct attack of the ligand Y upon the complex. This can better be seen in the following generic reaction:

$$PtL_3X + S \underset{}{\overset{k_1}{\rightleftharpoons}} PtL_3S + X \overset{+Y}{\rightleftharpoons} PtL_3Y + S$$

$$PtL_3X + Y \overset{k_2}{\rightleftharpoons} PtL_3Y + X,$$

where PtL_3X represents any platinum(II) complex undergoing reaction, S is the solvent, X is the leaving group, and Y is the entering group. The rate constant k_1 designates the rate determining step in the first of these reactions. A

verification of the feasibility of the solvent path came with the report of a series of reactions involving the replacement of the aquo ligand from $[Pt(dien)(H_2O)]^{2+}$ (dien = diethylenetriamine) by a number of different ligands (45). In each case the rate constant for the replacement of the aquo ligand was found to be larger than the previously determined rate constants for the hydrolysis reactions of $[Pt(dien)X]^+$ ($X = Cl^-$, Br^-, I^-). The applicability of this solvolysis path to reactions in solvents other than water has also been reported (34,38).

Mechanism of Reactions

The embodiment of this two path reaction into a reaction mechanism has taken the forms shown in Figure 1 (46, p. 422-423). In these figures, S is a solvent molecule, Y and Z are entering ligands (Y and Z may be identical ligands, and either may be a solvent molecule), X is the leaving group, A is a ligand cis to the reaction site, and L is the ligand trans to the reaction site. The same mechanism would be operative in each path of the bifurcated second order reactions, and also in first order reactions. In both the first order path of a second order reaction, and reactions which only have a first order overall reaction, Y will be a solvent molecule. For the mechanism in Figure 1b (47,48), the product will first be the square planar solvo

complex which will be extremely labile. This solvo complex will then proceed to react further, using the same mechanism, except now the solvent molecule will be the leaving group and the incoming group will be the ligand that yields the final product. The direct, second order reaction will pass through the trigonalbipyramid transition only once.

In the original formulation of the mechanism given in Figure 1a, Z was also a solvent molecule for first order reactions as well as second order reactions (5). This mechanism has been called a dissociative mechanism, and was thought to continue dissociating in this manner until a stable product was formed. This mechanism has fallen upon bad times, and has been repudiated by one of its authors (28, p. 103). It is appropriate to point out, however, there is no direct evidence to prove the existence of a trigonal bipyramid as the transition configuration, so that the angles in the equatorial plane of the transition state in Figure 1b could approach those of a square pyramid. The entering group could then fall into place as the leaving group left, or else the <u>trans</u> ligand could shift to a position opposite the entering ligand in a new square pyramid with the leaving group in the apical position. While this square pyramid transition cannot <u>a priori</u> be completely ruled out, the discovery of several five coordinated complexes of platinum(II), all of which have a trigonal bipyramid con-

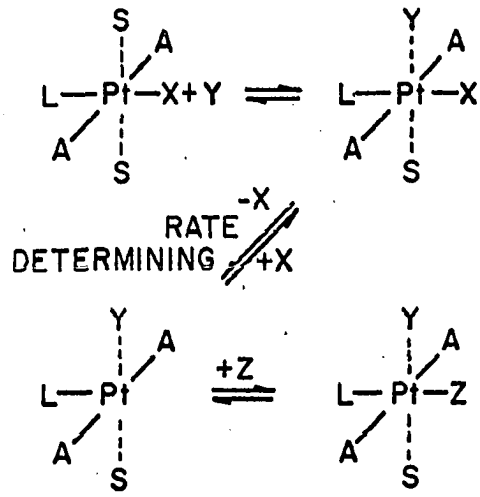

Figure 1a. Bimolecular reaction involving a square pyramid intermediate

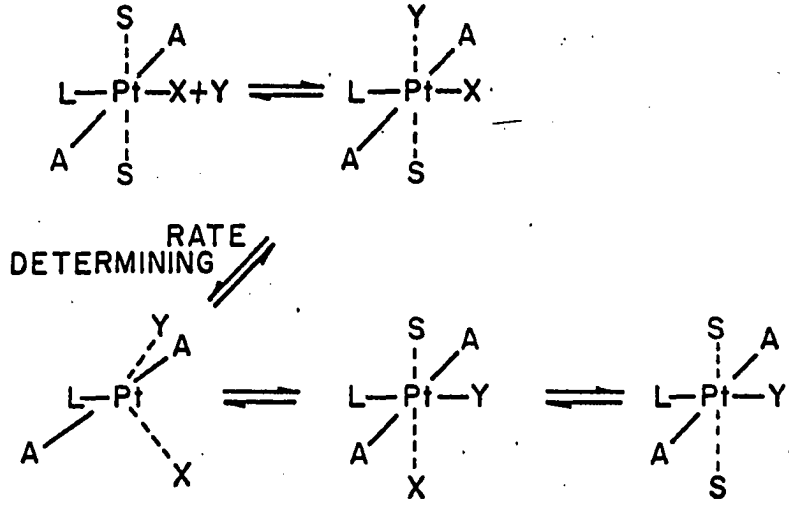

Figure 1b. Bimolecular reaction involving a trigonal bipyramid intermediate

figuration (49,50,51), adds weight to the arguments against the square pyramid (27, p. 44-48).

The mechanism involving the trigonal bipyramid is an associative mechanism, with the associative step determining the reaction rate. At the pregnant places in the preceding text, some of the evidence which favors an associative process in the role of rate determinant were indicated. In brief, these are: (1) the charge on the complex does not materially effect the reaction rate, (2) the ionic strength does not influence the reactions in a manner characteristic of dissociative mechanisms, (3) steric hindrance of the octahedral positions causes rate retardation, (4) solvation of the leaving group is not a determining factor, and (5) the reaction rate is strongly influenced by the nature of the incoming group. Some authors have opted in favor of a dissociation mechanism for complexes which are not highly sterically hindered, however. Adams et al. in studying the infrared spectra of platinum(II) complexes found that as the stretching frequency of a bond between the platinum and a ligand was decreased, the ligand became more labile. From this they suggest that, "a ligand of high trans-effect can exert its influence... by electron release in the σ-... co-ordinate bonds,...enhancing S_N1... substitution of the trans-ligand (52)." Belluco, Graziani, and Rigo concluded that a dissociative mechanism was possible in a series of

reactions they studied, because the reaction rates for the solvent paths in these particular reactions were greater than they had predicted from theory (40). Another possibility for a dissociative mechanism not involving sterically hindered complexes was the catalysis of certain platinum(II) complex reactions in the presence of $HC_2H_3O_2$, H_3BO_3, or HNO_2 (28, p. 103). This problem of catalysis was later found to be explicable in terms of charge enhancement in an associative mechanism, however (53).

Formulas Correlating Reaction Rates

A final excresence from the theories on the factors influencing nucleophilic reactivities has been a formula for correlating the nucleophilic displacement reactions of a given complex (38). Using t-$[Pt(pyridine)_2Cl_2]$ as a reference standard, an analogue of the Hammett equation was established:

$$\log k_y = sn_{Pt} + \log k_s, \qquad (1.2)$$

where k_y is a bimolecular constant for the nucleophic reagent (k_2 in Equation 1.1), k_s is a pseudo-first-order constant for a bimolecular nucleophilic reaction of the solvent (k_1 in Equation 1.1), s is a nucleophilic discrimination factor, and n_{Pt} is a nucleophilic reactivity constant. The last two terms, s and n_{Pt}, were the main features of

this formula, and require further explication.

The nucleophilic reactivity constant, n_{Pt}, was defined by the equation:

$$\log\left(\frac{k_Y}{k_s}\right)_o = n_{Pt}, \qquad (1.3)$$

where k_Y and k_s refer to the rate constants for the reaction of the ligand Y with t-[Pt(pyridine)$_2$Cl$_2$] in methanol at 30°C. A table of such constants was made up for a variety of ligands, and was taken to give the characteristic nucleophilic reactivity for each of these in reacting with platinum(II) complexes.

Using these values of n_{Pt}, a set of constants, s, which were characteristic of the reactions of other individual complexes were calculated. By reacting a given complex with a number of different reagents, and then plotting log k_Y, the log of the second order reaction rate of a particular reagent, as a function of n_{Pt}, the nucleophilic reactivity constant for that particular reagent, a straight line was obtained which had s as its slope and log k_s as its intercept. Thus, it was theoretically possible to predict a second order reaction rate for any reaction if the n_{Pt} of the reagent, the s of the complex, and k_s for the reaction of the complex with the solvent were known. It should be emphasized, however, that s is a function of both

the solvent and temperature. It was also observed that a strong inverse relationship existed between s and k_s.

In Equation 1.2 above, the Gibb's free energy of activation is basically being employed as the correlating factor, using the influence of the reagent on the reaction rates of the reference complex as the reagent characteristic, and the complex contribution to the reaction rate in a series of reactions as the substrate characteristic. There are other possible bases for correlation, however, and two of these have been tried (54,55,56). One of these employed the compensation effect (54,55), which is a relationship between the pre-exponential factor (frequency factor) and the activation energy from the Arrhenius equation; the other used the isokinetic relation (56), a relationship between the analogous quantities in the theory of absolute rates, the entropy and enthalpy of activation. At the present time the latter of these two has not been applied extensively to platinum(II) complexes, and the former has been applied in only a small number of cases, so a comprehensive analysis of their applicability is not possible at this time. The main difficulty in the study of these two treatments of reaction rates is that they are a correlation of a series of complexes differing from each other only in having a different ligand <u>trans</u> to the leaving group, with all other ligands in the complex, the entering group, and the

physical conditions all otherwise identical from one complex to the other. Unfortunately, there are not many such series available which have more than three or four members. This contrasts with the approach of Equation 1.2 above, in which the only variable in the series was the entering group. Much experimental data of this nature is available. A more complete treatment of these theories of reaction rate correlation is given in Appendix A.

Trans-effect

One of the early workers on the chemistry of platinum(II) complexes, Jorgenson, found that when $[Pt(NH_3)_2Cl_2]$ was synthesized using $[Pt(Cl_4]^{2-}$, a different product was obtained than that obtained when using $[Pt(NH_3)_4]^{2+}$ (57). The reaction of $[Pt(Cl_4]^{2-}$ with NH_3 resulted in c-$[Pt(NH_3)_2Cl_2]$, whereas the reaction of $[Pt(NH_3)_4]^{2+}$ with Cl^- yielded t-$[Pt(NH_3)_2Cl_2]$. If these two isomers of $[Pt(NH_3)_2Cl_2]$ are in turn reacted with thiourea (tu), the trans isomer will yield t-$[Pt(NH_3)_2tu_2]^{2+}$, while the cis isomer will yield $[Pt(tu)_4]^{2+}$. This reaction with thiourea is used to differentiate cis and trans diammines, and has been named Kurnakov's test after its discoverer (58).

In further studies of the cis and trans isomers of $[Pt(NH_3)_2Cl_2]$, Werner and Miolati (59), and Drew et al. (60) found that the conductivity of aqueous solutions changed

with time, thus indicating some chemical reaction. The change in conductivity was interpreted by Grinberg and Ryabchikov (61,62) and Jensen (63) to be the result of the acid hydrolysis reactions:

$$[Pt(NH_3)_2Cl_2] + H_2O = [Pt(NH_3)_2(H_2O)Cl]^+ + Cl^- \quad (1.4)$$

$$[Pt(NH_3)_2(H_2O)Cl]^+ + H_2O = [Pt(NH_3)_2(H_2O)_2]^{2+} + Cl^-. \quad (1.5)$$

These aqueous solutions were titrated with sodium hydroxide, and the acid strengths of aquo species in Equations 1.4 and 1.5 were determined (61,62,64). Further studies of the hydrolysis reaction of Equation 1.4 have been conducted for both isomers, with a consequent determination of reaction rate and equilibrium quotient for each reaction (5,19,20,65). The reaction rate for the trans isomer has been found to be higher than that of the cis isomer.

Each of the above differences is illustrative of what has come to be called the trans- effect (66). The trans-effect is exhibited by any group which affects the rate of substitution reactions of the ligand that is in the position trans to it in the square plane of the complex. The trans-effect is described in this manner because it places emphasis upon the most universally accepted manifestation of the trans-effect, the effect upon the rate of substitution reactions, without indicating the manner in which this manifes-

tation is caused. The main reason for being so vague is that no single extant theory on the trans-effect is capable of explaining all of the individual examples of its operation.

An explanation of the trans-effect suggested by Grinberg (67) was that an induced dipole on the central metal atom weakens the bond of the ligand in the position trans to the labilizing group, thus enhancing the rate of the substitution reactions of the leaving group. The dipole is induced on the platinum when the primary charge of the platinum(II) polarizes the electron cloud of the trans-labilizing ligand. The dipole induced on this polarized ligand in turn interacts with the electron cloud of the platinum to yield an increment in the electron charge density in the region of the ligand which is in linear opposition to the labilizing ligand. Figure 2, in which only the two ligands involved are shown, illustrates this. L is the trans-labilizing group, X is the leaving group, and the polarization dipoles are as illustrated. The increment in electron density causes a weakening of the bond of the leaving group, with a consequent increase in its rate of reaction. According to this theory, the higher the polarizability of the trans-labilizing group, the greater is its trans influence. This is in accord with experimental evidence.

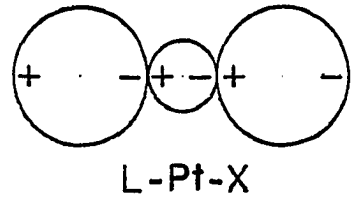

Figure 2. Distribution of charge in the induced dipoles in the L-Pt-X coordinates of trans-$[PtA_2LX]$

Some support for this thermodynamic interpretation of the trans-effect can be found in experimental determinations of the strength of the bond of the leaving group X in Figure 2 under the influence of various L ligands. Infrared studies of the stretching frequency of the halide-platinum bond when a variety of different ligands were trans to the halide have revealed a large number of cases in which the better the L group is as a trans-labilizing ligand, the lower the platinum-halide stretching frequency (52). Also, in X-ray determinations of the platinum-halide bond length in some platinum(II) complexes, the bond has been found to be longer when certain strongly trans-labilizing ligands were in the L position in Figure 2 (68,69). Both the shifting of stretching frequency to lower wave numbers, and the increase in bond length have been attributed to a weakening of the bond of the strongly labilized leaving group.

Further amplification on this polarization theory took

note that highly polarizable ligands which have large trans influence have low electronegativities, and form covalent bonds with platinum which involve electron transfer to the platinum. This transferal to the platinum leaves the directional nature of the trans-effect unexplained, however, because a general decrease in the strength of all the platinum-ligand bonds would be expected from a decrease in the net positive charge on the platinum. Syrkin attempted to explain the directionality on the basis of the platinum orbitals which are used in forming the covalent bonds with the ligands, and the effect upon the electron distribution in these orbitals when one of the ligands forms a highly covalent bond with the platinum (70). Considering the d, s, and two p orbitals of the platinum involved in the bonding, he claimed that resonance models for the system showed that strong covalent bonding by one of the ligands causes an increase in the covalent character of the bonds to ligands which are cis to the covalent ligand, and decrease in the covalency of the trans ligand. This lessening of covalent character was taken to correspond to a weakening of the bond of the trans ligand. This treatment involved the principle that the d orbital is of lower energy than the p orbital, and that if it were strongly involved in the bonding of one of the ligands, then by the directional nature of the d orbital, the ligand trans to the strongly bound ligand would

have a weaker bond.

Basolo and Pearson have proposed a different approach to this problem of polarizability as related to the trans-effect (46, p. 426). Enlisting the observation that those ligands which are easily polarized have low lying excited states, and that polarization can be explained in terms of the wave functions of these low lying excited states mixing with the wave function of the ground state (42), they proposed that the shift of electron density in the direction of the labilized ligand was caused by these hybrid obitals of polarization being directed toward the platinum.

The polarization approach to the trans-effect gives an explanation for those trans-labilizing ligands which cause an apparent weakening in the bonding of the ligand trans to themselves, but such a weakening is not always the rule. The olefins are some of the strongest trans-labilizing groups, yet measurements of the bond in the position trans to an olefin indicate that it is a normal bond (52,71). The explanation proffered for the trans labilization of these ligands involves the trigonal bipyramid transition state of Figure 1b above (47,48). First a coordinate system for the molecule is defined with the Pt(II) at the origin. The x and y axes are in the plane of the molecule and are directed toward the ligands, and the z axis is perpendicular to the plant of the molecule. In passing from a four coordinated

square plane to a five coordinated trigonal bipyramid, the filled platinum d_{xz} orbital is of such symmetry as to introduce destabilization of this transition state through electrostatic interaction with the entering group and the leaving group. This interaction can be reduced if the trans labilizing group has an available empty Π orbital which can accept the electrons of the platinum d_{xz} orbital. The result is a decrease in the electron density in the region of the entering and leaving group, and a stabilization of the trigonal bipyramid intermediate. Each of these theories is limited in its application, and both must be invoked for any attempt at a systematic explanation of all incidents of the trans-effect.

Several authors have noted the limitations in these two theories, and have attempted syntheses into a unified theory of the trans-effect. One of these has introduced the effect of polarization upon the Π orbitals of the trans labilizing ligand into the theory of the intermediate stabilization through Π-bonding (72). Here, the energy of the Π orbital of the trans labilizing ligand was coupled to the σ-bond between the ligand and the platinum. If the ligand is polarizable, its polarization causes a net shift of ligand charge toward the platinum. This shift decreases the electronic repulsion within the ligand with a resultant lowering of the energy of the empty Π orbital centered on the ligand. As

the energy of this Π orbital is lowered, Π-bonding with the d_{xz} orbital of the platinum becomes more favorable. The author claimed that in this fashion a ligand Π orbital which ordinarily would be of too high energy to Π-bond with the platinum could become usable in stabilizing the intermediate. Furthermore, this theory predicts that the more polarizable a ligand is, the greater is the lowering of its available Π orbital, and, consequently, the greater the stabilization of the reaction intermediate. In this manner the author has attempted to incorporate the observed parallel between polarizability and labilizing influence into the Π-bonding stabilization theory.

Another theory which incorporated both the σ- and Π-bonds into a unified operation of the trans-effect laid emphasis upon considering the trans ligands in pairs in any evaluation of the effective trans labilization (73). This theory considered the trans ligand pair, because of the interrelatedness of trans labilization and specific lability (leaving properties of a ligand). For example, while PEt_3 is a very strong trans labilizing group and Cl^- is rather weak, in the complex t-$[Pt(PEt_3)_2Cl_2]$, the Cl^- ligands are relatively labile, while the PEt_3 ligands are inert. In this complex, the strong labilization of the PEt_3 is less important than the low specific lability of PEt_3. Therefore, in order to adequately define the trans labilization, the in-

clusion of the labilized ligand was regarded as a requisite. Beyond this, a second factor included in this treatment was the degree of distortion that a trans ligand pair underwent upon the approach of the incoming ligand. On the basis of pure electrostatics, the order of mutual repulsion between point charges and electric dipoles as a function of the distance of separation is: charge - charge > charge - dipole > dipole - dipole. Besides the repulsion between the entering ligand and the ligands already bound to the platinum, the repulsion between the entering ligand and the filled antibonding d orbitals of the platinum comes into play. This repulsion causes a shifting of charge density towards the platinum. The ability of the bonded ligands to absorb this added charge from the platinum contributes to the overall stabilization of the intermediate by the reduction of electrostatic repulsion. This ability to accept additional charge from the platinum is a function of the polarizability of the ligand. The combination of these two factors, ligand - ligand repulsion and transition stabilization, determine which two ligands will be distorted the most, and thus become the equatorial plane of the trigonal bipyramid. Once the transition state has been achieved, the question of the leaving group becomes important. The leaving group is determined by three factors: charge on the ligand, the ability of the ligand to stabilize the transi-

tion state, and the solvation of the leaving group. The negative charge of a ligand will promote its leaving properties, owing to electrostatic repulsion. The factors which stabilize the transition state, empty low lying σ- and Π-orbitals on the ligand, decrease the lability of a ligand. Finally, ionic groups with high energy of solvation are displaced more easily than neutral groups, in polar solvents. These are the salient features of this second effort to form a unified trans-effect theory.

The third of the recent formulations of a coherent theory for the trans-effect divides the effect into a σ-trans effect and a Π-trans effect (27, p. 24-29).

In the σ-trans effect, the p orbitals of the platinum are the only orbitals capable of giving the directional character of the trans-effect. If the trans labilizing ligand has a strong σ interaction with the p orbital, the bond of the leaving group may be weaker. The greater the polarizability of the trans labilizer, the greater its σ overlap with p orbital of the platinum. This interraction is strengthened if the leaving group moves out of the plane to form the trigonal bipyramid intermediate. Because of the additional pair of electrons introduced by the entering group, however, the overall bonding of the transition state may be loosened.

The Π-trans effect differs from the original formulation

of the stabilization of the intermediate by π-bonding only in the consideration of all the d orbitals of the platinum which are capable of π interactions with the ligands. The delocalization of electronic charge by the trans labilizing group is again the important feature.

In evaluating any theory of the operation of the trans-effect, there are several touchstones whereby to judge their capabilities: 1) Can the theory account for the very high trans labilization exhibited by H^-, and CH_3^-? 2) Is the high stability of the bonding of NH_3 and OH^- explicable along with their weak trans-effect? 3) Can the high trans labilization of the olefins be explained while still retaining the normal bond character of the trans ligand? 4) Is the parallel between the polarizability of the ligand and its trans labilization meaningful within the context of the theory? 5) Is the directional character of the trans-effect a natural consequence of the theory without resorting to theoretical legerdemain? Examination of the preceding theories in light of these queries is revealing. While each theory has proficiency in explaining a large amount of the experimental data, each tends to be procrustean in handling ungainly data.

A final obfuscation of the mechanism of the trans-effect has been introduced by the report that t-$[Pt(PEt_3)_2ClH]$ reacts with pyridine with a first order

rate that is 1.4 times faster than the reaction of t-[$Pt(PEt_3)_2ClD$] (74). This secondary kinetic isotope effect is exactly of the same magnitude as the changes in the platinum-hydrogen and -deuterium vibrations observed in the infrared spectra.

Cis-effect

First mention of the existence of a cis -effect was thirty years after the trans-effect (75). The cis-effect is defined as an influence upon the rate of substitution reactions by the ligand which is cis to the reaction site. Since that first report, many observations of the operation of a cis-effect have been made, but the range of the cis influence does not approach the many orders of magnitude observed for the trans influence on reaction rates, so some authors have expressed the opinion that the cis influence is of insufficient moment to be dignified with a special name. In those cases of the cis-effect that have been reported, it appears that there is an inverse relationship between the trans-effect and the cis-effect: a group which strongly enhances the rate of reaction of groups trans to itself, tends to show little influence on the rate of reaction of groups cis to itself, with the reverse holding true for poor trans labilizing ligands (76). In some reactions involving ligands which are weak trans labilizers,

it has been found that the cis-effect may be of greater magnitude than the trans-effect (28, p. 99). The present state of experimental work involving systematic changes in the ligands cis to the reaction site is so fragmentary that definite conclusions concerning the ordering of ligands with respect to cis influence are not possible. The only working hypothesis for establishing experiments is the seeming inverse relationship between the cis and trans-effects. It was on this basis that the complexes were chosen for this study - PEt_3 is a very strong trans labilizing ligand and therefore, by hypothesis, a very weak cis labilizing ligand, while NH_3 is a very weak trans labilizing ligand, and therefore a very strong cis labilizing ligand.

Inasmuch as the well studied trans-effect lacks solid theoretical explanation, as is attested by the plethora of theories which are sometimes contradictory of one another, it is not too surprising that the less studied cis-effect has not been fit into an adequate theoretical framework. About the only attempts to deal with the cis-effect have been by authors of theories of the trans-effect who summarily state that their theory of the trans-effect also shows that the same mechanism operates to yield a weaker influence by the cis ligands. In the words of myriads of authors down through the ages, more research is required in this area.

EXPERIMENTAL

Materials

Platinum

The platinum used in the experiments was recovered from compounds used in other experiments at this laboratory and was originally from many sources. Because commercially obtained platinum contains traces of iridium, which can act as a catalyst, the platinum was purified using the method recommended by Jowanovitz et al. (77). Metallic platinum was dissolved in aqua regia and the solution was boiled to near dryness. Then a process of adding HBr solution and boiling to near dryness was used several times to drive off all the HNO_3. The solution was then treated with a concentrated solution of KBr to precipitate the sparingly soluble K_2PtBr_6. This latter salt was then recrystallized several times from H_2O, with the mother liquor being rejected after each recrystallization since it is the portion which is rich in iridium. Finally, the K_2PtBr_6 was reduced to platinum metal from a hot aqueous solution made strongly basic with NaOH, by the dropwise addition of hydrazine.

Chloro complexes of platinum

Four different chloro compounds of platinum- K_2PtCl_6, H_2PtCl_6, K_2PtCl_4, and $PtCl_2$- were required as intermediates for the preparation of the desired complexes.

Platinum which had been freed of iridium was dissolved in aqua regia. After repeated additions of excess concentrated HCl and boiling to near dryness, a fairly pure solution of H_2PtCl_6 was obtained. At this juncture two possible courses of action arose: addition of excess KCl caused the fairly insoluble K_2PtCl_6 to precipitate, or the H_2PtCl_6 solution was evaporated to dryness. In the latter case, the H_2PtCl_6 was first heated to approximately 150°C for a short while and then to 360-380°C for about two hours in a furnace with a slow current of air passing through the apparatus. At the end of this period, the resulting green solid was pulverized and reintroduced into the furnace for another hour at 360°C. The greenish $PtCl_2$ thus prepared was boiled with dilute HCl to remove any unchanged reactant, and was then dried at 360°C after having been washed twice with H_2O (78).

As for the K_2PtCl_6 which was prepared, a part was retained to be used in the preparation of $\underline{t}$-$[Pt(PEt_3)_2Cl_2]$, and the rest was reduced to K_2PtCl_4. The reduction to Pt(II) was achieved in two manners, a $K_2C_2O_4$ reduction (79) and a SO_2 reduction (80). In each of these reductions, the insoluble yellow K_2PtCl_6 was slowly converted into the quite soluble red K_2PtCl_4 by heating with the reducing compound over long periods. The SO_2 reduction had the advantage that no KCl was formed during the reduction, so that a purer

product was obtained without too much difficulty, The K_2PtCl_4 obtained by either method was purified by fractional crystallization with H_2O.

Trans-dichlorodiammineplatinum(II)

The t-$[Pt(NH_3)_2Cl_2]$ was prepared by the thermal decomposition of $[Pt(NH_3)_4]Cl_2$. The essential features of syntheses used for both of these complexes were first described by Reiset (2), but the more explicit directions for the preparation of $[Pt(NH_3)_4]Cl_2$ (81) and t-$[Pt(NH_3)_2Cl_2]$ (61), as given by later authors, were followed.

A hot concentrated solution of K_2PtCl_4 was combined with concentrated aqueous ammonia until a green precipitate of $[Pt(NH_3)_4]$ $[PtCl_4]$ was formed. When this precipitate began to form, a large excess of the ammonia solution was added; and the mixture was heated until all of this green Magnus' salt dissolved. Then the solution was evaporated to small volume, and the $[Pt(NH_3)_4]Cl_2$ was precipitated by the addition of a voluminous acetone-ether-alcohol solution. The white crystals were washed with ether and dried. These white crystals were then heated in an open dish with stirring to 250°C in a Wood's metal bath. The complex was so heated for approximately thirty minutes with the temperature being maintained ± 5°C. The resulting mass was next treated with hot 0.5M HCl to extract the t-$[Pt(NH_3)_2Cl_2]$ from other decomposition products. The complex compound

was relatively insoluble, so that it was recovered from hot aqueous solution by cooling. The coordination compound thus produced was recrystallized twice from 0.5M HCl and several additional times from H_2O until the ultraviolet spectrum was unchanged and agreed with published spectra (20). The spectrum obtained is given in Figure 3.

Trans-dichlorobis(triethylphosphine)platinum(II)

Two methods were employed for the synthesis of t-$[Pt(PEt_3)_2Cl_2]$. In each case PEt_3 was reacted with a chloroplatinate.

The PEt_3 was prepared by the Grignard reaction involving PCl_3, Mg, and EtBr. An ether solution of EtBr was treated with the Mg to form EtMgBr. The latter in turn reacted with the PCl_3 to yield the PEt_3. Each of these reactions could be rather violent because they were strongly exothermic and in volatile ether solutions, so the rate of each reaction was controlled by cooling with an ice bath. In addition, the PCl_3 was dissolved in ether and this solution was added dropwise to the ethereal EtMgBr solution. The PEt_3 was collected by vacuum distillation after all of the ether had been evaporated from the reaction solution.

In the first preparation of t-$[Pt(PEt_3)_2Cl_2]$, the PEt_3 was reacted with K_2PtCl_6 in a molar ratio of three PEt_3 to one K_2PtCl_6, in a H_2O solution (82). Upon standing for several days, a flocculent bleached precipitate formed,

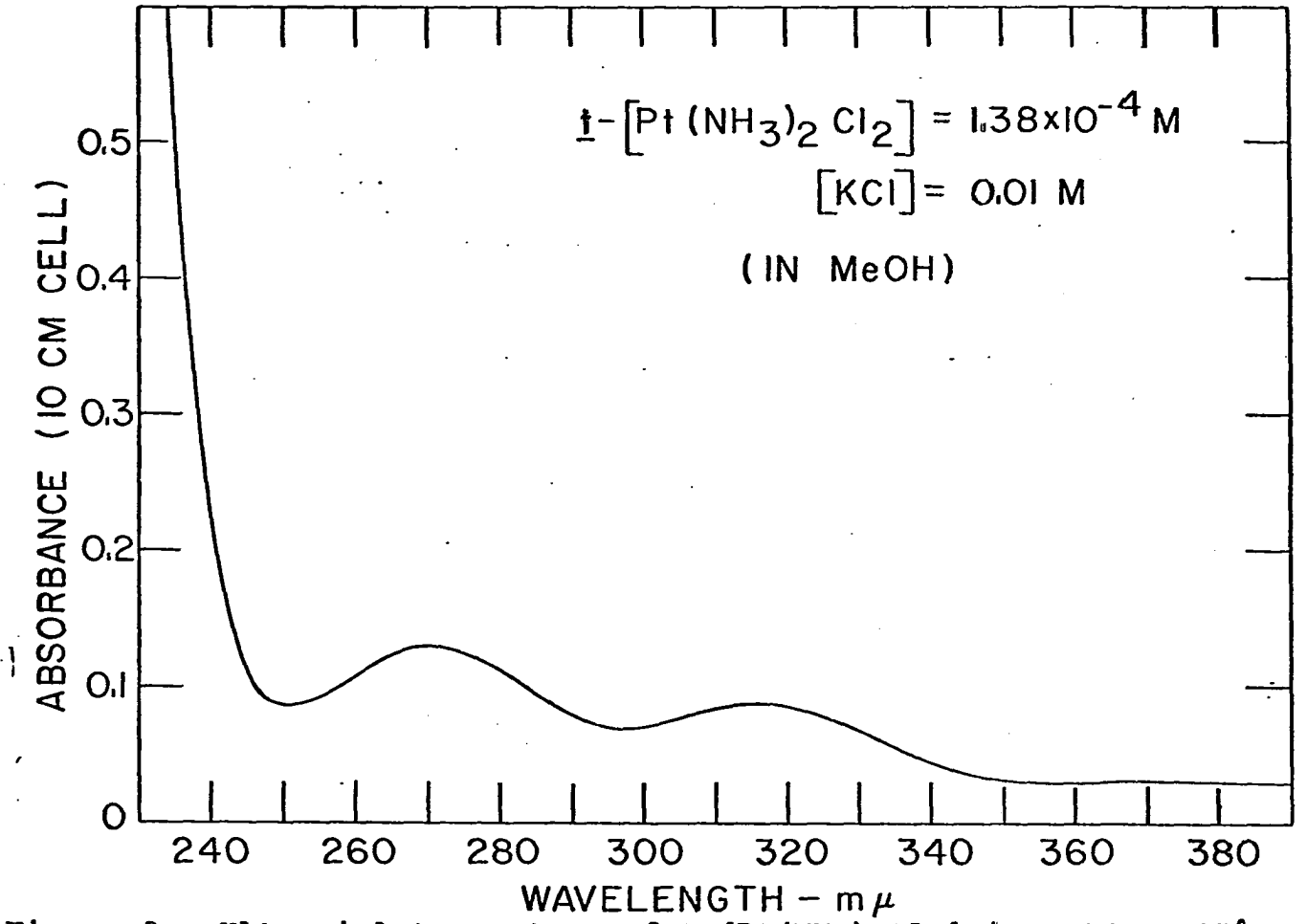

Figure 3. Ultraviolet spectrum of t-$[Pt(NH_3)_2Cl_2]$ in MeOH at 25°C. A 10 cm silica cell was used

which was collected by filtration.

The second preparation involved the reaction of PEt_3 with K_2PtCl_4 in a molar ratio of two PEt_3 to one K_2PtCl_4, in a H_2O solution (82). A reddish-brown precipitate of $[Pt(PEt_3)_4]$ $[PtCl_4]$ first formed, which was then converted to a mixture of cis and trans - $[Pt(PEt_3)_2Cl_2]$ by heating the precipitate in the mother liquor at 100°C for ten minutes. The $[Pt(PEt_3)_2Cl_2]$ formed by this procedure was a bleached precipitate, which was collected by filtration.

In each of these preparations the desired t-$[Pt(PEt_3)_2Cl_2]$ was extracted from any cis isomer by ether, in which the cis isomer is insoluble. By conducting this extraction at the boiling temperature of the ether and in bright light, a high yield of trans isomer was obtained from the second method above, as a consequence of the isomerization of the cis isomer. The bright yellow crystals of the trans isomer were obtained by evaporation of the ether. The pure complex was obtained by repeatedly recrystallizing the complex from methanol in a room lighted by red lights until an ultraviolet spectrum was obtained which did not change with additional recrystallization, and which correlated with a published spectrum (13). The ultraviolet spectrum of a specimen of the t-$[Pt(PEt_3)_2Cl_2]$ is given in Figure 4. The melting range of the complex was 142.0-142.3°C, which agrees well with published values of 142-143°C (9,63).

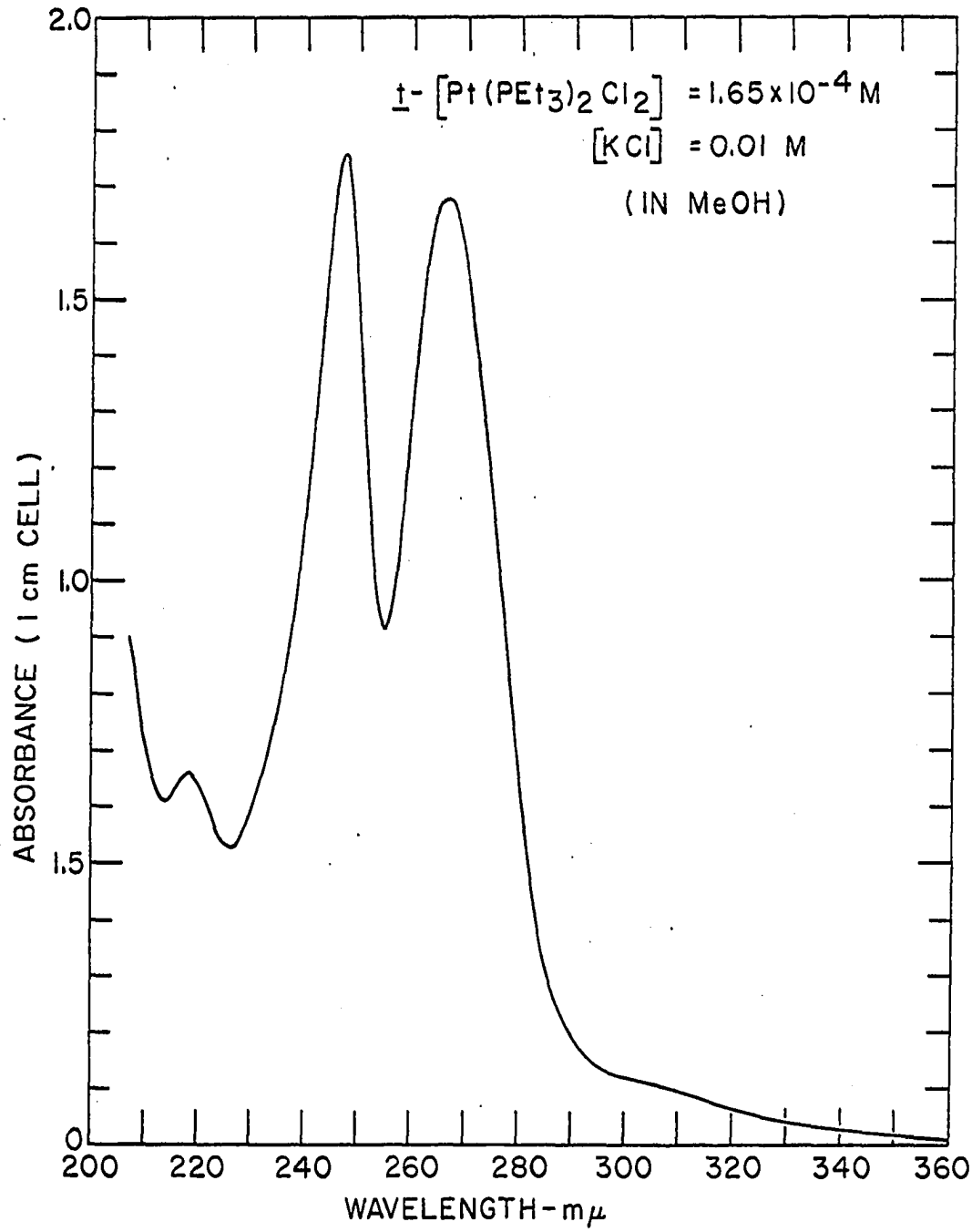

Figure 4. Ultraviolet spectrum of t-$[Pt(PEt_3)_2Cl_2]$ in MeOH at 25°C. A 1 cm silica cell was used

It should be noted, however, that values of 134°C (15) and 150°C (8) have also been reported for the melting point; the discrepancy possibly arises because the compound isomerizes at its melting point.

Trans-dichloroammine(triethylphosphine)platinum(II)

Prior to the synthesis of t-$[Pt(PEt_3)(NH_3)Cl_2]$, it was necessary to synthesize a chloro-bridged dimeric platinum (II) complex, sym-trans-di-μ-chloro-dichlorobis(triethylphosphine)diplatinum(II), t-$[Pt(PEt_3)_2Cl_4]$. This was achieved by mixing equimolar amounts of $PtCl_2$ and $[Pt(PEt_3)_2Cl_2]$ (either cis or trans, or a mixture of the two) and heating this mixture to 150°C with stirring (83). After the mixture started to become pasty, the temperature was raised to approximately 187°C where the mixture became fairly liquid. With the culmination of ten minutes heating with stirring at this temperature, a black charred mass resulted. When cooled and treated with acetone, however, the orangish-yellow dimer was extracted from the mass. After recrystallization several times from acetone, the ultraviolet absorption spectrum in methanol shown in Figure 5 was obtained. The absorption peak at 272 mμ was of some concern, because acetone had an absorption peak at this same wave length. The complex was recrystallized from methanol, but the spectrum remained unchanged. A neutron activation analysis for oxygen was obtained in order that the validity

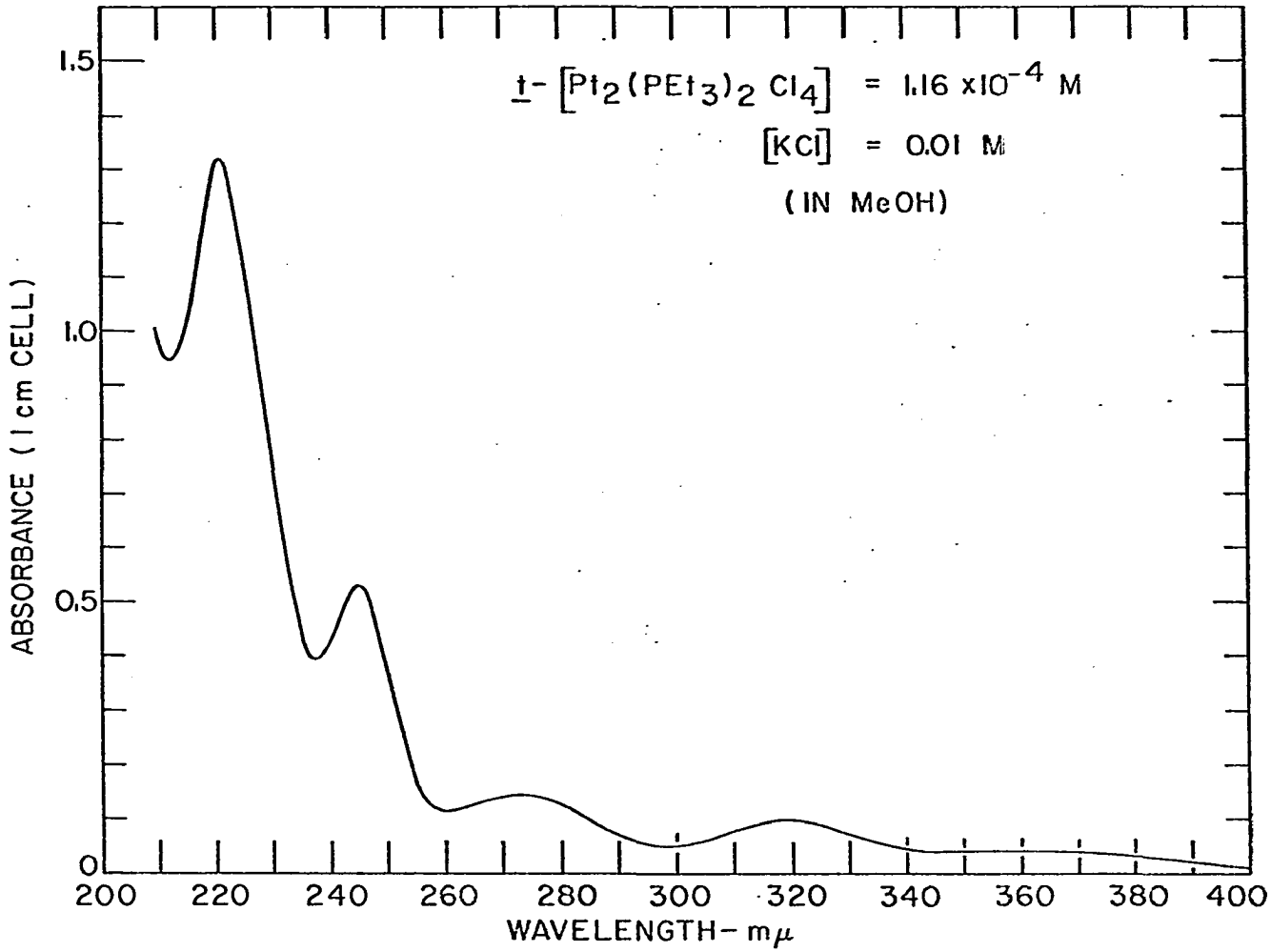

Figure 5. Ultraviolet spectrum of t-$[Pt_2(PEt_3)_2Cl_4]$ in MeOH at 25°C. A 1 cm silica cell was used

of the suspect peak as part of the spectrum might be determined. The complex was found to contain 790 ± 80 ppm by weight of oxygen, which would be insufficient acetone, if the oxygen were assumed to be present as acetone, to be noticeable in the ultraviolet spectrum on the basis of a reported extinction coefficient of 18.6 for the acetone transition at this wave length.

This dimeric complex was reacted with NH_3 to give the desired t-$[Pt(PEt_3)(NH_3)Cl_2]$ (16). In order to prevent further reaction of the product complex with NH_3, only two moles of NH_3 were added for every one mole of $[Pt_2(PEt_3)_2Cl_4]$. To this end, anhydrous NH_3 gas was bubbled into ethanol, and this solution was then standardized with $HClO_4$ in glacial acetic acid. The requisite amount of this standardized NH_3 solution was added to an ethanol solution of the dimer which had undissolved dimer present, and the mixture was stirred for three hours. At the end of this period, a slightly fluorescent, greenish-yellow solution had formed. The ethanol was allowed to evaporate at ambient temperature, leaving yellow crystals of t-$[Pt(PEt_3)(NH_3)Cl_2]$. The complex was recrystallized from petroleum ether having a boiling range of 80-100°C, until the infrared and ultraviolet spectra of the complex were unchanged. Because this complex had not previously been reported in the literature, and because the cleavage reaction of the dimer was reported to give either

isomer, the complex was subjected to a fairly comprehensive characterization. The ultraviolet spectrum, the infrared spectrum, and the mass spectrum are given in Figures 6, 7, and 8, respectively. The composition and structure of the complex were determined from interpretation of the infrared and mass spectra.

Interpretation of the infrared spectrum was somewhat facilitated by several studies on the infrared spectra of platinum(II) complexes which had been reported in the literature (52, 84, 85, 86, 87). While a comprehensive assignment of all the frequencies of the infrared spectrum was beyond the scope of the present study, sufficient information was obtained from relatively few assignments to enable the assessment of the structure.

In an extensive study of complexes having the cis and trans - $[Pt\ L_2X_2]$, where X = Cl, Br and L = neutral ligand, Adams et al. found that the Pt-Cl stretching frequency, ν (Pt-Cl), was fairly insensitive to ligands cis to it in the platinum(II) complex, and quite sensitive to the ligand trans to it (52). In addition, ν(Pt-Cl) was one very strong band at 339.5 $\pm$ 3.1 cm^{-1} when the two chloro ligands were trans to each other, and two very strong bands when they were cis. The cis chloro ligands had ν(Pt-Cl) shifted to lower frequencies than the frequencies found for the trans chlorides with the amount of shift being directly correlated to the

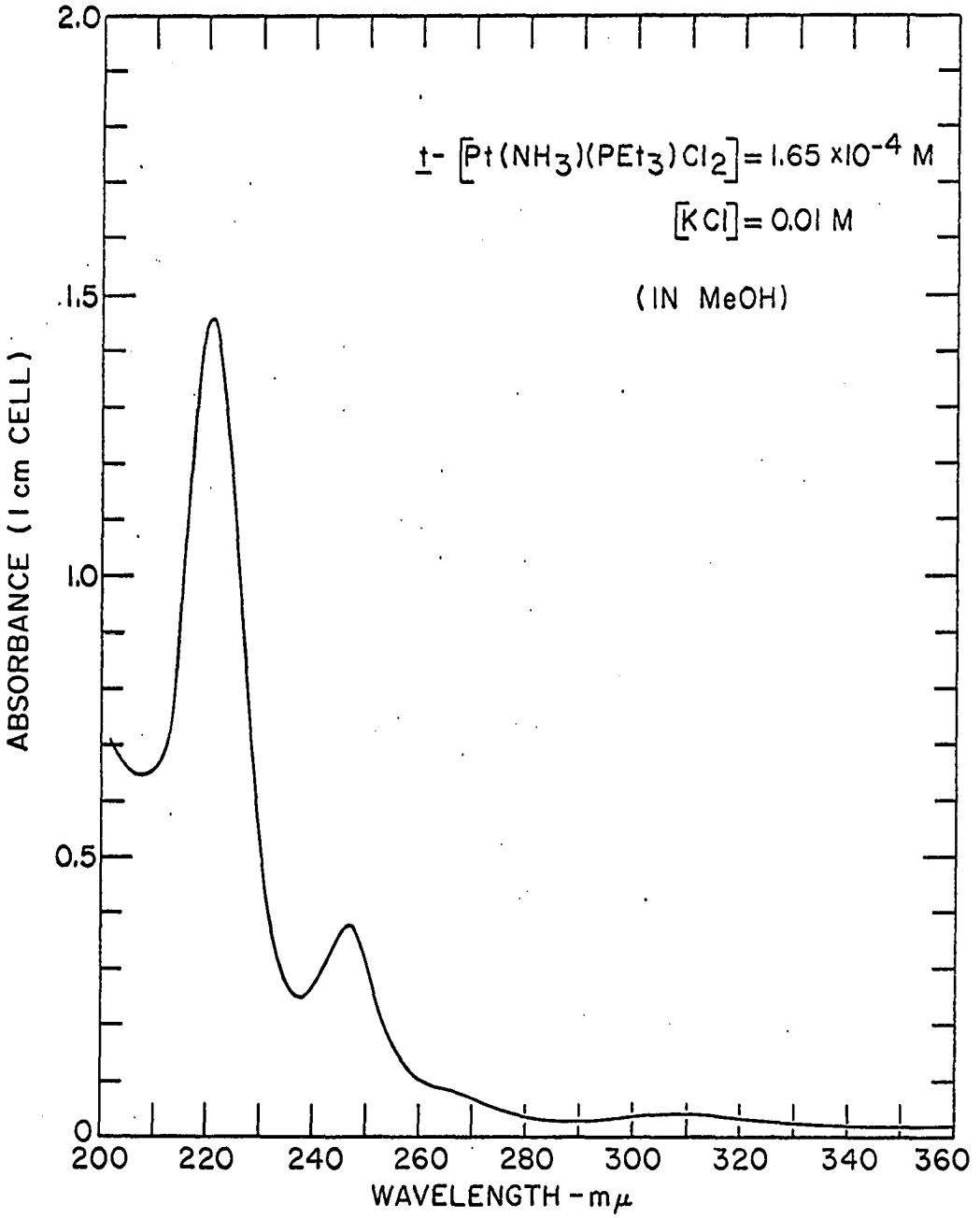

Figure 6. Ultraviolet spectrum of t-[Pt(PEt$_3$)(NH$_3$)Cl$_2$] in MeOH at 25°C. A 1 cm silica cell was used

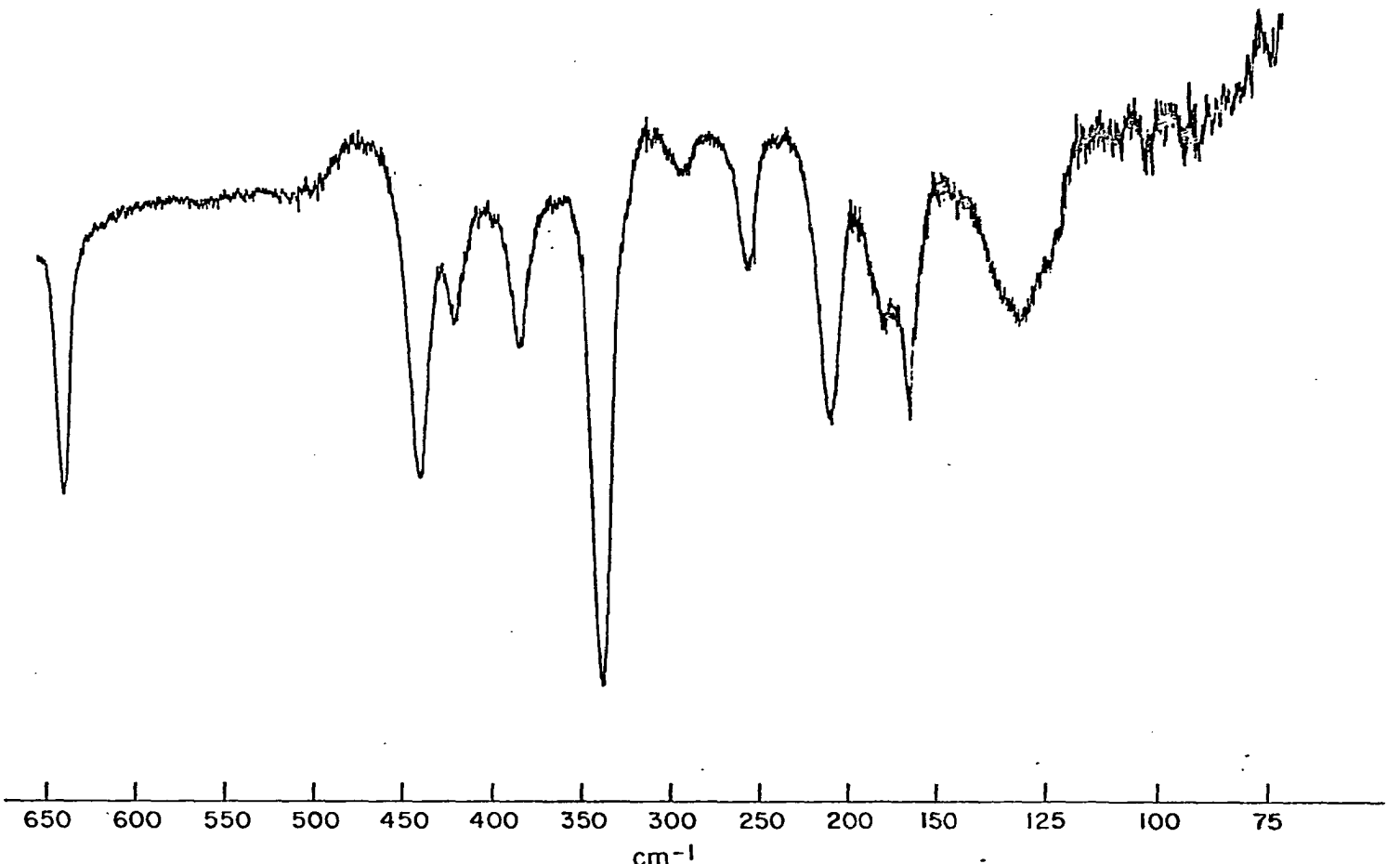

Figure 7a. Infrared spectrum of t-$[Pt(PEt_3)(NH_3)Cl_2]$ in the 70- 650 cm^{-1} region. The spectrum is of a nujol mull on a polyethlene sheet

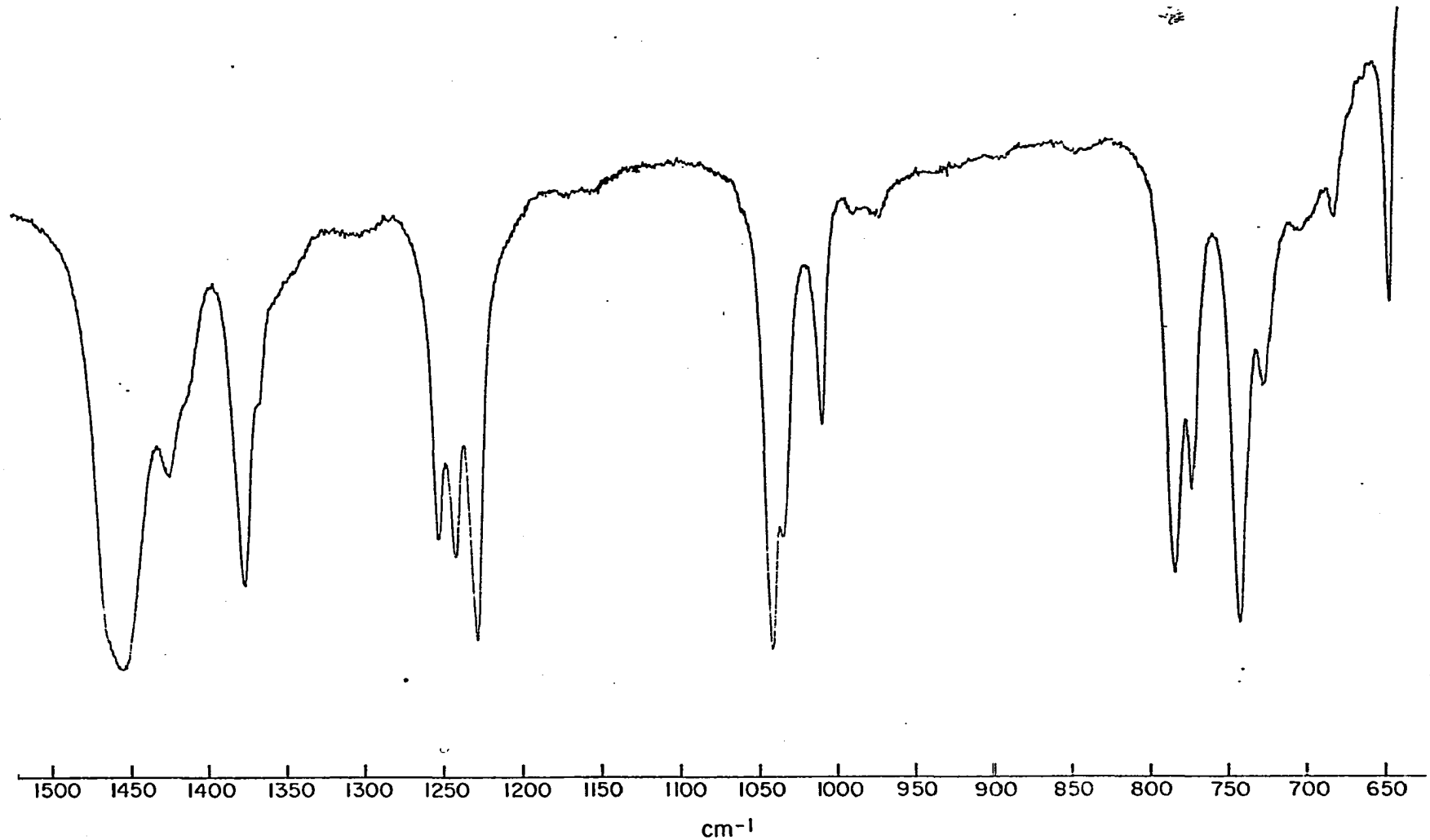

Figure 7b. Infrared spectrum of t-[$Pt(PEt_3)(NH_3)Cl_2$] in the 650- 1525 cm^{-1} region. The spectrum is of a nujol mull on a KBr window. The nujol bands are in the 1370 and 1460 cm^{-1} regions

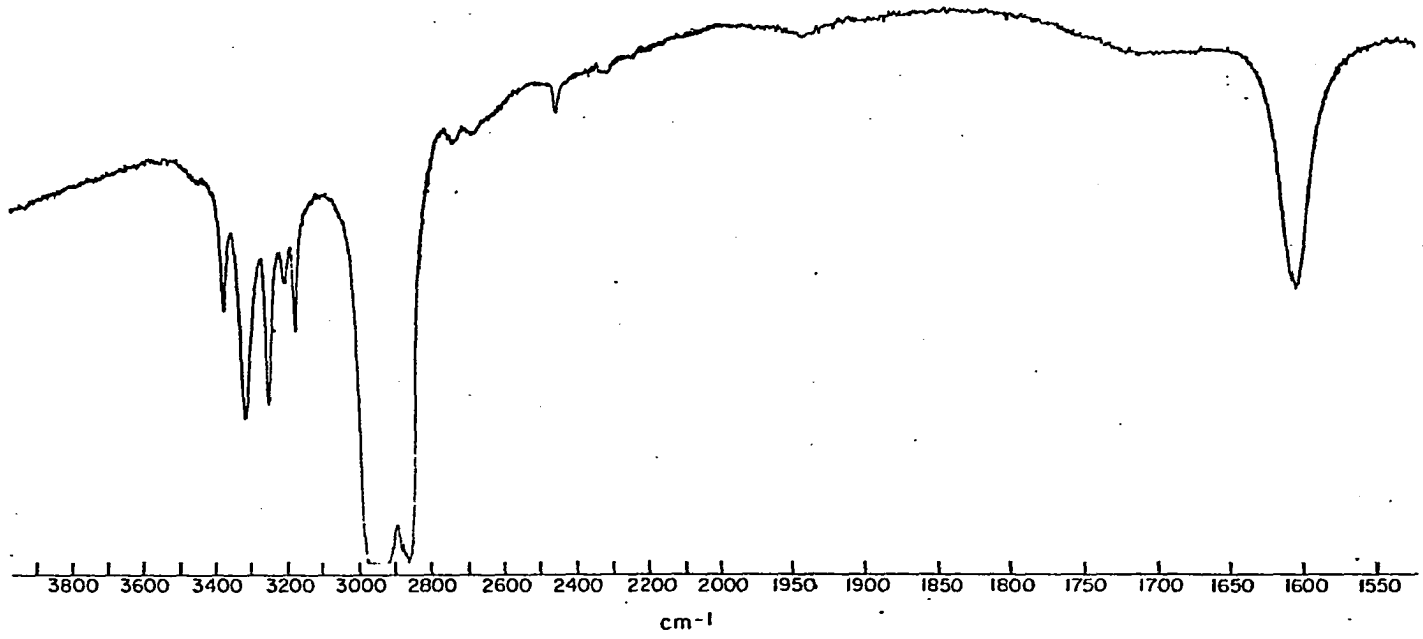

Figure 7c. Infrared spectrum of t-$[Pt(PEt_3)(NH_3)Cl_2]$ in the 1525- 3900 cm^{-1} region. The spectrum is of a nujol mull on a KBr window. The nujol bands are in the 2900 cm^{-1} region

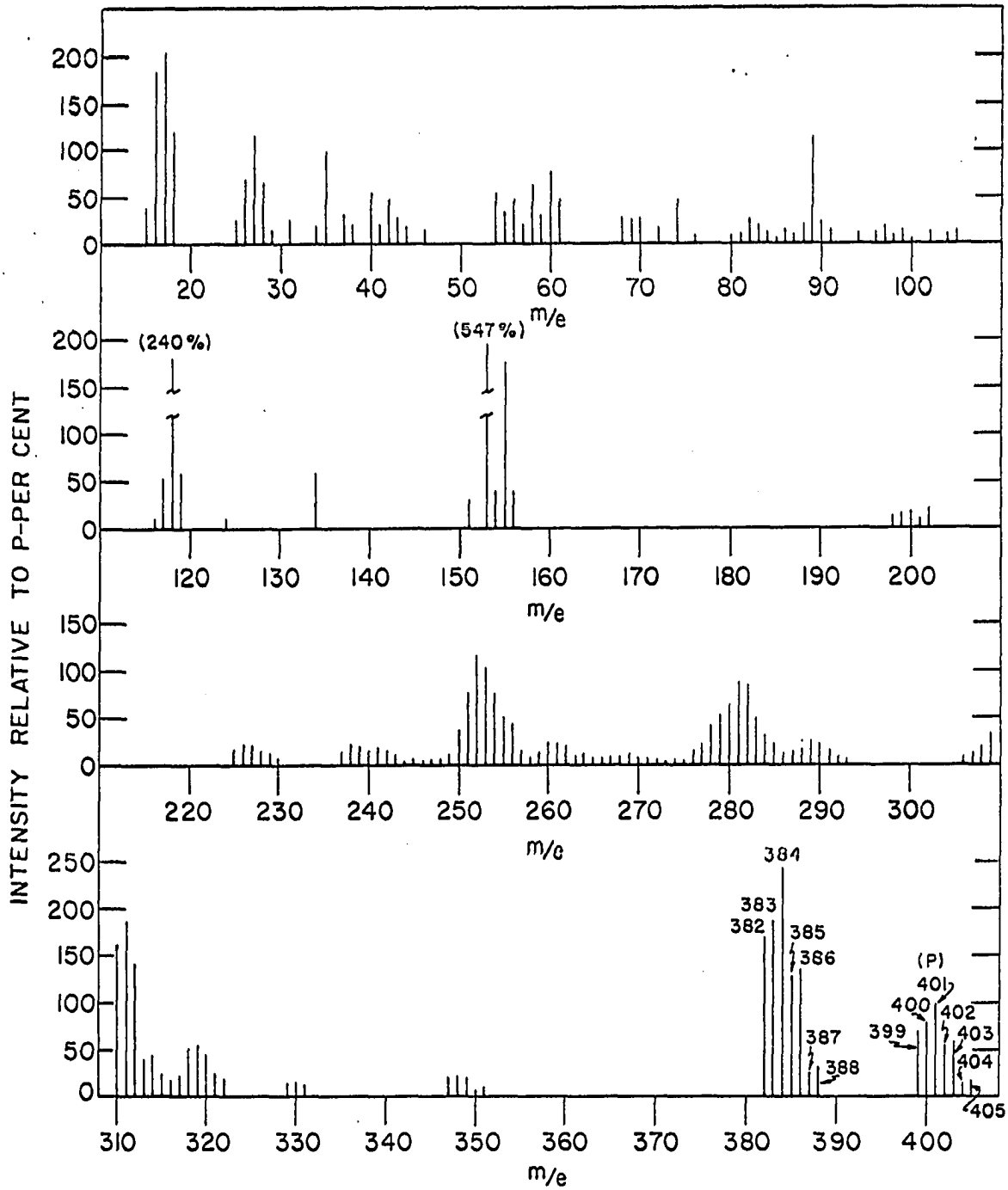

Figure 8. Mass spectrum of t-[Pt(PEt$_3$)(NH$_3$)Cl$_2$]. Intensities are relative to the intensity of the parent peak at 401

trans labilizing ability of the neutral ligand which was trans to the chloride, the strongly trans labilizing groups ordinarily caused greater lowering of ν(Pt-Cl) than the weakly trans labilizing groups. Location of ν(Pt-Cl) was simplified by the observation that they fell in the range 340- 269 cm^{-1} and were the most intense bands in the spectrum in that region.

A direct comparison of ν(Pt-Cl) in the study of Adams et al. (52) with the infrared spectrum of $[Pt(PEt_3)(NH_3)Cl]$ was not possible because of symmetry considerations. For t-$[Pt\ L_2Cl_2]$, where the two L ligands are the same, the molecule has a local D_{2h} symmetry, so that only the asymmetric ν(Pt-Cl) is infrared active. If this same complex now has two different L ligands, as in the case of the complex herein being considered, the local symmetry is reduced to C_{2v}, which has both the symmetric and asymetric ν(Pt-Cl) active in the infrared. For c-$[Pt\ L_2Cl_2]$ and c-$[Pt(PEt_3)(NH_3)Cl_2]$, the local symmetries are C_{2v}, and C_s respectively, both of which have the symmetric and asymmetric ν(Pt-Cl) infrared active. From these considerations, the assertion that direct comparison was impossible becomes rather obvious. Conclusions with respect to the structure are possible, however.

Adams et al. (52) did find that ν(Pt-Cl) was fairly independent of the ligand cis to it, but sensitive toward

the group trans to it. Also, they found that the cis complexes invariably had ν(Pt-Cl) shifted to lower frequencies, with both the symmetric and asymmetric stretches quite intense. In the spectrum shown in Figure 7, the most intense band in the far infrared is at 339.5 cm^{-1}. If the complex for which this is the spectrum was of trans configuration, although the symmetric stretch is also infrared active, the asymmetric stretch should fall in approximately the same position that it would if the molecule had D_{2h} symmetry. If the molecule were of cis configuration, however, ν(Pt-Cl) would be shifted to lower frequencies under the influence of the PEt_3 ligand, and two intense bands would be expected, corresponding to the symmetric and asymmetric modes.

Further evidence for assigning the configuration was derived from the N-H stretching modes, ν(N-H). For platinum(II) complexes, these bands fall in the 3000-3500 cm^{-1} region, and usually consist of just two immediately evident bands (84,85,86). A study of the spectrum for t-$[Pt(PPr_3^n)(NH_3)Cl_2]$ by Chatt, Duncanson, and Venanzi showed that in this complex ν(N-H) in the solid material consisted of five readily discernible bands at approximately 3363, 3300, 3243, 3210, and 3167 cm^{-1}, with relative intensities of 3300$\sim$3243>3167$\sim$3363>3210 cm^{-1} (84). The similarity between the complexes, t-$[Pt(PPr_3^n)(NH_3)(Cl_2]$ and

t-[Pt(PEt_3)(NH_3)Cl_2], and between their spectra in this region is patent.

The research of Goggin and Goodfellow (87) adds further confirmation to the foregoing analysis of ν(Pt-Cl), by enabling further assignment of the bands in the region of 250 to 450 cm^{-1}. From their work with a variety of triethylphosphine complexes of Pt(II), the following assignments become highly probable: 386 and 424 cm^{-1} bands are due to internal vibrations of PEt_3, the band at 291 cm^{-1} is probably due to the torsions of the methyl groups on the PEt_3, and the band at 254.5 cm^{-1} is probably the Cl-Pt-P in-plane deformation. The infrared spectrum of t-[Pt(PEt_3)$_2Cl_2$] which is included in the above research report bears a striking similarity in the 250-450 cm^{-1} region to the spectrum herein being analyzed, whereas the cis isomer's spectrum is quite dissimilar.

Finally, the only bands in the spectrum which can correspond to the deformation of the NH_3, to the NH_3 rocking, and to the Pt-N stretch fall at lower frequencies than those which have been found in platinum(II) complexes with a chloro ligand trans to the ammine (84,85,86). This behavior agrees with the presence of PEt_3 trans to the NH_3.

From all of the above considerations, it was concluded that the complex did indeed have a trans configuration. As a check of purity, the infrared spectrum was rerun after the

complex had been recrystallized twice more using a fractional extraction technique. The spectrum was found to be unchanged. Preliminary to obtaining the mass spectrum of this complex, a vacuum sublimation was performed on a small sample in order to test the volatility of the solid. It was found that the complex would begin to sublimate at approximately 110°C, but as the temperature was raised to 130°C, the sublimation ceased and the residue changed from a light yellow to an orange-yellow. Ultraviolet spectra of MeOH solutions of the sublimate and of the residue revealed that while the sublimate had the same spectrum as the starting material, the residue had the same spectrum as the dimeric t-$[Pt_2(PEt_3)_2Cl_4]$. Initial efforts at obtaining the mass spectrum encountered the same phenomenon. The temperature of the complex was raised too high, and only NH_3 was detected by the mass spectrometer. After some modification in handling technique, the mass spectrum given in Figure 8 was obtained.

Interpretation of the entire mass spectrum was rendered difficult by the presence of the hydrogens on PEt_3. A large proliferation of ions differing by one mass unit resulted, as can be seen in Figure 8. The identification of the complex on the basis of the mass spectrum was still a very real possibility, however, because of the natural isotopic distribution. On the basis of isotopic abundances of Pt^{192}

0.78%, Pt^{194} 32.8%, Pt^{195} 33.7%, Pt^{196} 25.4%, Pt^{198} 7.23%, Cl^{35} 75.4%, Cl^{37} 24.6%, C^{12} 98.89%, C^{13} 1.11%, H^{1} 100%, N^{14} 100%, P^{31} 100%, a mass of 401 was calculated to be the expected parent peak, P, for the mass spectrum of t-$[Pt(PEt_3)(NH_3)Cl_2]$, with the peaks about P having intensities of (P-2) 68.0%, (P-1) 73.0%, (P+1) 50.8%, (P+2) 58.5%, (P+3) 10.8%, (P+4) 15.6%, relative to the intensity of P. In the experimental mass spectrum shown in Figure 8, P was found to fall at 401 mass units with no ions of mass greater than the masses grouped around the parent peak being detected. The surprising aspect of the mass spectrum was that a more intense set of bands was centered at a position 17 mass units lower than P- the parent compound minus the NH_3 ligand. The PEt_3 has been reported as weakening the bond of the ligand trans to it. Coupled with the ordinary stability of the NH_3 bond to platinum(II), the mass spectrum appears to offer graphic evidence for the weakening of the bond trans to PEt_3, as well as giving added evidence for the configuration of the complex. The experimental relation of the satellite peaks to the parent were (P-2) 70.6%, (P-1) 77.7%, (P+1) 54.7%, (P+2) 59.8%, (P+3) 15%, (P+4) 17% of P. All of these values agreed to within 10% of the calculated values, except for the (P+3) band. The magnitude of the disagreement in this case, as well as all of the other disparities, was attributable to

difficulties in estimating the exact base line and the exact peak height in the mass spectrogram. If instead of the grouping around mass 401, the peaks around 384 were considered, the same calculated distribution should hold true, but now the experimental intensities were much greater and therefore the relative intensities were less affected by uncertainties in the base line and peak height. When this was done, the relative intensities were (P-2) 71.0%, (P-1) 77.2%, (P+1) 52.7%, (P+2) 57%, (P+3) 11.5%, (P+4) 13.8%. This was closer overall agreement with the calculated values than found for the higher region. From the mass spectrum it was concluded that the complex had the correct mass and isotopic distribution for $[Pt(PEt_3)(NH_3)Cl_2]$, and that the weakness of the Pt-N bond indicated that the NH_3 was <u>trans</u> to PEt_3. The presence of NH_3 in the complex was demonstrated by the detection of mass 17 ions in fairly high concentration, as was the presence of Cl demonstrated by the detection of high concentrations of ions of mass 35 and 37 in a ratio of 3:1. Interestingly, no free platinum was found in the 192-198 mass region, and only the slightest hints of any peaks were found in the half-mass region.

Efforts to obtain a melting point encountered the difficulty reported above. When the temperature reached 130°C, the complex began to melt, but rather than completely

melting, the complex decomposed and solidified as the dimer. It was thus impossible to measure a melting point as an added indication of the purity of the complex. From the spectral data it was concluded that the complex was pure, however.

Additional platinum complexes

Because of anomolies encountered during the experimentation - these will be discussed in the next chapter - three additional platinum complexes were prepared: trans-tetrachlorobis(triethylphosphine)platinum(IV), t-$[Pt(PEt_3)_2Cl_4]$; cis-dichlorobis(triethylphosphine)-platinum(II), c-$[Pt(PEt_3)_2Cl_2]$; and trans-chlorohydridobis-(triethylphosphine)platinum(II), t-$[Pt(PEt_3)_2(H)Cl]$.

The t-$[Pt(PEt_3)_2Cl_4]$ was prepared by bubbling chlorine gas for two minutes through a benzene solution of t-$[Pt(PEt_3)_2Cl_2]$ (88). The benzene and excess chlorine were immediately removed by evaporation under reduced pressure, and the residue was recrystallized five times from acetone. The resultant golden-yellow crystals of t-$[Pt(PEt_3)_2Cl_4]$ were slightly soluble in methanol, which proved to be no handicap, because only a very dilute solution of the complex was required.

The white c-$[Pt(PEt_3)_2Cl_2]$ was prepared as described above under the first method for preparing t-$[Pt(PEt_3)_2Cl_2]$. As was stated there, a mixture of the

two isomers was prepared, and the trans isomer was extracted by ether. The cis isomer which remained after this extraction was recrystallized from chloroform several times and finally from ethanol. This compound is quite soluble in methanol.

The final complex, t-$[Pt(PEt_3)_2(H)Cl]$, was prepared by the reaction of hyrazine with an aqueous suspension of c-$[Pt(PEt_3)_2Cl_2]$ (89). The mixture was heated on a steam bath for an hour, at which time a colorless oil formed. When the mixture was cooled, the oil solidified into nearly pure, white crystals of the product. The hydrido-complex was recrystallized several times from 2:1 aqueous methanol. It was very soluble in methanol. The ultraviolet spectra of all three of these complexes are given in Figure 9.

Other chemicals

All of the other chemicals used in this research were of analytical reagent grade, meeting the specifications of the American Chemical Society. The methanol used was of spectrochemical grade. The potassium chloride (KCl), sodium hydroxide (NaOH), methanol (MeOH), and potassium acid phthalate (KHP) were obtained from the Baker Chemical Company or the General Chemical Company. The anhydrous ammonia gas (NH_3) and anhydrous hydrogen chloride gas (HCl) were obtained from the Matheson Company. The petroleum ether was obtained from the Skelly Oil Company.

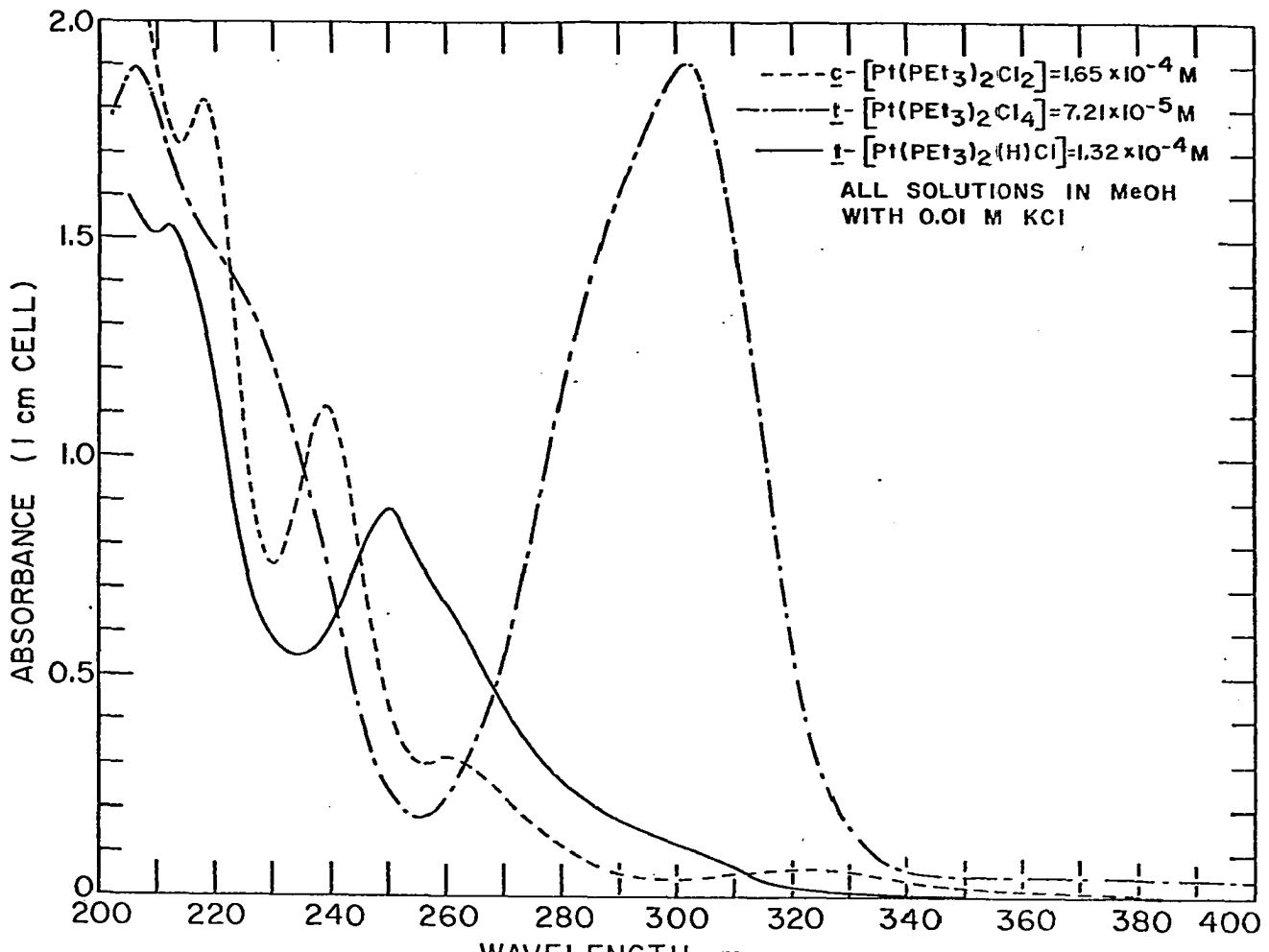

Figure 9. Ultraviolet spectra of c-$[Pt(PEt_3)_2Cl_2]$, t-$[Pt(PEt_3)_2Cl_4]$, and t-$[Pt(PEt_3)_2(H)Cl]$ in MeOH at 25°C. A 1 cm silica cell was used for each spectrum

The MeOH was checked in the conductivity cells and was found to have a specific conductivity at 25°C of 1.0×10^{-6} ohm^{-1} cm^{-1}. The International Critical Tables did not have unambiguous values for the specific conductivity, but the values given were in the region of 10^{-6} ohm^{-1} cm^{-1}.

Solutions

All of the reactions took place in MeOH solutions containing 0.01M KCl. The KCl served the dual purpose of suppressing the amount of solvolysis of the complex in the solution, and of bringing the resistance of the solution into the 1000-10000 ohm region. The 0.01 KCl solutions were prepared prior to the dissolution of the complex by weighing out the requisite amount of solid KCl and then dissolving this in a volumetric flask filled to the mark with MeOH at the temperature at which the experiments were to be conducted. All other solutions were made up by using these KCl solutions.

The volumes of the volumetric flasks were not corrected for glass expansion, because calculations showed that the change in flask volume in going from the calibration temperature of 20°C to the higher temperature fell within the range of uncertainty of the original calibration. The calculations showed that the maximum possible error in the volume introduced by not making the temperature correction would be less than 0.1%. The volumetric apparatus used in

these experiments met the class A specifications of the National Bureau of Standards.

The NH_3 solutions were prepared by bubbling anhydrous NH_3 into MeOH and then adding a weighed amount of KCl sufficient to make the solution 0.01M in KCl. Solutions for the individual experiments were made by diluting this stock NH_3 solution with 0.01M KCl-MeOH. The concentration of NH_3, in the individual experiments was determined by dissolving aliquots of the solutions in a large volume of water and then titrating the NH_3 with a standard sulfamic acid solution to a methyl red endpoint. The accuracy of the methyl red endpoint was checked in several trials using a pH meter with glass electrodes, and was found to correspond to the endpoint measured by the pH changes. The aliquots of the MeOH solutions of NH_3 were dissolved in large volumes of H_2O (approximately 25 ml of NH_3 solution in 300 ml of H_2O) in order to reduce the volatility of the NH_3 during the titrations.

The $\underline{t}$-$[Pt(PEt_3)_2Cl_2]$ and $\underline{t}$-$[Pt(PEt_3)(NH_3)Cl_2]$ reaction solutions were prepared by weighing the required amount of the solid compound into a dry volumetric flask and then filling to the mark with a NH_3 solution previously adjusted to the desired NH_3 concentration. The reaction was timed from the moment of introduction of the NH_3 solution into the flask. These two complexes dissolved rapidly

enough in MeOH that this procedure was possible. A few solutions were made up by first dissolving the complex in KCl solution, and then adding NH_3 solution to this, in order to test whether there were any aging effects in the solutions.

The t-$[Pt(NH_3)_2Cl_2]$ solutions were more difficult to prepare both because of the limited solubility of the complex in MeOH and because of the slow rate of dissolution. Perforce, therefore, all of the experiments involving t-$[Pt(NH_3)_2Cl_2]$ were started by adding an NH_3 solution to the already dissolved complex. Again, in the preparation of all the solutions, the NH_3 was present in a 0.01 M KCl solution, and any MeOH used for preparing solutions was itself 0.01M in KCl. Zero time for all the reactions was the moment of addition of NH_3 to the complex.

Instruments

The conductivity changes were measured with a type 716C capacitance bridge manufactured by the General Radio Company. The output from the bridge was first amplified by a Tektronix type 122 low level preamplifier. The preamplifier was powered by a solid state power supply designed and constructed at this laboratory. The signal from the preamplifier was fed into a General Radio type 1231-B amplifier and null detector. A type 1231-P5 interstage filter was incorporated into the

amplifier circuit. The balancing resistors were a General Radio type 1432 M decade resistance set (five decades of 1, 10, 100, 1k, and 10k ohm steps), supplemented with a type 510 decade (0.1 ohm steps). The accuracy of the decades were ± 0.15% for the 1 ohm/step decade, ± 0.05% for the 10, 100, 1k, and 10k ohm/step decades, and ± 0.5% for the 0.1 ohm/step decade. The balancing capacitors were General Radio type 980 M and 980N decades of 0.01 ± 1% μf/step and 0.001 ± 1% μf/step, respectively. The signal generator was a Hewlett-Packard 200 CD wide range oscillator. The arrangement of the bridge is shown in Figure 10. In actual experimental practice, the capacitors C_b and C_p were set at one value throughout the course of an experiment, and capacitor C_n was adjusted to bring the capacitance of the conductivity cell, C_x, into balance. The resistance of the solution in the conductivity cell, R_x, was measured with the resistors R_p.

The conductivity cells used for the kinetics studies were designed to conform to the recommendations of Jones and Bollinger (90), and were constructed at this laboratory. Three cells were used in the experimentation. The cell constants of the cells were determined using a 0.02 N KCl solution in H_2O. The cell constants of the three cells were 6.386, 6.382, and 6.323 cm^{-1}.

The conductivity cells were thermostated during ex-

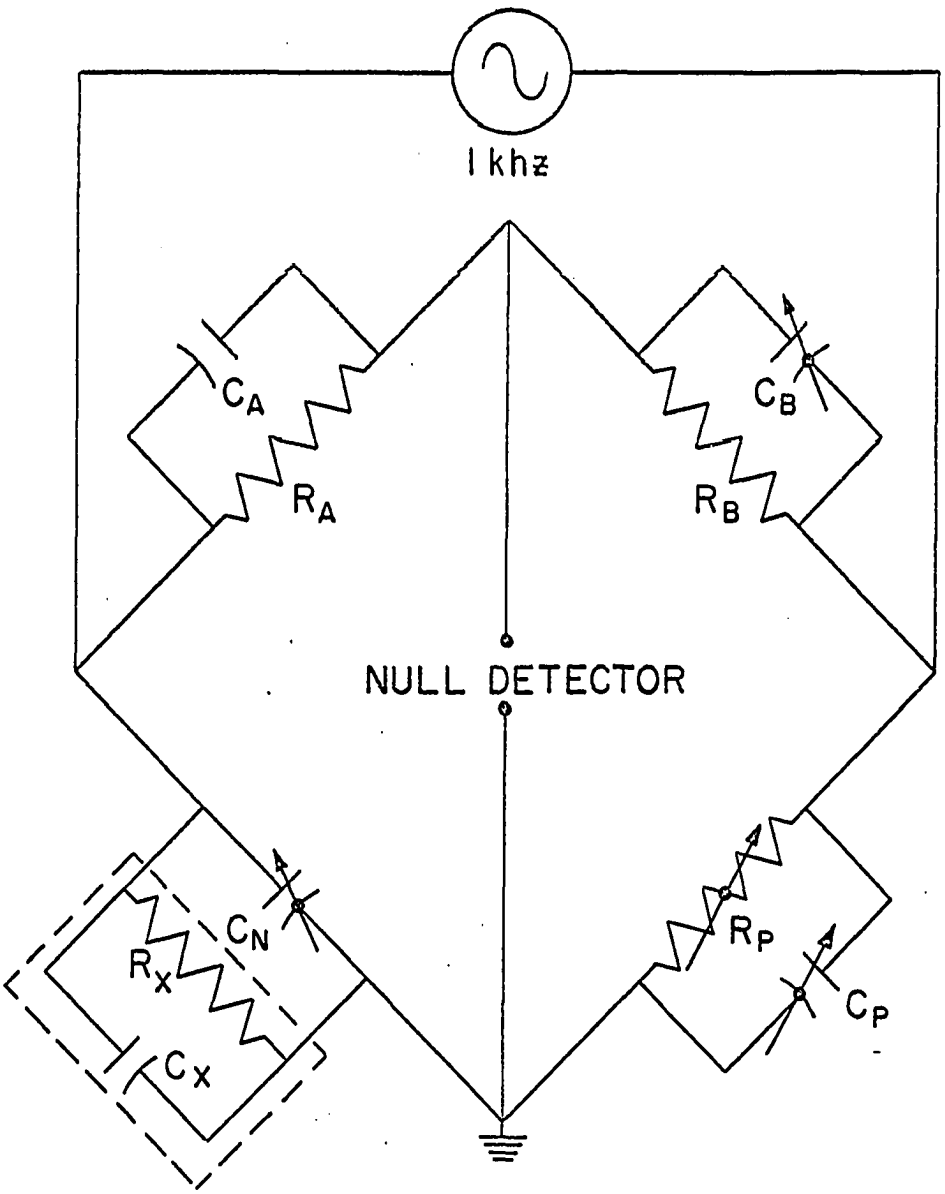

Figure 10. Schematic diagram of the conductance bridge. C_A, C_B, C_P, R_A, and R_B all remained fixed during any series of experimental measurements. C_N and R_P were varied to balance R_X and C_X of the conductance cell

perimental measurements, by partial immersion in a constant temperature bath. This bath used a modified Sargent S-84805 water bath for circulating, heating, and containing the thermostating liquid, a Fenwal Electronics type GB32P8 glass probe thermistor for temperature sensing, and a regulator designed and constructed at this laboratory for temperature control. The thermostating liquid was General Electric 10-C transformer oil. The temperature was maintained at $\pm$ 0.02°C of the set point by this bath.

The kinetics studies which used spectral changes were studied by means of a Cary Recording Spectrophotometer Model 14. The cell compartments of this instrument were thermostated by circulation of H_2O from a Bronwill Scientific constant temperature circulator, which maintained the temperature to $\pm$ 0.05°C.

A Corning Model 12 pH meter along with a Beckman 40498 glass electrode and 39170 fiber type calomel reference electrode were used for end-point determination in all titrations employing the pH meter.

Viscosities were measured using a Ubbelohde viscometer. The densities of the solutions were measured with a pycnometer.

The infrared spectra between 70 cm^{-1} and 800 cm^{-1} were obtained from a Beckman IR 11 Far Infrared Spectrometer using a mineral oil mull on a polyethylene sheet. The

spectrum between 600 cm^{-1} and 4000 cm^{-1} was obtained from a Beckman IR 7 prism grating spectrometer using a mineral oil mull on a KBr window.

The mass spectrum was made by direct insertion of the sample into the ion chamber of a modified General Electric Analytical Mass Spectrometer. The vapor pressure during the actual run was 10^{-6} torr. The ionizing beam was 70 volt electrons with a 10 μa current.

An IBM System 360/50 digital computer was used for all calculations involving a computer. Whenever computer generated plots were employed, the results of the calculations from the 360/50 were used by an IBM 1401 digital computer to generate the plots.

Procedures

Conductivity measurements

Before any kinetics experiments were performed, the behavior of the systems being studied was checked under the actual experimental conditions. The first observation was that no matter what MeOH solution was introduced into the conductivity cell, the resistance initially dropped at a very rapid rate, followed by a stabilization after approximately 15 minutes. This initial change was ascribed to temperature effects caused by the cooling of the MeOH solutions as they were being poured into the conductivity cell.

A similar phenomenon was previously observed at this laboratory when working with H_2O solutions, and was shown to be a temperature effect when a room temperature change caused a reversal to an initial rapid increase in resistance. This rapid initial change in resistance arises because of the sensitivity of the equivalent conductance to changes in temperature (for KCl in MeOH at 25°C, for example, a 1°C change in temperature causes a 1.4% change in the limiting equivalent conductance) and the relatively high resistances for the solutions (most solutions were in the 6000 ohm region). It was found that the duration of the initial change could be minimized by having all the solutions in the same thermostatic bath as the conductivity cell, and by having the conductivity cell contain a solution of composition similar to that of the solution which was to be introduced into it. In this way, the systems all started out at the same temperature, and the number of rinsings of the conductivity cell were kept to a minimum. As a general rule, the amount of manipulation of the solutions was kept to a minimum in order to keep the temperature factors minimal.

As for the individual solutions themselves, KCl in MeOH, NH_3 and KCl in MeOH, and solutions of the various complexes and KCl in MeOH all had the rapid initial change followed by a levelling off. While the resistance of these

solutions was relatively stable for short durations, over several hours time all of them would exhibit a slow drop in resistance. This very slow change was ascribed to a slow leaching of ions from the pyrex of the conductivity cells.

For all the conductivity measurements, the maximum potential experienced by the solutions in the conductance cells was 0.25 volts when the bridge was at maximum imbalance. To test whether the current flowing through the solutions caused any heating, a KCl-MeOH solution was introduced into the cell and was allowed to sit for a time without any current flowing through it, in order to stabilize. The measuring current was then turned on, and no change in the resistance of the solution was observed during 20 minutes while the current was continuously flowing through the solution. Despite this, however, the current to the cells was turned off between measurements.

The conductivity cells did not have platinized electrodes, but preliminary measurements at several different frequencies yielded the same solution conductivity, indicating no polarization problems in the cell. This being true, and because changes in conductivity were of interest rather than absolute conductivities, only one measuring frequency was required. The frequency used for all experimental measurements was 1 khz. In actual practice, the

conductivities obtained in this manner were extremely good, as was showed by the experimentally found equivalent conductance of KCl in MeOH from these measurements agreeing to within 1% with values found using far more elaborate equipment and techniques than those which were practical for kinetics studies.

There were three reasons for using unplatinized electrodes for the measurements. The great area of platinized electrodes could tend to cause concentration of the platinum complexes near the electrodes through absorption. Because the solutions were all of low complex concentration ($<10^{-3}$M) and the reaction rates were dependent upon the complex concentration, any such inhomogeneities in complex concentration would cause errors in the experimental results. Also, the large area of platinized electrodes could act as a catalyst in any reactions, particularly if there were concomitant increase in concentrations at the electrode. Finally, because a fairly volatile solvent was being used, unreproducibility of the electrode conditions through adsorption of atmospheric gases on the platinized electrodes could introduce difficulties into the experiments. Since the main reason for using platinized electrodes (reduction of polarization) did not appear to exist in the cells without platinization, polished platinum discs were used for the above stated reasons.

The signal generator was separated from the capacitance bridge and detector by 40 feet in order to minimize noise in the detector from this source.

The reaction solutions were prepared in the manner described above in the section on preparation of solutions. The reaction was timed from the moment of mixing the complex with NH_3 solution. As soon as the solutions were prepared, they were introduced with rinsing into the conductivity cell, and conductivity measurements were initiated. The reacting solutions were allowed to remain in the cells during the entire period of the reactions with NH_3 and, in most cases, for a fairly long time afterwards. Current was flowing through the solutions only when measurements were actually being made.

The mixing and storing of the solutions as well as the conductivity thermostating bath were all in a room lighted only by red light. This was done because research had indicated that the isomerization reactions of these complexes was induced by light in the ultraviolet region (13). The light sensitivity of the complexes required the measuring apparatus and the conductivity cells to be in separate rooms. The transmission lines necessitated by this separation of the measurer and the measured did not introduce any errors into the measurement of resistances using the 1 khz signal, as was shown by obtaining the same value for the resistance

of a carbon resistor measured at the bridge and at the end of the transmission line.

Spectrophotometric measurements

Although the major portion of the experimentation employed conductivity measurements, some spectrophotometric measurements were conducted in order to ascertain whether the conductometric method was influencing the reactions. The solutions were prepared and handled in approximately the same manner for the spectrophotometric measurements as they were for the conductivity measurements. The complete spectrum between 400 mμ and 240 mμ was recorded at regular time intervals after the reaction was started. The time during which the solutions were subjected to any wave length of light which could cause isomerization was minimized by using a fairly rapid scan rate (the isomerization reaction was reported to require several hours of constant exposure to light before appreciable isomerization occurred in the absence of any catalysts (13)).

The recorded time for the start of each scan, plus the known scan rate enabled the determination of the time after the inception of the reaction at which the absorption of the solution was recorded at any given wave length. Between scans, the solutions were removed from the spectrophotometer beam path, while still remaining in the thermo-

stated cell compartments of the spectrophotometer. Silica spectrophotometric cells were used for the measurements.

RESULTS

As was stated in the previous chapter, the primary measuring technique employed in the experimentation was measurement of changes in the conductance of the solutions. For each of the three complexes studied, the portions of the reactions which were significant for the measurements can be represented as follows:

$$A \longrightarrow \underset{[B]}{B^{+}} + Cl^{-}$$

$$B^{+} \longrightarrow \underset{[C]}{C^{2+}} + Cl^{-},$$

where [B] and [C] are the concentration of B^{+} and C^{2+} respectively, at time t. If the Cl^{-} produced by each reaction is considered separately, it will be seen that the increase in Cl^{-} concentration becomes equal to [B] + 2[C]. Using Kohlrausch's law, the ionic contribution to the conductance becomes,

$$\lambda_{B}[B] + \lambda_{Cl}[B] + 2\lambda_{C}[C] + 2\lambda_{Cl}[C] = \Lambda_{B}[B] + 2\Lambda_{C}[C], \tag{3.1}$$

where λ is the ionic equivalent conductance, Λ is the equivalent conductance, and the factor 2 preceding λ_{C} converts the concentration of C^{2+} from molarity to normality. The conductance L at any time t is given by the equation,

$$L(t) = \frac{1}{R(t)} = L(0) + \frac{1}{1000K}\left(\Lambda_{B}[B] + 2\Lambda_{C}[C]\right), \tag{3.2}$$

where R(t) is the resistance of the solution in the conductivity cell at time t, L(O) is the specific conductance of the solution at t = O, and k is the cell constant. The concentrations [B] and [C] in Equation 3.2 signify the time dependent concentrations of these species, with the exact time dependency of these quantities to be given when each complex is considered individually. The basic form of Equation 3.2 is derived from the definition for equivalent conductance and from electrolytes in solution behaving in the manner of resistors in parallel. Because Equation 3.2 was used as the basis for the analysis of the conductivity measurements, the features of it and Equation 3.1 will be treated more extensively in the following pages.

Tacit in Equation 3.2 is the constancy of the Λ's throughout the course of the reactions. In all of the experiments, the concentration of complex was less than 10^{-3}M, which meant that at most the Cl^- concentration would increase by 2×10^{-3}M, and 10^{-3}M of complex cations would be added to the solution. The vast majority of reactions had KCl concentration of 0.01M. Examination of Figure 11 shows that variations in Λ for 0.01M KCl solutions caused by changes in concentration of this magnitude are at most 2% (91,92). In the experimental solutions, however, this change would be piecemeal because the rate constant for the second ammonation reaction was approximately ten times

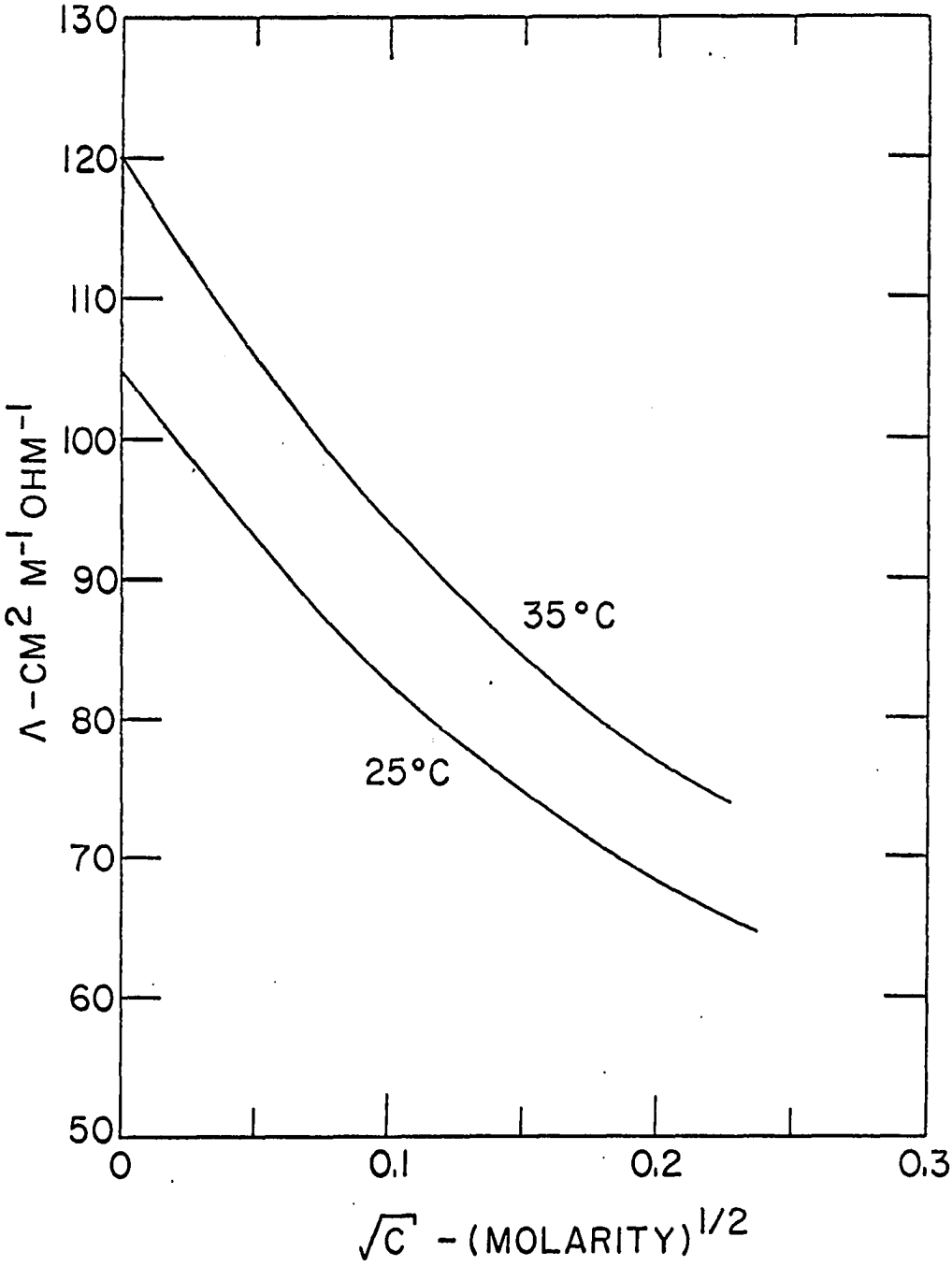

Figure 11. Equivalent conductance of KCl vs. the square root of the molarity at 25° and 35°C

smaller than that for the first ammonation reaction. Consequently, the ions from the first ammonation reaction would be completely added to the solution before the second ammonation reaction had proceeded appreciably, so that the changes in Λ would be small for each reaction.

With respect to the independent mobility of the ions, as incorporated into Equation 3.1, research on the transference numbers for KCl solutions in MeOH indicated that Kohlrausch's law of the independent migration of ions was valid for KCl at least up to the limit of the determination, 0.02M (93). In the present research, except for two solutions of 0.03M KCl, all of the experiments had KCl concentrations of 0.01M or less.

The picture is somewhat clouded by the NH_3 in solution, because of its interaction with the methanol, a solvent which has acid properties very similar to those of H_2O (94). In a measurement of the conductivity of an NH_3- MeOH solution at 35°C, the ionization constant for NH_3 in MeOH was estimated as 2×10^{-6}, from the assumption that the ions formed yield an equivalent conductance of approximately 100. On this basis, a 1M solution of NH_3 in MeOH would yield an additional concentration of ion of approximately 10^{-3}M. The resultant increase in ionic strength and lowering of equivalent conductances of the ions should have remained constant throughout the reaction, with regard to this

ionization, however, because all of the reactions had a minimum of sixtyfold excess of NH_3 present, which meant that the NH_3 concentration remained essentially constant.

Besides the acid-base reaction of NH_3 with MeOH, the changes in the physical properties of the solvent due to the dissolved NH_3 which does not undergo the acid-base reaction must be considered. Treatment of this problem is somewhat handicapped by the dearth of information, both experimental and theoretical, but a semi-quantitative description is possible. Germane to the consideration are the observations that both NH_3 and MeOH are neutral molecules, they are both capable of forming hydrogen bonds, the dielectric constants of the pure materials are not too disparate (at 20°C, ε=15.5 for NH_3 and 33.1 for MeOH (95)), and the highest mole fraction of NH_3 was 0.05 (most solutions had less than half this concentration of NH_3, however). The last of these observations would tend to indicate that any changes in the dielectric constant which did occur were probably slight. The neutral charge of the two materials would also lead to this conclusion. The hydrogen bonding characteristics of both species would undoubtedly have been of greatest importance in determining the final dielectric constant of the solution. Each of these compounds can act both as a donor and as a receiver in hydrogen bond formation, which, then coupled with size and geometrical considerations,

would tend to indicate that the NH_3 should have very little disruptive influence upon the structuring within the MeOH. A quantitative feel for the magnitude of any such changes is obtained by noting that a solution of 10% by weight of H_2O in MeOH has a measured dielectric constant of 35.7 at 25°C as compared to 31.5 for pure MeOH and 78.54 for pure H_2O at 25°C (the discrepancy between this value for the dielectric constant of pure MeOH and the previously cited value represents the difference between 20°C and 25°C) (96). The net result of these admittedly qualitative considerations (but necessarily so, because of the state of the art) is that the hydrogen bonding consideration also indicates little change in the dielectric constant of the MeOH upon introducing NH_3 at the concentration levels of interest here. An empirical formula which has been shown to give good approximations for dielectric constants of dilute solutions is (97),

$$D = w_1 D_1 + w_2 D_2,$$

where w_1 is the weight fraction and D_1 the dielectric constant for pure component 1, and D is the dielectric constant for the solution. When this equation is applied to the 10% by weight of H_2O in MeOH above, the calculated value of D is 36.2 which is 1.4% off from the experimental value of 35.7, even though the concentration of H_2O is slightly

beyond the claimed range of validity for the equation. Applying this equation to the most concentrated NH_3-MeOH solution encountered in this experimentation (3% by weight of NH_3), at 20°C the calculated value of the dielectric constant for the solution is 32.6, compared to 33.1 for pure MeOH.

Another property of the solutions which influence variations in the equivalent conductance is the viscosity. In order to ascertain if any large changes in viscosity would result from addition of NH_3 to the KCl-MeOH solutions, the viscosity of a MeOH solution containing 2.6 M NH_3 and 0.01 M KCl was compared with that of a MeOH solution containing 0.01M KCl alone. It was found that the viscosity of the solution containing NH_3 was 0.8% lower than that of the solution containing no NH_3. The highest NH_3 concentration used in any of the experiments was 1.31M, and the vast majority of the experiments had NH_3 concentration less than 0.65M, so it seems safe to say that changes in equivalent conductance due to viscosity changes caused by the dissolved NH_3 were negligible.

Still another factor in solutions which can cause changes in the dielectric constant is the ions which are present. The ions in the solution have made the measurement of the dielectric properties of ionic solutions extremely difficult. The advent of wave guide techniques

has helped to remedy this situation, however, and some pertinent comments can be made with respect to the MeOH solutions. A study of the dielectric constant of aqueous solutions containing electrolytes of various valence types indicated that the dielectric constant of the solution could be represented up to 2N by the equation (98),

$$\varepsilon = \varepsilon_w + 2\bar{\delta}c,$$

where ε is the dielectric constant of the solution, ε_w is the dielectric constant of pure H_2O, $2\bar{\delta}$ is a molar depression constant which is approximately additive for the separate ions ($2\bar{\delta} = \delta^+ + \delta^-$ for a 1:1 electrolyte, $2\bar{\delta} = \delta^+ + 2\delta^-$ for a 1:2 electrolyte, etc.), and c is the molarity of the solute. The values for $\bar{\delta}$ ranged from -5 for KCl and RbCl, up to -15 for $MgCl_2$, -14 for $BaCl_2$, and -22 for $LaCl_3$ (the highest value reported). With the assumption that MeOH solutions can be represented by the same form of equation, and that the $\bar{\delta}$ values for the MeOH solutions do not diverge greatly from the H_2O values, at the highest ion concentrations used in the present experimentation the dielectric constant should be changed by less than 1%.

The above concern for the dielectric constant of the solvent arises because of the influence that changes in dielectric constant has on both ionic association and the equivalent conductance. In the Bjerrum equation and the

more recent Fuoss and Krauss equation for ion pair formation (99,100), the association quotient for ion pairs is a function of $(|z_1 z_2|)e^2/(aDkT)$, where z_1 and z_2 are the charges on the two ions forming the pair, e is the charge on the electron, a is the distance between centers of the two ions forming the pair, D is the dielectric constant of the medium, k is the Boltzmann constant, and T is the absolute temperature. Further, in the Onsager treatment of equivalent conductance, both the electrophoretic effect and the relaxation effect are found to be functions of $1/DT$. Because the NH_3 concentration in the experimental solutions had values ranging from 0.04M to 1.3 M, the effect of the NH_3 upon the dielectric constant has to be considered, particularly in view of the use of Equation 3.2 as the basis for the analysis of the data.

The effect of ionic association on the electrical properties of the solution is not apparent in Equation 3.2, but becomes more so if the Λ's in that equation are stated in a different form. For any electrolyte which is incompletely dissociated in solution, the degree of dissociation, α, is defined as $\alpha=\Lambda/\Lambda^*$, where Λ is the experimental equivalent conductance, and Λ^* is the hypothetical equivalent conductance for the electrolyte at that concentration if it behaved as a strong electrolyte. Ordinarily Λ^* is calculated from the equivalent conductances of strong elec-

trolytes at the concentration of interest. For example, the value of Λ^* for acetic acid (HAc) is calculated from the equivalent conductances of HCl, NaCl, and NaAc solutions, all of which are strong electrolytes, at the concentration of the HAc solution: $\Lambda^*_{HAc} = \Lambda_{HCl} - \Lambda_{NaCl} + \Lambda_{NaAc}$. The degree of dissociation of HAc can then be calculated with the formula $\alpha = \Lambda/\Lambda^*$. This latter formula can be rearranged to give $\Lambda = \alpha\Lambda^*$, which is the form of interest in the present context. It should be noted that this treatment is equally valid for ion pairs as well as for undissociated molecules.

The association quotient for the equilibrium between the free ions and the ion pairs is defined as,

$$K_A = \frac{[p_i, n_i]}{[p_i][n_i]} ,$$

where $[p_i, n_i]$ is the concentration of the ion pairs for complex i, and $[p_i]$ and $[n_i]$ are the concentrations of the unassociated positive and negative ions from the particular complex of interest. Under conditions in which the negative ion is present in a large, relatively constant excess concentration, b, this equation assumes the form,

$$K_A = \frac{1}{b} \frac{[p_i, n_i]}{[p_i]} ,$$

which indicates that at any time the ratio of the concentration of ion pairs to that of free positive ions is a con-

stant under the stated conditions. The only provisos are the establishment of rapid equilibrium, b remaining constant, and the quotient, K_A, not changing during the measurements for any experiment. The low range of concentration changes during the reaction, along with the large excesses of the substituents of the solutions other than the complex, assure that K_A will remain static for any experiment (it would be noted that all of the above remarks rest upon an unstated constancy of temperature, a condition which was averred in the previous chapter). The equation for K_A stated in terms of the degree of dissociation of ion pairs, α_i, is,

$$K_A = \frac{1}{b} \frac{1-\alpha_i}{\alpha_i}$$

which can be rearranged to give,

$$\alpha_i = \frac{1}{K_A b + 1} \qquad (3.3)$$

Thus, under the conditions stated, the degree of dissociation of the ion pairs of the charged complex ions will be constant.

When ion pairs are formed, however, there is a change in the conductance properties. The ion pairs formed by the first ammonation product will be neutral because they involve a 1:1 electrolyte. These ion pairs can therefore be handled by introducing the expression $\Lambda^*_B \alpha_B [B]$ into

Equation 3.2 in place of $\Lambda_B[B]$. An idea of the order of magnitude of α_B could be obtained from values of the association constant for KCl in MeOH at 25°C. Unfortunately, there is not agreement on this constant, but it is reasonable to say that the association constant probably lies between 1.202 (92) and 14.7 (91).

The ion pairs formed by the doubly charged complex ion resulting from the second ammonation reaction are not neutral, so their conductance contribution must be taken into account. Thus, the term $2\Lambda_C[C]$ in Equation 3.2 assumes the form $2\Lambda_C^*\alpha_C[C] + \Lambda_p(1-\alpha_C)[C]$, where Λ_p is the equivalent conductance of the ion pairs. Introduction of the terms accounting for ion association into Equation 3.2 yields,

$$L(t)=L(0)+\frac{1}{1000k}(\Lambda_B^*\alpha_B[B]+(2\Lambda_C^*\alpha_C+\Lambda_p(1-\alpha_C))[C]). \quad (3.4)$$

Examination of this equation reveals that it can be treated in the same form as Equation 3.2 if the Λ's and α's remain constant during the individual reactions.

In all of the previous discussion, the behavior of KCl under various conditions was presented as a model for the expected behavior of the products of the ammonation reactions. While the Cl^- ions formed by the reactions will obviously fit into such a comparison quite readily, the situation with regard to the complex ions requires further

elucidation. In general, the complex ions were larger than the K^+ ions, and also larger than the solvent molecules, which would tend to decrease their migration rate through the solution because of viscosity considerations (101). In addition, these ions would have less interaction with the solvent than K^+ because of their larger size. Both of these factors would mean that their would be a greater tendency toward ion pair formation for the complex ions than for K^+. For the product of the first ammonation reaction, this would be opposed by a larger effective volume for the distribution of charge. The product of the second ammonation, being doubly charged, would have a greater tendency to form ion pairs because of electrostatic considerations. Other than the differences in ionic association, and lower equivalent conductances than K^+, the principal consideration herein is whether the values for Λ and α remained approximately constant throughout the reactions. In the case of KCl, this was shown by the preceding treatment to be a good approximation. While there are obvious differences between K^+ and the complex ions, experimental evidence indicated that such a parallel in behavior between the K^+ and complex ions existed as will be seen from the following section.

Besides acting as a medium for the treatment of the complex ion behavior in the solutions, the previous dis-

cussions involving KCl had the ancillary function of showing that the quantity L(0) in Equation 3.2 was constant throughout the course of the ammonation reactions.

Trans-dichloroammine(triethylphosphine)platinum(II)

The experimental data for the ammonation reactions of t-$[Pt(PEt_3)(NH_3)Cl_2]$ will be treated first because it exhibits characteristics found in the other two systems, while not involving the complexities found in the t-$[Pt(PEt_3)_2Cl_2]$ system, nor the limitations of the t-$[Pt(NH_3)_2Cl_2]$ system. The rate constants for the kinetic paths in the t-$[Pt(PEt_3)(NH_3)Cl_2]$ ammonation were ascertained by using a computer generated plot of a calculated L(t) *vs.* t for each experiment, and ocmparing this plot with a superimposed plot of the experimental values for L(t) *vs.* t. The ammonation reactions of t-$[Pt(PEt_3)(NH_3)Cl_2]$ were found to have the kinetic paths,

$$\underset{[A]_0-[B]-[C]}{t\text{-}[Pt(PEt_3)(NH_3)Cl_2]}+NH_3 \xrightarrow{k_1} \underset{[B]}{c\text{-}[Pt(PEt_3)(NH_3)_2Cl]^+}+Cl^- \qquad (3.5)$$

$$c\text{-}[Pt(PEt_3)(NH_3)_2Cl]^+ + NH_3 \xrightarrow{k_2} \underset{[C]}{[Pt(PEt_3)(NH_3)_3]^{2+}}+Cl^-, \qquad (3.6)$$

where $[A]_0$ is the concentration at t=0 and $[A]_0-[B]-[C]$ is the concentration at t for t-$[Pt(PEt_3)(NH_3)Cl_2]$, [B] and [C] are the concentrations at time t for the indicated complexes

(these two had zero concentration at t=0), and k_i is the rate constant for the indicated reaction. Inasmuch as the starting material is a nonelectrolyte, only the product formation is significant for conductivity measurement. The differential equations to describe the rate were taken as:

$$\frac{d[B]}{dt} = k_1[NH_3]([A]_0 - [B] - [C]) - k_2[NH_3][B]$$

$$\frac{d[C]}{dt} = k_2[NH_3][B].$$

These equations were used along with the condition that $[A] + [B] + [C] = [A]_0$. In the rate equations the concentration of the NH_3 can be written in terms of its initial concentration, $[NH_3]_0$, and its change with time in terms of the complex concentrations,

$$[NH_3] = [NH_3]_0 - [B] - 2[C],$$

where the factor 2 arises because two NH_3 are used and two Cl^- released for the formation of each $[Pt(PEt_3)(NH_3)_3]^{2+}$. Introduction of this expression into the two differential equations of interest yields,

$$d[B]/dt = k_1([NH_3]_0-[B]-2[C])([A]_0-[B]-[C]) - k_2([NH_3]_0-[B]-2[C])[B] \qquad (3.7)$$

$$d[C]/dt = k_2([NH_3]_0-[B]-2[C])[B] \qquad (3.8)$$

Although the reactions were conducted under pseudo-first-order conditions (i.e. a large excess of NH_3), because a computerized treatment was employed, changes in the NH_3 concentration with time were included for completeness. Equations 3.7 and 3.8 were part of the arithmetic statement functions in a Runge-Kutta numerical integration program. The equations used in the computer program were more complete than Equations 3.7 and 3.8, having the provision to handle successive reversible reactions. By introducing rate constants equal to zero for the reverse reactions, however, the functions in the computer program reduce to Equations 3.7 and 3.8. A listing of the full computer program is given in Appendix B. The values for [B] and [C] which resulted at each time, t, were used by the computer to calculate values for L(t) by means of Equation 3.2. Then these calculated values for L(t) were plotted as a function of t, and the experimentally determined values of L(t) were superimposed on this plot for comparison. Closeness of fit between the two sets of L(t) values was the criterion for the validity of the constants used in the equations.

It can be seen from Equation 3.2 that besides the values for [B] and [C] obtained from the numerical integration of Equations 3.7 and 3.8 values for L(0), Λ_B, Λ_C, and k had to be supplied for the computer calculation of L(t). The cell

constant, k, was measured experimentally using an aqueous KCl solution. The initial value for the specific conductance, L(O), was obtained by extrapolation back to t=0 on the plot of experimental values of L(t) as a function of t. The extrapolation was necessitated by the initial sharp rise in conductance which was described in the preceeding chapter. Values of Λ_B and Λ_C were initially estimated using the equivalent conductance formula of Amis which related equivalent conductance in one solvent system to that in another solvent system (102),

$$\frac{\Lambda_0 \eta \mu}{D} = \text{constant},$$

where η is the viscosity of the pure solvent, μ is the dipole moment calculated from the mole fraction and dipole moments of the pure solvent and solute by the expression ($\mu=N_1\mu_1 + N_2\mu_2$), and D is the dielectric constant of the pure solvent. Basolo et al. (26) determined the molar conductance for t-$[Pt(o\text{-}tolyl)(py)(PEt_3)_2]NO_3$ in ethanol at 25°C (py is pyridine) and this value, 34 cm^2 $mole^{-1}$ Ohm^{-1}, along with the appropriate value of η, μ and D for EtOH at 25°C and MeOH at 35°C was used in the Amis equation to get a first approximation for Λ_B and Λ_C. The value measured by Basolo et al. was in a very dilute solution with no added electrolyte, so a further adjustment up to the concentrations of interests here had to be made. The approximate

value for Λ_B so obtained, 79 $cm^2 mole^{-1}$ Ohm^{-1}, should still be slightly higher than the value for the present complex, because the ionic equivalent conductance of Cl^- is lower than that of NO_3^- in alcohol solutions. While the Amis equation yields only an approximate value for the equivalent conductance in going from one solvent to another, the value so obtained can be useful as a gauge of the amount of association occurring in the solutions. The measured value of Basolo et al. was for a very dilute solution, so that there should have been no ion pair formation. The closeness of approach of the values found in this experimentation to the value extrapolated from the research of Basolo et al. will thus be an indicator of association. The values of Λ_B and Λ_C were then adjusted in the computer input until a good fit of the calculated and experimental values of L(t) was obtained. This circuitous manner of obtaining these constants was necessitated by an inability to synthesize either c-$[Pt(PEt_3)(NH_3)_2Cl]Cl$ or $[Pt(PEt_3)(NH_3)_3]Cl_2$ to measure their equivalent conductances.

The initial values for k_1 and k_2 were obtained by resolving a plot of $\log(L(\infty)-L(t))$ vs. t into two components corresponding to the first and second ammonation reactions. The rationale for this procedure is found in the pseudo-first-order approximation to the differential equations which represent the rates of change in concentration during

the reactions. Making the substitution $k_i' = k_i[NH_3]$, where k_i' is taken to be constant throughout the course of the reaction, the differential equations become,

$$\frac{d[A]}{dt} = -k_i'[A]$$

$$\frac{d[B]}{dt} = k_1'[A] - k_2'[B]$$

$$\frac{d[C]}{dt} = k_2'[B],$$

where [A] is the concentration of t-$[Pt(PEt_3)(NH_3)Cl_2]$ at time t, and [B] and [C] are the concentrations at time t of c-$[Pt(PEt_3)(NH_3)_2Cl]^+$ and $[Pt(PEt_3)(NH_3)_3]^{2+}$, respectively. These differential equations are integrated using the initial conditions that $[A]=[A]_0$, $[B]=[C]=0$, at $t=0$, to yield,

$$[A] = [A]_0 \exp(-k_1't)$$

$$[B] = \frac{k_1'[A]_0}{k_2'-k_1'} \left(\exp(-k_1't) - \exp(-k_2't)\right)$$

$$[C] = \frac{[A]_0}{k_2'-k_1'} \left(k_1' \exp(-k_2't) - k_2' \exp(-k_1't)\right) + [A]_0$$

At $t=\infty$, these equations reduce to $[A](\infty)=[B](\infty)=0$, and $[C](\infty)=[A]_0$. Substitution of these values into the appropriate places in Equation 3.2 and subtraction of L(t) from L(∞) yields,

$$L(\infty)-L(t) = \frac{[A]_0}{1000k\ (k_2'-k_1')}\ ((2\Lambda_C k_2'-\Lambda_B k_1')\ \exp(-k_1't)$$

$$-(2\Lambda_C k_1'-\Lambda_B k_1')\ \exp(-k_2't)). \qquad (3.9)$$

Equation 3.9 is the equation which was tactitly being employed in the resolution of the plot of log $(L(\infty)-L(t))$ *vs.* t into two components. The slopes of the lines which resulted from the resolution were the pseudo-first-order rate constants, k_1' and k_2'. These were entered on two separate graphs of k_i' as a function of $[NH_3]$, one plot for k_1' *vs.* $[NH_3]$, and one for k_2' *vs.* $[NH_3]$. When the values for all the experiments had been entered on these graphs, the slopes of straight lines which could be passed through the points were taken as initial values of k_1 and k_2. The values for k_1, and k_2 in Equation 3.7 and 3.8 were then adjusted in the computer input along with the values of Λ_B and Λ_C until a subjective fit was obtained to the experimental L(t) values using the same values of k_1, k_2, and Λ_B for all the experiments. Λ_C was treated as indicated below.

During the process of fitting the calculated conductance curve to the experimental values, it was found that Λ_C was dependent upon the initial complex concentration. This observation resulted because of an inability to obtain a good fit during the course of the second ammonation reaction unless the value for Λ_C was decreased somewhat when the

initial complex concentration was increased. No such variation was found for the first ammonation reaction (again, the tenfold difference in the rate constants for the first and second ammonation reactions allowed the assignment of conductance changes as arising from either the first or second ammonation reaction). The reason for this variation in Λ_C upon changing the initial complex concentration is found in the approximation used to obtain Equation 3.3. The Cl^- concentration in all of the present experiments was at least ten times larger than the highest complex concentration, so that considering the Cl^- concentration constant seemed to be a good approximation. The Cl^- and complex concentrations were close enough, however, that the approximation of the degree of dissociation, α, remaining constant throughout the reaction would fail if the association quotient, K_A, was large. This is exactly what happened for the product of the second ammonation reaction. The association quotient for the product of the first ammonation reaction was sufficiently low that the approximation held good there, so that Λ_B did not have to be changed when the initial complex concentration was changed. That the degree of dissociation for the singly charged complex was high can be seen by comparing the value of 67.9 $cm^2N^{-1}Ohm^{-1}$ for Λ_B at 35°C given in Table 2 below with the value of 79 $cm^2N^{-1}Ohm^{-1}$ estimated above from the experimental value of Basolo

et al.

The failure of Equation 3.3 when Λ_C for solutions of different initial complex concentration were compared did not mean that the approximation was also invalid during the course of the individual reactions, however. The reasons for this were that the Cl^- from the first reaction was completely added before the second reaction had proceeded appreciably, and that the higher amount of association for the second ammonation product reduced the amount of free Cl^- added by the second reaction upon going to completion. Therefore, the amount of change in the Cl^- concentration during the second ammonation reaction would be small enough that Λ_C would remain approximately constant during the entire second ammonation reaction. As a test of the validity of this approximation the relation involving the degree of dissociation, α_C, was written in a form which included variations in the Cl^- concentration with time. If $[Cl^-]=[Cl^-]_0 + [B] + [C] + \alpha_C[C]$, where $[B] + [C]$ is the Cl^- added by the first ammonation reaction, $\alpha_C[C]$ is the free Cl^- added by the second ammonation reaction, and $[Cl^-]_0$ is the concentration of the KCl, then Equation 3.3 becomes,

$$\alpha_C = \frac{1}{K_A[Cl^-] + 1} \qquad (3.10)$$

The denominator of this equation has been written as a

function of α_C in order to simplify the mathematical treatment. This equation was used in conjunction with the Runge-Kutta numerical integration program. For the α_C in the denominator of the equation, the value calculated during the previous integration interval was used. This did not introduce an appreciable error because the intervals of integration were so small that the Cl^- increments were always less than 3×10^{-6} moles/ℓ as compared to the initial Cl^- concentration of 0.01M. Since [B]=[C]=0 initially, the initial value for α_C was simply given by Equation 3.3,

$$\alpha_C = \frac{1}{K_A[Cl^-]_0 + 1} \quad .$$

As the Runge-Kutta program calculated [B] and [C], these quantities were used to calculate α_C for two values of the association quotient, K_A=10 and K_A=200. For a solution with the highest complex concentration used in the present experiments and the values at 35°C for k_1 and k_2 given in Table 2, α_C was found to have changed by less than 2.5% during the final 90% of the second ammonation reaction for K_A=200.

For K_A=10, α_C had changed by less than 1% when the first ammonation reaction reached 95% of completion, which can be interpreted as a verification that α_B remains essentially constant during the first ammonation reaction, because

Equation 3.10 would also describe the change in α_B with changes in the Cl^- concentration.

Two other exceptions to the fitting procedure were an experiment which had KCl=0.03M, and an experiment which had 2% by volume (1.3% by weight) of H_2O added to the solution. In both of these experiments, the values for k_1, and k_2 were the same as for all the other experiments, but changes in the value of Λ_B and/or Λ_C were required. The reasons for using different values for Λ_B and Λ_C in the high $[Cl^-]$, experiment are patent, but the change in Λ_C for the experiment with H_2O added requires some elaboration.

The reason for conducting an experiment with H_2O added was the need to determine what effect any H_2O in the solutions might have on the rate constants. Since no special effort was made to remove the traces of H_2O present in the spectrochemical grade MeOH (less than 0.02% by weight), and because even if so treated, atmospheric H_2O can be absorbed during the manipulation of the solutions, the effects of H_2O were studied by adding a quantity of H_2O far exceeding any that might be present from other sources. It was found that although there was no apparent change in the rates of the reactions nor in the value for Λ_B, there was an increase in Λ_C. The reasons for such a change were twofold. First, there was the increase in the bulk dielectric constant caused by the very high dielectric constant of pure H_2O - using the

formula given previously, the theoretical dielectric constant for MeOH containing 1.3% by weight H_2O is 32.1 compared to 31.5 for pure MeOH. Second, and probably the more important of the two, was the superior solvating ability of the H_2O as compared to the MeOH. Selective solvation by the H_2O of the ions in the solution, particularly the Cl^-, would cause an increase of the effective dielectric constant experienced by these ions (selective solvation in solutions of mixed solvents is a phenomenon which is becoming well documented by nuclear magnetic resonance studies (103)). The net result of both factors was a decrease in the formation of associated pairs, which would have been more marked for ion pairs involving the doubly charged $[Pt(PEt_3)(NH_3)_3]^{2+}$ ion because of its greater degree of association than for the less associated $\underline{c}$-$[Pt(PEt_3)(NH_3)_2Cl]^+$. This change in the association was reflected in Λ_C, which includes the degree of dissociation of ion pairs, as was shown above.

The values of k_1, k_2, Λ_B, Λ_C, and the initial conditions for all the experiments involving $\underline{t}$-$[Pt(PEt_3)(NH_3)Cl_2]$, both at 25°C and 35°C, are given in Table 2. Because of the method employed to determine the rate constants, the errors in the values for k_1 and k_2 could not be stated in precise numerical fashion. In lieu of this, the computer generated plots for all these experi-

Table 2. Ammonation of t-$[Pt(PEt_3)(NH_3)Cl_2]$

Temp. °C	$[Pt(PEt_3)(NH_3)Cl_2]_0$ mM	$[NH_3]_0$ mM	$[KCl]_0$ mM	$10^4 \times k_1$ $M^{-1}sec^{-1}$	$10^4 \times k_2$ $M^{-1}sec^{-1}$	Λ_B $cm^2Ohm^{-1}N^{-1}$	Λ_C $cm^2Ohm^{-1}N^{-1}$
25[a]	0.277	1310	10	5.45	0.49	59.1	48.2
	0.480	1310	10	5.45	0.49	59.1	47.8
	0.592	989	10	5.45	0.49	59.1	47.4
	0.601	600	10	5.45	0.49	59.1	47.4
	0.803	1240	10	5.45	0.49	59.1	47.1
35	0.241	100	10	14.2	1.2	67.9	55.4
	0.649	89.9	10	14.2	1.2	67.9	52.7
	0.649	41	10	14.2	1.2	67.9	52.7
	0.650	173	10	14.2	1.2	67.9	52.7
	0.787	604	10	14.2	1.2	67.9	52.7
	0.951	100	10	14.2	1.2	67.9	51.0
	0.167	201	10	12.3	1.2	-[b]	-[b]
	0.622	320	30	14.2	1.2	56.3	41.3
	0.657[c]	352	10	14.2	1.2	67.9	55.8

[a]At 25°C; for the first ammonation reaction, $\Delta H^{\ddagger} = 16.9$ kcal/mole, $\Delta G^{\ddagger} = 21.9$ kcal/mole, $\Delta S^{\ddagger} = -17$ kcal/mole - deg; for the second ammonation reaction, $\Delta H^{\ddagger} = 16$ kcal/mole, $\Delta G^{\ddagger} = 23$ kcal/mole, $\Delta S^{\ddagger} = -23$ cal/mole-deg.

[b]Measurements were made with a spectrophotometer.

[c]Contained 2% by volume of H_2O.

ments have been reproduced in Appendix C.

Also to be found in Table 2 is the result of an experiment in which a spectrophotometer was the measuring device. The ultraviolet absorption spectrum changes of the solution during the ammonation reactions are shown in Figure 12. The changes in the absorption peak for t-$[Pt(PEt_3)(NH_3)Cl_2]$ at 247 mμ were used to determine both k_1 and k_2. The absorbance at infinite time, $A(\infty)$, at 247 mμ was readily obtainable, thus enabling a plot of $\log(A-A(\infty))$ against t. This plot was resolved into two components, the slopes of which yielded the values of k_1 and k_2 found in Table 2. The mathematical justification for the resolution of the $\log(A-A(\infty))$ *vs.* t curve into two components is quite similar to that employed for the conductivity equation, except in this case the values for [A], [B], and [C] are substituted into the equation for absorbance:

$$A = l\varepsilon_A [A] + l\varepsilon_B [B] + l\varepsilon_C [C], \qquad (3.11)$$

where A is the absorbance as a function of time, ε_i is the extinction coefficient of the complex i at the wavelength being utilized, and l is the length of the absorption path. When the values for [A], [B], and [C] found by the pseudo-first-order integration of the rate equations are substituted into the equation for $A-A(\infty)$, with the conditions that $[C](\infty) = [A]_0$, $[A](\infty) = [B](\infty) = 0$, the resulting equation

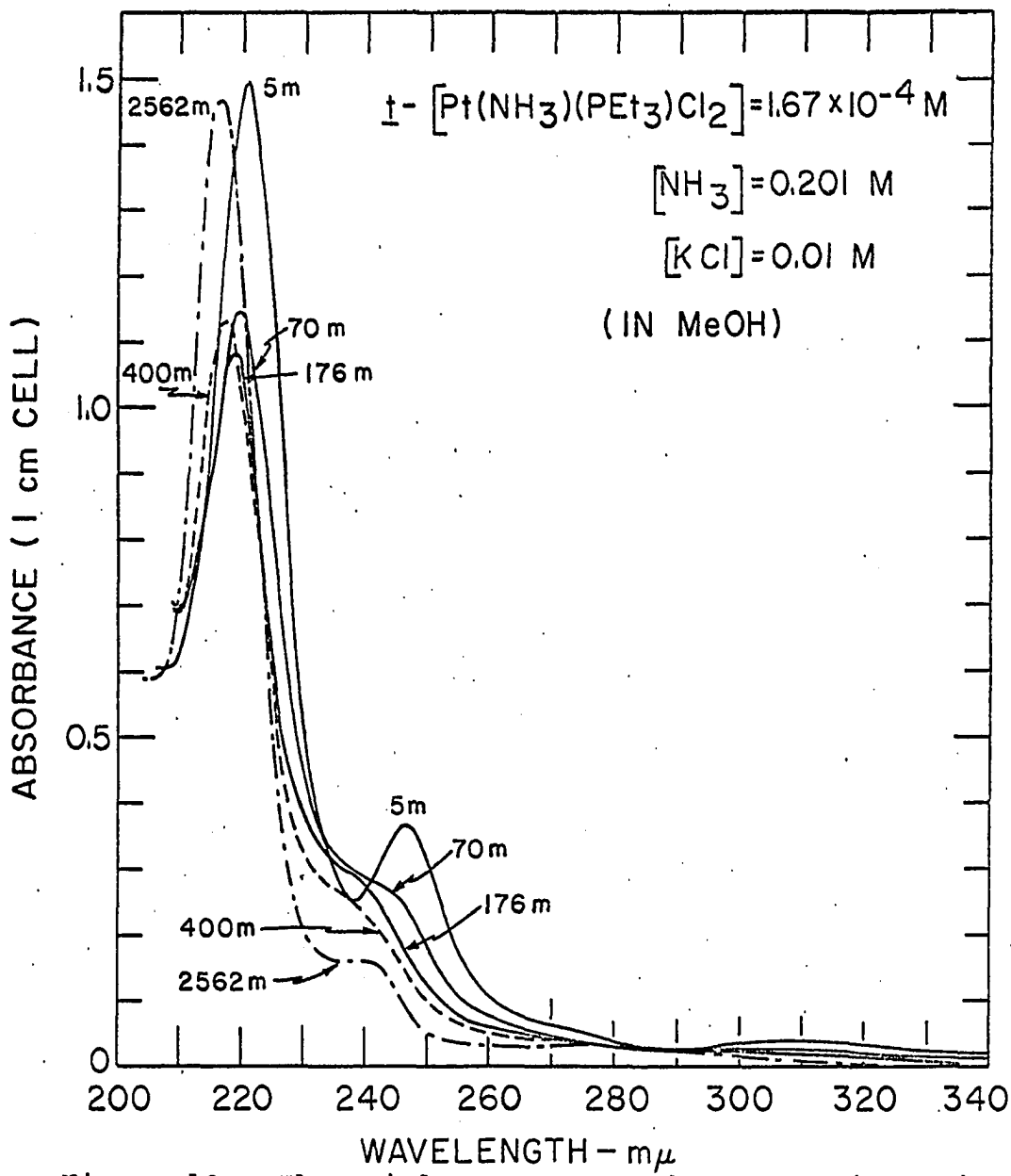

Figure 12. Ultraviolet spectra taken at various times during a t-$[Pt(PEt_3)(NH_3)Cl_2]$ ammonation experiment at 35°C. The time recorded is the elapsed reaction time when the spectral sweep started at 400 mμ. A 1 cm silica cell was used

is

$$A - A(\infty) = l[A]_0(\varepsilon_A + \frac{\varepsilon_B k'_1 - \varepsilon_C k_2'}{k_2' - k_1'}) \exp(-k'_1 t)$$

$$+ \frac{l k_1' [A]_0}{k_2' - k'_1} (\varepsilon_C - \varepsilon_B) \exp(-k_2' t).$$

Here again, the slopes of the two lines obtained by the resolution of log(A-A(∞)) vs. t, will be the pseudo-first-order rate constants, k_1' and k'_2. The values of k_1 and k_2 given in Table 2 were obtained by dividing k_1' and k'_2 by the NH_3 concentration.

It will be noted that k_1 and k_2 are given as second-order rate constants, as would be expected from rate equations of the form of Equations 3.7 and 3.8. The justification for writing Equations 3.7 and 3.8 in a form which has dependence on both the concentration of the complex and of the NH_3 for both ammonation reactions comes from experimental evidence. In obtaining initial estimates for k_1 and k_2 using the pseudo-first-order approximation and a plot of log (L(∞)-L(t)) as a function of t, the resolved curves corresponding to the first and second ammonation reactions were both linear on log plots, indicating that both reactions were first order in the concentration of the complex. A qualitative appreciation of this first-order dependence for the first reaction can be obtained by examining the

plots in Appendix C. It will be seen that for experiments in which the NH_3 was approximately the same, but in which the complex concentration was changed, that the break in the curve corresponding approximately to the termination of the first ammonation reaction occurs at about the same time for each. This is what would be expected for first-order dependence. The first order dependence of both reactions upon the concentration of NH_3 was shown by the linear relationship between the pseudo-first-order rate constants, k_1', obtained from the resolved conductivity curves, and the NH_3 concentration.

Some question existed concerning the reversibility of the second ammonation reaction, because the second ammonation reaction for t-$[Pt(PEt_3)_2Cl_2]$ was found to be reversible. Although NH_3 when bonded to Pt has been found to be extremely inert, as was previously stated, for the ammonation reactions of t-$[Pt(PEt_3)_2Cl_2]$ there was an equilibrium reaction for the second ammonation reaction because of steric interaction between the ethyl groups on the phosphine and the ligands cis to the phosphine - this will be considered more thoroughly when t-$[Pt(PEt_3)_2Cl_2]$ results are presented. In order to test whether this same sort of steric reversal of the reaction occurred for t-$[Pt(PEt_3)(NH_3)Cl_2]$, advantage was taken of the ultraviolet absorption spectrum differences of the complexes

found in solution. Examination of Figure 12 shows that as the t-$[Pt(PEt_3)(NH_3)_2Cl]^+$ was formed, the absorption peak at 221 mμ decreased. As the much slower second ammonation reaction proceeded, however, a new absorption peak began to appear at 215 mμ. The conclusion drawn was that $[Pt(PEt_3)(NH_3)_3]^{2+}$ had an intense absorption peak at 215 mμ, while c-$[Pt(PEt_3)(NH_3)_2Cl]^+$ did not. Through this difference in the absorption spectra, the irreversibility of the second ammonation reaction was demonstrated. A solution containing only complex and NH_3 was allowed to stand until the first and second reactions had proceeded to a steady state. To one aliquot of this solution, NH_4Cl was added in the form of a MeOH solution. To a second aliquot of this solution, a MeOH solution of HCl was added. To a third aliquot, pure MeOH was added. The three resulting solutions all had the same concentration of complex, and the two solutions to which MeOH solutions were added had the same concentration of NH_4Cl, with the postulate that the neutralization reaction between NH_3 and HCl went to completion. The big difference between the solutions were that the NH_3 concentration in the solution to which HCl had been added was one-fourth the NH_3 concentration in the other two solutions, and that one solution contained no added Cl^-. The ultraviolet absorption spectra of the solutions was recorded after these solutions had again been allowed to

reach a steady state, and it was found that the two solutions containing Cl^- had the same spectrum, within the accuracy of the spectrophotometer in this region with MeOH, and that there had been only a small change in the spectrum upon the addition of Cl^-. The changes that did occur in the spectrum in going from a solution with no added Cl^- to one containing added Cl^- were mainly in the region of 200-210 mμ. These changes were totally explicable in terms of ionic association, and decreased spectrophotometer sensitivity in the 200-210 mμ region because of increased optical density in both solution and reference solution upon the addition of NH_4Cl in high concentration (approximately 0.2M). The solvent itself has a fair absorption in this region, causing the spectrophotometer slit to widen, with a resultant decrease in sensitivity, and the added NH_4Cl enhanced this effect. The spectra were also in good agreement with the final spectrum of the experiment shown in Figure 12, which had a Cl^- concentration of 0.01 and approximately the same NH_3 and complex concentration, so it was concluded that the reaction was not appreciably reversible.

One last finding in the ammonation reactions of t-$[Pt(PEt_3)(NH_3)Cl_2]$ as well as in the reactions for the other two complexes was that there was a gradual upward drift in the conductivity after the ammonation reactions of

the complex had clearly reached a steady state - in some experiments having high NH_3 concentrations, the conductivity remained steady for several days before this slow upward drift could be detected. Added to this change in conductivity was the observation that there was no apparent concomitant change in the ultraviolet absorption spectrum. The conclusion drawn was that although ions were being introduced into the solution, these ions were not coming from any obvious changes in the complex present in the solution. The changes in conductivity corresponded to an ion concentration which was less than 10^{-3}M over the course of two months, so the actual determination of the ions was somewhat precluded. The probable cause of this rise in ionic concentration was discovered when a solution containing only KCl and NH_3 dissolved in MeOH was also found to have a slow increase in conductivity over long periods of time, which was undoubtedly due to a very slow leaching of ions from the glass of the container by the basic solution. This leaching process was found to occur even in MeOH solutions containing only KCl, by other workers (92). Because this process added ions to the solution at such a slow rate it did not interfere with the primary measurements, and was therefore ignored in the treatment of the data. The variations in the rate at which these ions came into solution - in some cases several days elapsed

before any changes were observed - is the type of behavior which would be expected from a process which would be dependent, among other things, on the condition of the glass surface in the conductivity cell at any particular time.

The activation parameters of the two ammonation reactions were calculated from the rate constant at 25° and 35°C, and are also given in Table 2. The Arrhenius equation was used to calculate the Arrhenius activation energy, E_a, and the enthalpy of activation, $\Delta H^{\ddagger}$, was derived from it. The Gibb's free energy of activation, $\Delta G^{\ddagger}$, was calculated by the free energy relationship of the theory of absolute reaction rates. The entropy of activation, $\Delta S^{\ddagger}$, was calculated from the enthalpy and free energy of activation.

Trans-dichlorodiammineplatinum(II)

As a means to correlating the results of this study with the experimental results available for H_2O systems, t-$[Pt(NH_3)_2Cl_2]$ was admirably suited. Not only did it fit into the series of complexes in which the ligand cis to the reaction site was systematically varied, but also, its ammonation reactions in H_2O had been studied. One disadvantage associated with t-$[Pt(NH_3)_2Cl_2]$ was that in both H_2O and MeOH it dissolves at an excruciatingly slow rate, and has a limited solubility. In MeOH the highest concentration obtainable was 1.46×10^{-4}M, at 35°C, and this re-

quired 12 hours to dissolve. This limited solubility of the complex imposed a limitation upon the experimentation which was possible with this complex. No large variation in the initial complex concentration was possible. Furthermore, the noise level in the solutions during the ammonation reactions of this coordination compound was quite high, and placed a limitation upon the precision of the conductance measurements of this complex. At 25°C the noise problem is unchanged, but both the solubility of the complex and the equivalent conductances of the ammonation products are lower than at 35°C. The restriction on the precision of the conductance measurements that results from these factors made the measurement of the ammonation kinetics at 25°C unfeasible with the available instruments.

The extinction coefficient of the most intense absorption peak in the ultraviolet region (exclusive of the charge transfer peak in the far ultraviolet) was found to be 100 in MeOH, while the extinction coefficient of the surrounding valleys was on the order of 55; the products of the ammonation reactions were of similar low intensity in this region, so spectral determination of the rate constant was also precluded by the low solubility of the complex.

While the above limitations restricted the variation in experimental conditions, sufficient latitude was still

available to determine that the reactions were first-order in both NH_3 and complex concentrations, and were represented by the following equations:

$$\underline{t}\text{-}[Pt(NH_3)_2Cl_2] + NH_3 \xrightarrow{k_1} [Pt(NH_3)_3Cl]^+ + Cl^-$$

$$[Pt(NH_3)_3Cl]^+ + NH_3 \xrightarrow{k_2} [Pt(NH_3)_4]^{2+} + Cl^-.$$

This is the same form as the ammonation reactions of $\underline{t}$-$[Pt(PEt_3)(NH_3)Cl_2]$, so the same differential equations for the rate of reaction are applicable. In the analysis of the ammonation of this complex, however, the pseudo-first-order approximation was used exclusively, inasmuch as the lowest NH_3 concentration was 1000 times greater than the complex concentration. Thus, a plot of $L(\infty)-L(t)$ *vs.* t was resolved into two components using the relationship of Equation 3.9. The pseudo-first-order rate constants, k_1' and k_2', which resulted from this resolution were then used in a least-squares program in the computer to fit the equations,

$$k_1' = k_1[NH_3] + k_s,$$

$$k_2' = k_2[NH_3] ,$$

where k_1 and k_2 are the second order rate constants which are dependent upon the NH_3 concentration, and k_s is the

pseudo-first-order rate constant for the reaction of the starting complex with the solvent. The inclusion of k_s in the equation for k_1' does not effect the mathematics of the integration which yielded Equation 3.9, because k_s will be a constant term also. The only requirement in the integration was that k_1' be constant throughout the course of any given reaction.

The inclusion of k_s in the equation for the pseudo-first-order rate constant, k_1', was based on the observation that a plot of k_1' vs. $[NH_3]$ had a non-zero intercept on the k_1' axis at $[NH_3]=0$. This type of intercept has been found to be the rate constant for the solvolysis reaction for nonreversible reactions of Pt(II) complexes. The inclusion of an additional reaction path in the first ammonation reaction can be represented by the following equation,

$$\underline{t}\text{-}[Pt(NH_3)_2Cl_2] + MeOH \xrightarrow{k_s} \underline{t}\text{-}[Pt(NH_3)_2(MeOH)Cl]^+ + Cl^-.$$

At this point there are two possible reactions which the solvated complex can undergo,

$$\underline{t}\text{-}[Pt(NH_3)_2(MeOH)Cl]^+ + NH_3 \longrightarrow \underline{t}\text{-}[Pt(NH_3)_2(MeO)Cl] + NH_4^+,$$

and

$$\underline{t}\text{-}[Pt(NH_3)_2(MeOH)Cl]^+ + NH_3 \longrightarrow [Pt(NH_3)_3Cl]^+ + MeOH.$$

Of these two, the proton transfer reaction is probably favored because of the acid strength of MeOH. Also, in aqueous

systems the ammonation reaction of this complex has been found to yield the hydroxo complex through a solvolysis path as a competing reaction. The rate of reaction of the t-$[Pt(NH_3)_2(MeOH)Cl]$ would be greater than the solvolysis step, so that k_s would be the limiting rate constant for this kinetic path.

In passing, it should be noted that a solvolysis path was not found in the ammonation reactions of the other two compounds of this study. For the reactions of t-$[Pt(PEt_3)_2Cl_2]$ other authors have found that the reaction with MeOH is too slow to be measured (38). A theoretically predicted value for the rate constant of the reaction of MeOH with t-$[Pt(PEt_3)_2Cl_2]$ is several orders of magnitude smaller than any known rate constant for reactions of this complex. A kinetic path involving the solvolysis of t-$[Pt(PEt_3)_2Cl_2]$ can therefore be excluded from consideration. As for the ammonation reactions of t-$[Pt(PEt_3)(NH_3)Cl_2]$, no indication was found for a solvolysis path in either a k_i' *vs.* $[NH_3]$ plot or in the computer treatment of both ammonation reactions.

Table 3 contains the initial concentrations of all the experiments; the observed pseudo-first-order rate constants, k_1' and k_2'; and the rate constants, k_1, k_s, and k_2 obtained by the least-squares treatment in the computer. The standard deviations calculated by the least-squares program

are also included in Table 3.

Table 3. Ammonation of t-$[Pt(NH_3)_2Cl_2]$ at 35°C

$[Pt(NH_3)_2Cl_2]_0$ mM	$[NH]_0$ mM	$[KCl]_0$ mM	$10^5 \times k'_1$ sec^{-1}	$10^5 \times k'_2$ sec^{-1}
0.135	166	10	34.0[a]	3.11[b]
0.139	168	10	30.4	3.45
0.135	463	10	62.5	9.17
0.146	496	10	66.8	10.8
0.134	589	10	82.5	10.9

[a]From the computer least-squares fit of these values to the equation $k'_1 = k_1 [NH_3] + k_s$, $k_1 = 1.13 \times 10^{-3} \pm 0.08 \times 10^{-3} M^{-1}$ sec^{-1}, $k_s = 1.3 \times 10^{-4} \pm 0.3 \times 10^{-4} sec^{-1}$.

[b]From the computer least-squares fit of these values to the equation $k'_2 = k_2 [NH_3]$, $k_2 = 1.98 \times 10^{-4} \pm 0.07 \times 10^{-4} M^{-1}$ sec^{-1}.

A plot of L(t) vs. t for one of the experiments is given in Figure 13a. The slow rise in the conductance due to the leaching out of ions from the glass cells is evidenced by the linear portion of the curves at long times. This linear portion has been extrapolated back to zero, as shown by the dashed line in Figure 13a. Figure 13b contains a $\log(L(\infty)-L(t))$ vs. t plot for the same experiment, as well as the resolved portions of the plot. The extrapolated line in Figure 13a was used as $L(\infty)$ values in obtaining Figure 13b.

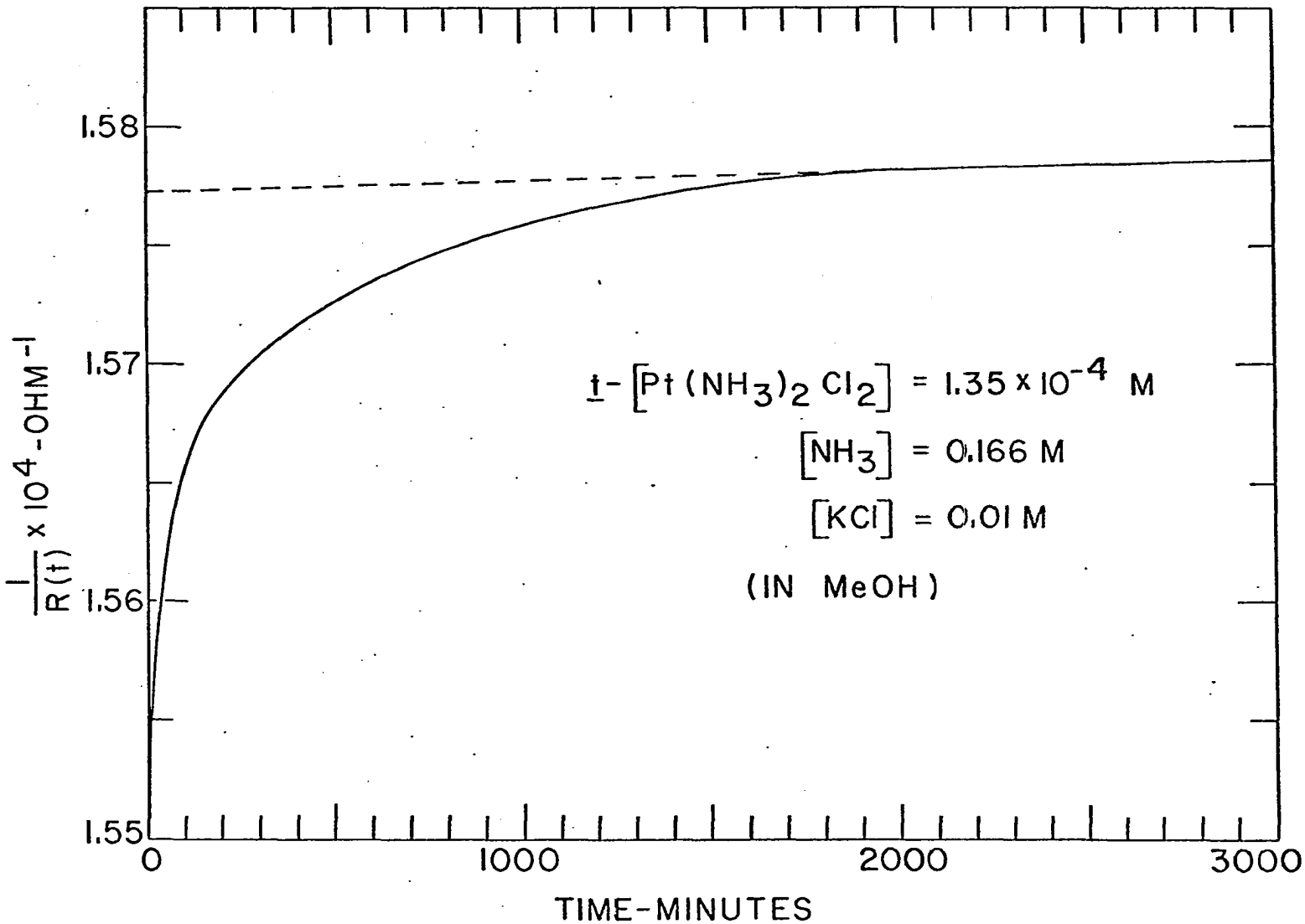

Figure 13a. Conductance plot for a t-[Pt(NH$_3$)$_2$Cl$_2$] ammonation experiment at 35°C

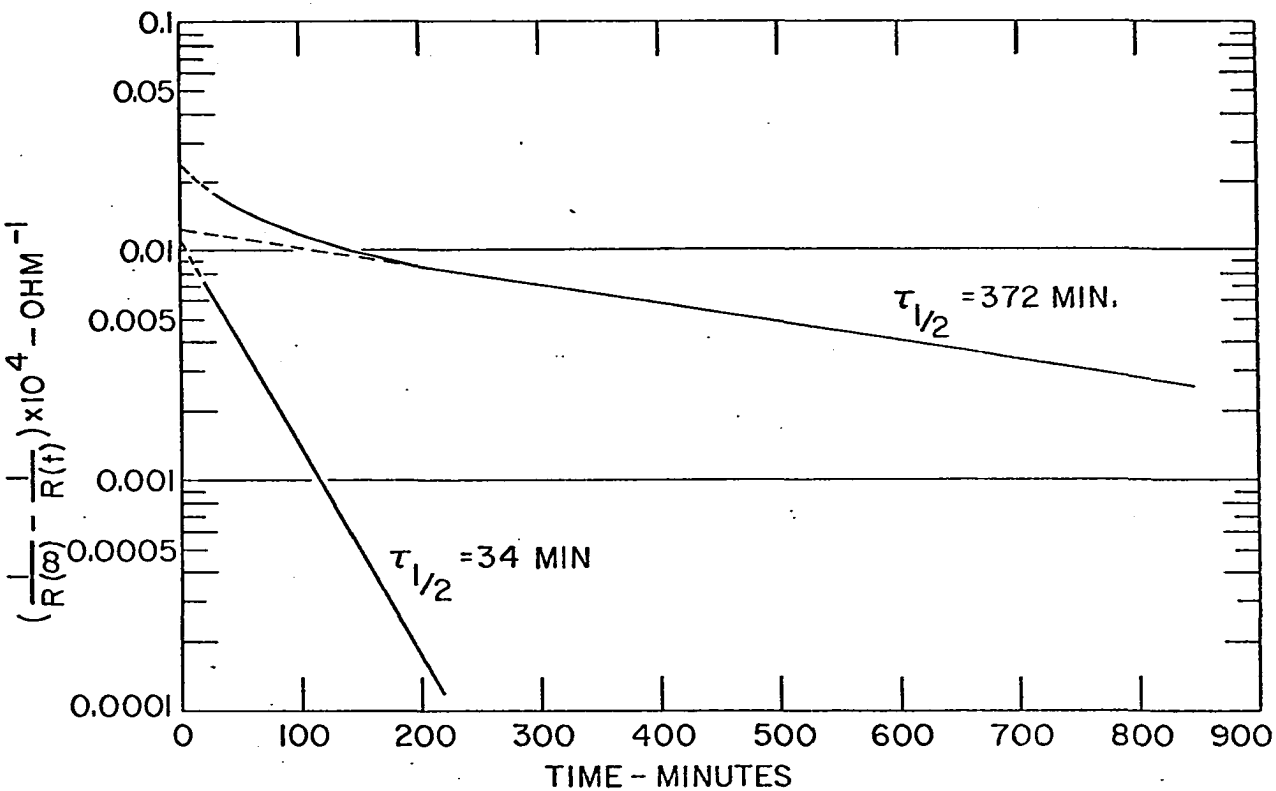

Figure 13b. Semilog plot of the conductance(∞) minus the conductance(t) vs. the elapsed reaction time for the experiment given in Figure 13a. The extrapolated line in Figure 13a was used as the conductance(∞). The semilog plot is resolved into two components corresponding to the first and second ammonation reactions

Trans-dichlorobis(triethylphosphine)platinum(II)

While the reactions of the other two compounds were rather uncomplicated, those for t-$[Pt(PEt_3)_2Cl_2]$ turned out to be much more complex. The complexity of these ammonation reactions was manifested in two ways. First, the rate of change in the conductivity started out rather slowly, compared to the rates for the other two complexes studied, but then the rate would slowly increase until it had approximately doubled. This increase in the rate of change of the conductivity was reproducible under varying starting conditions - changes in the complex concentration, NH_3 concentration, Cl^- concentration, and temperature. The time between the inception of the experiment, and the first evidence of the increase in the rate of change of the conductivity (hereafter called the induction period), was shortened when either the complex or NH_3 concentrations were increased. The second manifestation of the complexity of these ammonation reactions was the reversibility of the second ammonation reaction, with an equilibrium being established.

One of the first questions that arose was whether or not the change in rate corresponded to a positive acceleration of the reaction rate, or just the removal of some retardation to the reaction: was there catalysis, removal of an inhibitor, or a competing reaction. In an attempt to answer

this question, reactions were run in which several impurities had been added to the starting solution in order to see what effect these would have on the reaction. The impurities chosen, t-$[Pt(PEt_3)_2Cl_4]$, c-$[Pt(PEt_3)_2Cl_2]$, t-$[Pt(PEt_3)_2(H)Cl]$, were complexes which might logically be formed in any reactions competing with the ammonation reaction. Each of these would then have the possibility, if it were so formed in competing reaction, of reacting rapidly with the NH_3 and/or acting as a catalyst for the ammonation reacts of t-$[Pt(PEt_3)_2Cl_2]$. Of these three complexes, the latter two would be expected to complete their ammonation reactions almost instantaneously, because of the very high trans labilization by PEt_3 and H^-. The solution containing the Pt(IV) complex was allowed to react a few minutes with the NH_3 solution before the reactions of t-$[Pt(PEt_3)_2Cl_2]$ were started, in order to better duplicate the conditions which would prevail in a solution in which this oxidation product was formed in a competing reaction. The results of these experiments were quite negative. In each case, there still existed the induction period followed by an increase in rate, except that in the cases of the added t-$[Pt(PEt_3)_2Cl_4]$ and t-$[Pt(PEt_3)_2(H)Cl]$ the increase in rate was not as great as in experiments of comparable starting concentrations of t-$[Pt(PEt_3)_2Cl_2]$ and NH_3 without these added materials. In the experiment with added

c-$[Pt(PEt_3)_2Cl_2]$, however, the increase in rate was of the same magnitude as that found in solutions not containing any added materials. In sum added c-$[Pt(PEt_3)_2Cl_2]$ did not appear to influence the reaction rate, but added t-$[Pt(PEt_3)_2Cl_4]$ and t-$[Pt(PEt_3)_2(H)Cl]$ caused the induction period to be extended.

In still another variation on the starting conditions, an aliquot of an experimental solution which had reached steady state condition was added to a second solution at the beginning of its reaction (the reacted solution was added to the NH_3 solution and allowed to come to equilibrium, and then this solution was added to solid t-$[Pt(PEt_3)_2Cl_2]$ in a volumetric flask). In this case, the reaction proceeded at a high rate from its inception, without any apparent induction period.

In Figure 14, a composite of these four experiments and a normal experiment is shown. The scale on the ordinate axis was chosen so as to suitably compare the various curves. While all of the solutions which are incorporated into Figure 14 were of approximately the same concentration, their variation can be seen in Table 4, where the initial concentrations for all these solutions is given.

Another possibility, and one which has been found to occur in the reactions of some other platinum complexes, was that the induction period corresponded to the second-

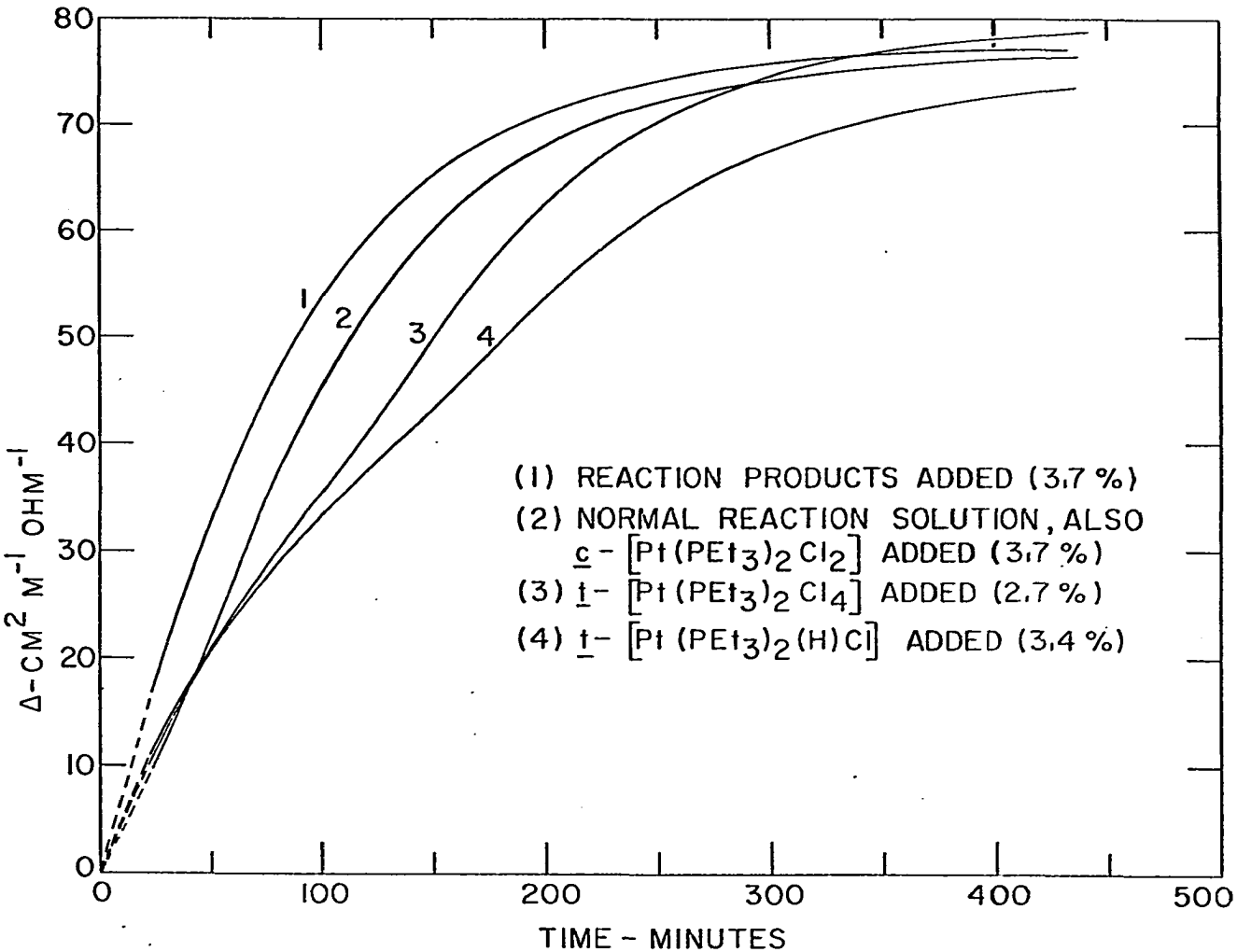

Figure 14. Influence of four added foreign complexes on the conductance changes during the t-$[Pt(PEt_3)_2Cl_2]$ ammonation reactions. The exact concentrations of the solutions are given in Table 4. $\Delta=1000k(L(t)-L(0))/[Pt(PEt_3)_2Cl_2]$, where $L(t)=1/R(t)$

Table 4. Ammonation of t-$[Pt(PEt_3)_2Cl_2]$ in solutions with added impurities

$[Pt(PEt_3)_2Cl_2]_0$ mM	$[NH_3]_0$ mM	$[KCl]_0$ mM	Impurity added	$[Impurity]_0$ mM
0.651[a]	218	10	-[b]	0.0238[c]
0.650[d]	199	10	c-$[Pt(PEt_3)_2Cl_2]$	0.0242
0.644[e]	180	10	-[f]	-[f]
0.608[g]	201	10	t-$[Pt(PEt_3)_2Cl_4]$	0.0165
0.627[h]	202	10	t-$[Pt(PEt_3)_2(H)Cl]$	0.0213

[a]Curve 1 in Figure 14.

[b]An equilibrium mixture of t-$[Pt(PEt_3)_2(NH_3)Cl]^+$ and t-$[Pt(PEt_3)_2(NH_3)_2]^{2+}$.

[c]Initial concentration of the t-$[Pt(PEt_3)_2Cl_2]$ solution that was allowed to react with 0.218M NH_3 and 0.01M KCl until an equilibrium was established.

[d]Curve 2 in Figure 14.

[e]Curve 2 in Figure 14 also represents this reaction.

[f]This is a normal ammonation reaction without any added compound.

[g]Curve 3 in Figure 14.

[h]Curve 4 in Figure 14.

order reaction of the reagent with the complex, and a concurrent reaction of the complex with the solvent to form the extremely labile solvated species, which then reacts with the reagent to form the product. In some systems having this second reaction path, the reaction rate has ex-

hibited the same sort of behavior observed for t-$[Pt(PEt_3)_2Cl_2]$, an induction period followed by an increase in rate. Experiments were performed in which the complex was dissolved in a KCl-MeOH solution, allowed to stand for approximately 12 hours, and then the ammonation reaction was started. The induction period was still observed, contrary to the results observed using aged solutions for complexes having an alternate path involving a solvolysis reaction of the complex.

From this set of observation, the conclusion was drawn that inhibition of the reaction followed by an increase in rate when the inhibitor was either deactivated or chemically reacted, could not adequately explain the system. If inhibition of the reaction was occuring, then there should have been evidence of this even though the starting solution contained some of the products. In experiments which had no reaction products added, the change to a higher rate took place over a span of time almost as great as a half-time for the reaction (vide Figure 14, in which a normal experiment is included for comparison.

Similarly, the lack of difference between fresh and aged solutions ruled out any kinetic path involving a reaction with solvent. Isomerization, formation of the hydride, and oxidation to a Pt(IV) species also were excluded as the source of the change in rate because of the experiments per-

formed with these materials added. Additionally, electrophilic catalysis could be ruled out on the basis of a study by Belluco et al. (53), in which they found that the reactions of t-$[Pt(PEt_3)_2Cl_2]$ were not affected by electrophilic catalysts which did catalyze the reactions of some other Pt(II) complexes. Finally, both conductance and spectrophotometric evidence indicated that the second ammonation reaction was very much slower than the first ammonation reaction and continued for a long duration after the first reaction was completed for this complex as well as for the other two studied, so that the increase in rate could not be ascribed to a slow reaction followed by a faster subsequent reaction.

A possible clue to what might have occurred was found in research reported by Teggins et al. (104,105). In studying exchange reactions involving bromo complexes of Pt(II), they found what might be termed nucleophilic catalysis or enhanced nucleophilicity. In the electrophilic catalysis of Belluco et al., the proposed mechanism was an electrophilic ligand entering the axial position of the square-plane, to form a square pyramid. The ligand in the apex of this square pyramid transition state, being electrophilic, caused a decrease in electron density in the other axial position of the square-plane. This decrease in electron density in turn enhanced the rate of attack by a

nucleophilic ligand from that direction. In contrast to this, the proposed mechanism for the nucleophilic catalysis of Teggins et al. involved the formation of a transition state in which a Pt-Br-Pt bridge was formed. This single bridge, being extremely labile, immediately reacted with an incoming ligand. This catalysis involved a nucleophilic attack on one Pt(II) complex by a bromo ligand coordinated to another Pt(II) complex. The nucleophilicity of the incoming bromo ligand coordinated to the Pt(II) was much greater than free Br^-, so that the rate of bridge formation was greater than the rate of attack by the free Br^-. The rate of bridge cleavage was even greater, so the consequent overall exchange rate was greatly enhanced. Additionally, Lokken and Martin (106) proposed Pt-Cl-Pt bridging as a mechanism for Cl^- exchange in Zeise's salt, $K[Pt(C_2H_4)Cl_3]$.

In the present system, the PEt_3 ligands would be a favorable factor in the formation of a Pt-Cl-Pt bridge, as compared to the C_2H_4 ligand in Zeise's salt. In their studies of halide bridged dimeric platinum(II) complexes, Chatt and Venanzi found that Pt-Cl-Pt bridging was much more stable when PEt_3 was coordinated to the platinum, than when C_2H_4 was the neutral ligand (16,107). They also found that Pt-Br-Pt bridging was more stable than Pt-Cl-Pt bridging, which could account for fewer cases of the chloro bridging being proposed as a transition state in platinum(II)

reactions than bromo bridging.

After a mechanism involving nucleophilic catalysis was proposed, the questions arose as to which complex was the catalyst, and what reaction was catalyzed. The latter of these two questions was the easier to answer, because both spectral and conductance evidence indicated that the second ammonation reaction was much slower than the first, and continued long after the first reaction was completed. Also, the spectral changes during the reactions indicated that the rate of disappearance of the starting complex, t-$[Pt(PEt_3)_2Cl_2]$, increased with time during the initial phases of the reactions. Thus, the first ammonation reaction was proposed as the catalyzed reaction.

The catalyst was much more difficult to assign. The starting material and its solvolysis products were ruled out by the experiment involving added reaction products, and the experiments involving aged complex solutions. Deciding which of the products could be the catalyst was much more onerous, and rate laws involving each one as the catalyst were tried. The second ammonation product, $[Pt(PEt_3)_2(NH_3)_2]^{2+}$ was slightly favored, because of the lack of an induction period in the experiment in which reaction products at low concentrations were added to a reaction at its inception. The concentration of the added Pt(II) was 3.7% of the concentration of the

t-$[Pt(PEt_3)_2Cl_2]$ present, yet there was no apparent induction period despite the existence of a period extending almost one half-time in solutions without any added products. This was interpreted to mean that the product from the much slower second ammonation reaction must be of importance.

Besides the puzzling behavior of the reaction during its initial phases, as the first ammonation reaction approached completion, a very sharp change in the rate of conductivity change was observed, and after a slow, slight increase in conductivity, the reaction ceased. The total change in the conductance for the reactions fell far below what would be expected for both ammonation reactions going to completion, however. To narrow the possible explanations of this behavior, an experiment was performed in which no KCl was added, so that ionic association would be at a minimum (the only ions present being from the reaction of NH_3 with MeOH, and the ions from the complex ammonation), and so that any reverse reactions dependent upon Cl^- concentration, if such existed, would be minimized. When this was done, while there was still a very sharp break in the rate of conductivity change, there was a continuing slower rise in specific conductance of a more pronounced degree up to an eventual steady state. Even in this experiment, while the net change in specific conductance up to the sharp break was of the order expected from the ions of the first

ammonation going into solution, the net change during the slower portion fell far short of what would be expected for completion of the second reaction, even if there were considerable association occurring (which there should not have been under the stated conditions). This behavior has been found by other researchers, and was not too difficult to explain. In determining the crystal structure of t-$[Pt(PEt_3)_2Cl_2]$, Messmer and Amma (108) found that there was a fairly high degree of non-bonding interaction between the Cl and the carbons of PEt_3, and that a distortion of the P-Pt-Cl bond angle resulted. A similar result was found in the structural determination of t-$[Pt(PEt_3)_2(H)Br]$, in which the Br-Pt-P angle was determined to be approximately 94^0 (68). Also, from molecular models it was seen that there would be a great deal of interaction between the NH_3 and PEt_3 ligands in t-$[Pt(PEt_3)_2(NH_3)_2]^{2+}$, which would be reduced if a Cl was substituted for one of the NH_3 ligands. In fine, the second ammonation reaction was reversible because of steric factors, and as a consequence an equilibrium was established which favored the less hindered t-$[Pt(PEt_3)_2(NH_3)Cl]^+$. While there was no evidence to indicate reversibility for the first ammonation, the steric hindrance existing in the complex was evidenced by a lower rate of reaction during the induction period than would be expected on the basis of the other two complexes studied.

An experiment which was followed spectrophotometrically in the ultraviolet region is shown in Figure 15a. The salient features of this composite figure are: the absorbance peaks at 267 mμ and 247.5 mμ disappear during the early phases of the reaction, and a new absorbance peak at 233 mμ concomitantly grows into the spectrum; at longer times, the absorbance peak at 233 mμ begins to disappear, but at a much slower rate than the rate at which it grew into the spectrum. In Figure 15b the absorbance values at 267 mμ for this experiment are plotted as a function of time. This plot shows the same sort of behavior encountered in the conductance plots--an induction period followed by an increased rate of change. Figure 15b also indicates that the upper limit for the concentration of the starting material remaining in the solution after 300 minutes of reaction time is 20% of the initial concentration, on the basis of an extinction coefficient of 10200 at 267 mμ for t-$[Pt(PEt_3)_2Cl_2]$. The application of this extinction coefficient to the absorbance at 267 mμ after 1500 minutes in Figure 15a indicates that a maximum of 14% of the initial concentration of t-$[Pt(PEt_3)_2Cl_2]$ could be present in the solution at that time. This is an upper limit on the concentration which would only be realized if no other species in the solution absorbed at this wavelength.

These observations were interpreted to mean that there

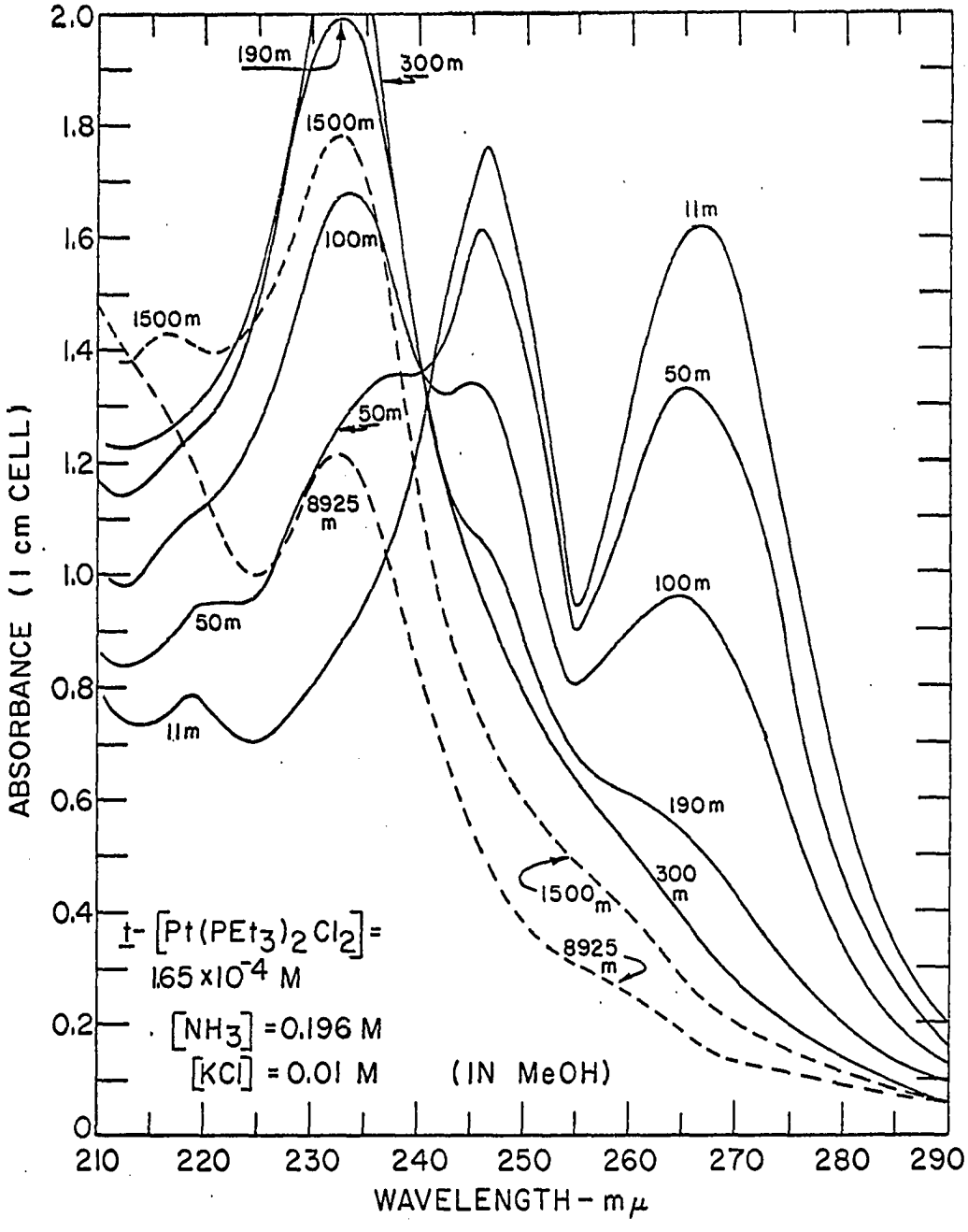

Figure 15a. Ultraviolet spectra taken at various elapsed reaction times during a t-$[Pt(PEt_3)_2Cl_2]$ ammonation experiment at 35°C. The spectral sweep started at 400 mμ at the indicated time

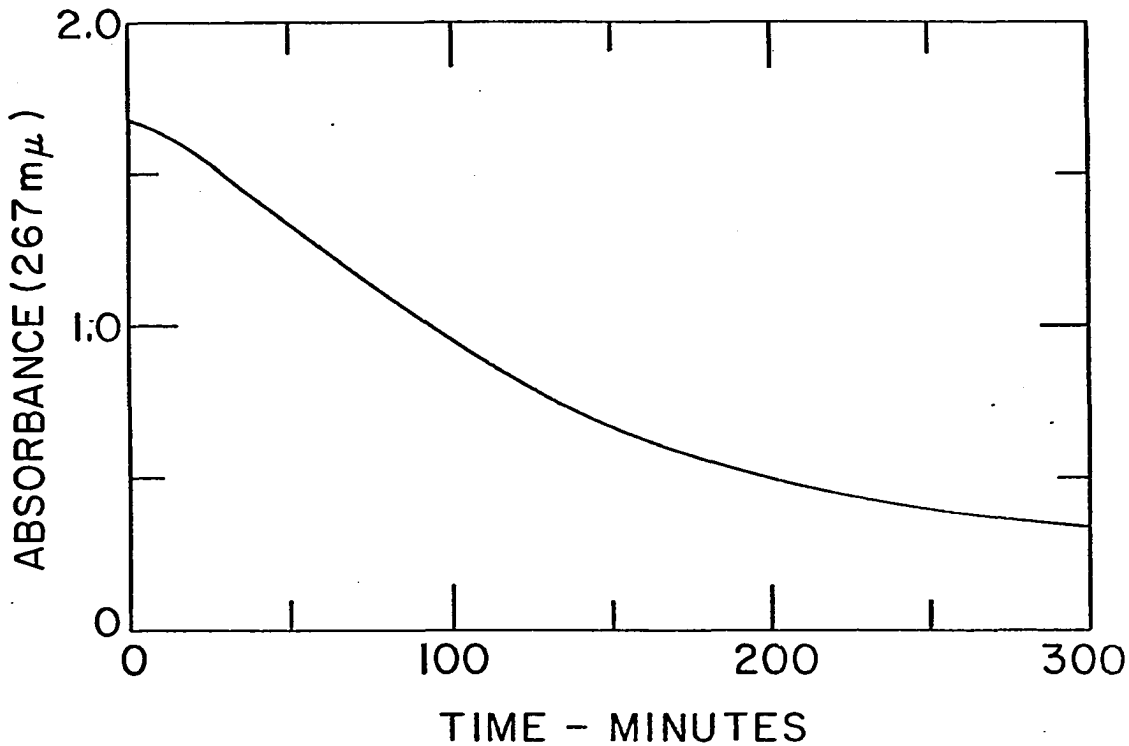

Figure 15b. Changes in the ultraviolet absorbance at 267 mμ vs. the elapsed reaction time for the experiment in Figure 15a. A 1 cm silica cell was used

is an initial reaction which removes t-$[Pt(PEt_3)_2Cl_2]$ from the solution, and that the rate with which this complex disappears increases with time until a maximum rate is achieved. The compound formed by the reaction has a strong absorbance peak at 233 mμ. This product in turn reacts slowly and disappears in part from the solution, as evidenced by a gradual decrease in the absorbance peak at 233 mμ. This peak continues to be quite large, however, which is in accord with the presence of an equilibrium for this reaction.

As stated previously, other studies of the reaction of NH_3 with t-$[Pt(PEt_3)_2Cl_2]$ concluded that the cis isomer was formed by the reaction (14,15). This finding was checked by comparing the ultraviolet spectrum of a solution resulting from the reaction of t-$[Pt(PEt_3)_2Cl_2]$ with NH_3, with the spectrum of a solution of similar composition containing c-$[Pt(PEt_3)_2Cl_2]$ in place of the trans isomer. Figure 16 repeats the 8925 minute spectrum found in Figure 15a, and compares it with the spectrum resulting from the reaction of c-$[Pt(PEt_3)_2Cl_2]$ with NH_3. Although the spectrum for the reaction of c-$[Pt(PEt_3)_2Cl_2]$ with NH_3 in Figure 16 is that measured 1200 minutes after the inception of the reaction, the spectrum had remained unchanged for better than 1000 minutes. The differences between the two spectra in Figure 16 indicate that while some cis isomer may be present

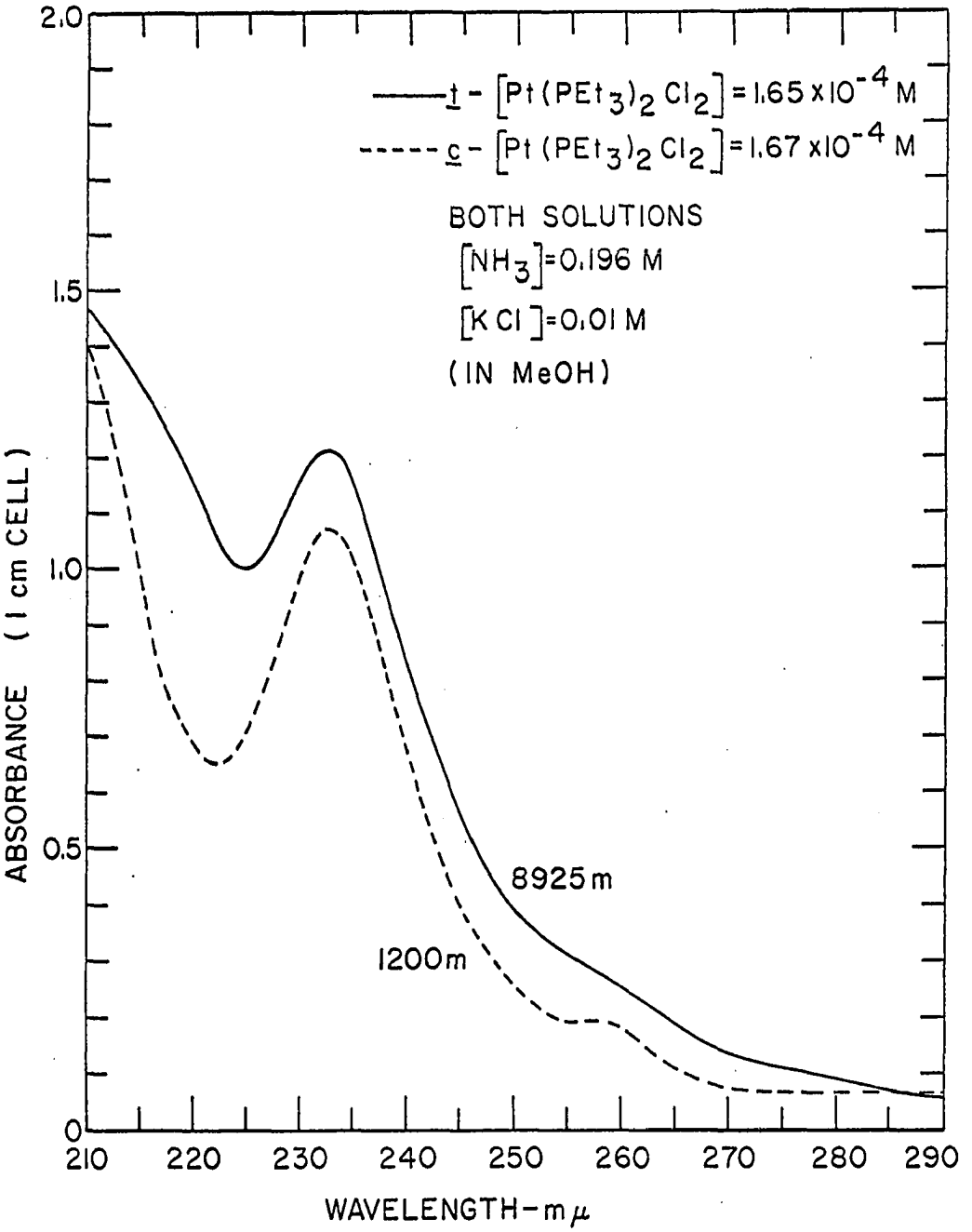

Figure 16. Ultraviolet spectrum of t-$[Pt(PEt_3)_2Cl_2]$ ammonation experiment compared with ultraviolet spectrum of c-$[Pt(PEt_3)_2Cl_2]$ ammonation experiment at 35°C. The elapsed reaction time for each is indicated

in the solution resulting from the reaction of the trans isomer with NH_3, the trans solution contains other complexes. Indeed, the partial isomerization of the trans isomer was expected, as stated previously, but the process was kept to a minimum by running the experiments in a room lighted only with red lights. The previous research on the reaction of t-$[Pt(PEt_3)_2Cl_2]$ with NH_3 was performed before the light sensitivity of the isomerization reaction was known, so in the absence of any statement regarding special precautions in this respect, it can probably be assumed that the isomerization reaction in the previously reported research was light induced, and therefore rather rapid. If the spectrum after 8925 minutes in Figure 15a is compared with the spectrum after 1500 minutes in the same figure, it is seen that the isomerization reaction does not account for the gradual disappearance of the absorbance peak at 233 mμ, because an absorbance peak at 217 mμ continued to grow in as the peak at 233 mμ decreased. This growth of the peak at 217 mμ was interpreted as being due to the second ammonation reaction of t-$[Pt(PEt_3)_2Cl_2]$.

In summary, the pertinent observations regarding the ammonation reactions of t-$[Pt(PEt_3)_2Cl_2]$ are: the overall ammonation reactions are given by the equations,

$$\underline{t}\text{-}[Pt(PEt_3)_2Cl_2] + NH_3 \longrightarrow \underline{t}\text{-}[Pt(PEt_3)_2(NH_3)Cl]^+ + Cl^- \quad (3.12)$$

$$\underline{t}\text{-}[Pt(PEt_3)_2(NH_3)Cl]^+ + NH_3 \rightleftharpoons \underline{t}\text{-}[Pt(PEt_3)_2(NH_3)_2]^{2+} + Cl^- . \quad (3.13)$$

In addition to these simple reactions, there is some other path for the formation of $\underline{t}$-$[Pt(PEt_3)_2(NH_3)Cl]^+$ which is not operative during the initial minutes of the reaction, but which becomes operative as the ammonation reactions proceed. This additional kinetic path does not involve a solvolysis reaction, nor isomerization, nor oxidation to Pt(IV), nor formation of a hydride, but does involve one of the products of the ammonation reactions. Furthermore, the addition of $\underline{t}$-$[Pt(PEt_3)_2Cl_4]$ or $\underline{t}$-$[Pt(PEt_3)_2(H)Cl]$ in low concentrations causes the induction period to be extended markedly, with the eventual increase in reaction rate being much less than would be the case without any added material. The first ammonation reaction is much faster than the second ammonation reaction, and both of these appear to be finished before any isomerization becomes evident. The initial ammonation reaction (before the rate begins to increase), the reaction during the catalyzed portion, and the final ammonation reaction are all first-order dependent upon $[NH_3]$. The final equilibrium is shifted by changes in $[Cl^-]$, so there

is Cl^- dependence in the reverse reaction of the final ammonation reaction. Finally, the initial ammonation reaction and the final ammonation reaction both exhibit first-order dependence upon the complex concentration; the order of the dependence of the reaction rate upon complex concentration during the period of enhanced rate could not be determined satisfactorily.

Several mechanisms which potentially fulfilled all the constraints of the experimental findings were used in a computer treatment of the experimental data. Each mechanism involved the formation of a chloride bridged binuclear intermediate from one molecule of the starting compound, and one of the product complex ions.

One of the mechanisms which was tried involved the following reactions:

$$\underline{t}\text{-}[Pt(PEt_3)_2Cl_2] + NH_3 \xrightarrow{k_1} \underline{t}\text{-}[Pt(PEt_3)_2(NH_3)Cl]^+ + Cl^-$$

$$\underline{t}\text{-}[Pt(PEt_3)_2(NH_3)Cl]^+ + NH_3 \underset{k_{-2}}{\overset{k_2}{\rightleftharpoons}} \underline{t}\text{-}[Pt(PEt_3)_2(NH_3)_2]^{2+} + Cl^-$$

$$\underline{t}\text{-}[Pt(PEt_3)_2(NH_3)_2]^{2+} + \underline{t}\text{-}[Pt(PEt_3)_2Cl_2] \underset{k_{-1i}}{\overset{k_{1i}}{\rightleftharpoons}}$$

$$\underline{t}\text{-}[(PEt_3)_2(NH_3)\ PtClPt(PEt_3)_2Cl]^{2+} + NH_3$$

$$\underline{t}\text{-}[(PEt_3)_2(NH_3)PtClPt(PEt_3)_2Cl]^{2+} + NH_3 \xrightarrow{k_{2i}}$$

$$2\underline{t}\text{-}[Pt(PEt_3)_2(NH_3)Cl]^+.$$

This mechanism was rejected because it could not duplicate the induction period. The reason for this was that the diammine product was used up as fast as it was formed, so that the buildup to the concentration necessary for the approximate doubling of reaction rate was never achieved. Thus, the material responsible for the enhancement of the reaction rate must have increasing concentration during the reaction if there is to be the induction period followed by the increased rate of reaction.

The two following reaction sequences were also used in treating the experimental data. Each involved the formation of a chloride bridged binuclear intermediate between the starting material and one of the reaction products. Each was found capable of giving a close approximation to the experimental results, except for a major shortcoming which will be treated subsequent to the formulation of the reactions involved in each. For the first of the two, the intermediate is formed by a reaction between the first reaction product and the starting compound:

$$\underline{t}\text{-}[Pt(PEt_3)_2Cl_2] + NH_3 \xrightarrow{k_1} \underline{t}\text{-}[Pt(PEt_3)_2(NH_3)Cl]^+ + Cl^-$$

$$\underline{t}\text{-}[Pt(PEt_3)_2Cl_2] + \underline{t}\text{-}[Pt(PEt_3)_2(NH_3)Cl]^+ \underset{k_{-1i}}{\overset{k_{1i}}{\rightleftharpoons}}$$

$$\underline{t}[(PEt_3)_2ClPtClPt(PEt_3)_2(NH_3)]^{2+} + Cl^-$$

$$\underline{t}\text{-}[(PEt_3)_2ClPtClPt(PEt_3)_2(NH_3)]^{2+} + NH_3 \xrightarrow{k_{2i}}$$

$$2t\text{-}[Pt(PEt_3)_2(NH_3)Cl]^+$$

$$\underline{t}\text{-}[Pt(PEt_3)_2(NH_3)Cl]^+ + NH_3 \underset{k_{-2}}{\overset{k_2}{\rightleftharpoons}}$$

$$\underline{t}[Pt(PEt_3)_2(NH_3)_2]^{2+} + Cl^-,$$

For the sake of brevity, the concentration of

$\underline{t}\text{-}[(PEt_3)_2ClPtClPt(PEt_3)_2(NH_3)]^{2+}$ will be written as

$[Pt_2(PEt_3)_4(NH_3)Cl_2]^{2+}$ in the treatment which follows.

The rate equations of interest here are:

$$\frac{d[Pt(PEt_3)_2(NH_3)Cl]^+}{dt} = k_1[NH_3]\ [Pt(PEt_3)_2Cl_2]$$

$$-k_{1i}[Pt(PEt_3)_2Cl_2]\ [Pt(PEt_3)_2(NH_3)Cl]^+$$

$$+ k_{-1i}[Cl]\ [Pt_2(PEt_3)_4(NH_3)Cl_2]^{2+}$$

$$+2k_{2i}[NH_3]\ [Pt_2(PEt_3)_4(NH_3)Cl_2]^{2+}$$

$$- k_2[NH_3]\ [Pt(PEt_3)_2(NH_3)Cl]^+$$

$$+k_{-2}[Cl^-]\ [Pt(PEt_3)_2(NH_3)_2]^{2+},$$

$$\frac{d[Pt_2(PEt_3)_4(NH_3)Cl_2]^{2+}}{dt} = k_{1i}[Pt(PEt_3)_2Cl_2]$$

$$[Pt(PEt_3)_2(NH_3)Cl]^+$$

$$-k_{-1i}[Cl^-]\ [Pt_2(PEt_3)_4(NH_3)Cl_2]^{2+}$$

$$-k_{2i}[NH_3]\ [Pt_2(PEt_3)_4(NH_3)Cl_2]^{2+},$$

$$\frac{d[Pt(PEt_3)_2(NH_3)_2]^{2+}}{dt} = k_2[NH_3]\ [Pt(PEt_3)_2(NH_3)Cl]^+$$

$$-k_{-2}[Cl^-]\ [Pt(PEt_3)_2(NH_3)_2]^{2+}\ .$$

The steady-state approximation, that the concentration of the intermediate is always very small, and that consequently its rate of change can be made approximately equal to zero, was used to resolve the above three rate equations into their final form (i.e. $d[Pt_2(PEt_3)_4(NH_3)Cl_2]^{2+}/dt \approx 0$, so that the second of the above equations can be solved for $[Pt_2(PEt_3)_4(NH_3)Cl_2]^{2+}$):

$$\frac{d[Pt(PEt_3)_2(NH_3)Cl]^+}{dt} = k_1[NH_3]\ [Pt(PEt_3)_2Cl_2]$$

$$+ \frac{k_{1i}[NH_3]\ [Pt(PEt_3)_2Cl_2]\ [Pt(PEt_3)_2(NH_3)Cl]^+}{(k_{-1i}/k_{2i})\ [Cl^-] + [NH_3]}$$

$$-k_2[NH_3]\ [Pt(PEt_3)_2(NH_3)Cl]^+$$

$$+ k_{-2}[Cl^-]\ [Pt(PEt_3)_2(NH_3)_2]^{2+}$$

$$\frac{d[Pt(PEt_3)_2(NH_3)_2]^{2+}}{dt} = k_2[NH_3]\ [Pt(PEt_3)_2(NH_3)Cl]^+$$

$$-k_{-2}[Cl^-][Pt(PEt_3)_2(NH_3)_2]^{2+}\ .$$

These two differential equations were used as arithmetic function statements in a Runge-Kutta numerical integration program. The resultant concentrations of the ionic complex species as a function of time were then introduced into Equation 3.9 in the same manner as was used for the t-$[Pt(PEt_3)(NH_3)Cl_2]$ reactions considered previously. The values for k_1, k_{1i}, k_{-1i}/k_{2i} (these two constants were used in the form of a ratio), k_2, k_{-2}, Λ_A and Λ_B were varied until a set of constants was obtained which would yield a good fit of the calculated conductance curve to the experimental conductance curve.

The same process was used for the following sequence of reactions:

$$\underline{t}\text{-}[Pt(PEt_3)_2Cl_2] + NH_3 \xrightarrow{k_1} \underline{t}\text{-}[Pt(PEt_3)_2(NH_3)Cl]^+ + Cl^-$$

$$\underline{t}\text{-}[Pt(PEt_3)_2(NH_3)Cl]^+ + NH_3 \underset{k_{-2}}{\overset{k_2}{\rightleftharpoons}} \underline{t}\text{-}[Pt(PEt_3)_2(NH_3)_2]^{2+} + Cl^-$$

$$\underline{t}\text{-}[Pt(PEt_3)_2Cl_2] + \underline{t}\text{-}[Pt(PEt_3)_2(NH_3)_2]^{2+} \underset{k_{-1i}}{\overset{k_{1i}}{\rightleftharpoons}} \underline{t}\text{-}[(PEt_3)_2ClPtClPt(PEt_3)_2(NH_3)_2]^{2+}$$

$$\underline{t}\text{-}[(PEt)_2ClPtClPt(PEt_3)_2(NH_3)_2]^{2+} + NH_3 \xrightarrow{k_{2i}} \underline{t}\text{-}[Pt(PEt_3)_2(NH_3)Cl]^+ + \underline{t}\text{-}[Pt(PEt_3)_2(NH_3)_2]^{2+} + Cl^-$$

For the sake of brevity, the concentration of $\underline{t}\text{-}[(PEt_3)_2ClPtClPt(PEt_3)_2(NH_3)_2]^{2+}$ will be written as $[Pt_2(PEt_3)_4(NH_3)_2Cl_2]^{2+}$ in the treatment which follows.

The rate equations for these reactions are:

$$\frac{d[Pt(PEt_3)_2(NH_3)Cl]^+}{dt} = k_1[NH_3][Pt(PEt_3)_2Cl_2] - k_2[NH_3][Pt(PEt_3)_2(NH_3)Cl]^+ + k_{-2}[Cl^-][Pt(PEt_3)_2(NH_3)_2]^{2+} + k_{2i}[NH_3][Pt_2(PEt_3)_4(NH_3)_2Cl_2]^{2+},$$

$$\frac{d[Pt_2(PEt_3)_4(NH_3)_2Cl_2]^{2+}}{dt} = k_{1i}[Pt(PEt_3)_2Cl_2]$$
$$[Pt(PEt_3)_2(NH_3)_2]^{2+}$$
$$-k_{-1i}[Pt_2(PEt_3)_4(NH_3)_2Cl_2]^{2+}$$
$$-k_{2i}[NH_3][Pt_2(PEt_3)_4(NH_3)_2Cl_2]^{2+},$$

$$\frac{d[Pt(PEt_3)_2(NH_3)_2]^{2+}}{dt} = k_2[NH_3][Pt(PEt_3)_2(NH_3)Cl]^{+}$$
$$-k_{-2}[Cl^-][Pt(PEt_3)_2(NH_3)_2]^{2+}$$
$$-k_{1i}[Pt(PEt_3)_2Cl_2][Pt(PEt_3)_2(NH_3)_2]^{2+}$$
$$+k_{-1i}[Pt_2(PEt_3)_4(NH_3)_2Cl_2]^{2+}$$
$$+k_{2i}[NH_3][Pt_2(PEt_3)_4(NH_3)_2Cl_2]^{2+}.$$

Again applying the steady-state approximation, the following equations result:

$$\frac{d[Pt(PEt_3)_2(NH_3)Cl]^{+}}{dt} = k_1[NH_3][Pt(PEt_3)_2Cl_2]$$
$$-k_2[NH_3][Pt(PEt_3)_2(NH_3)Cl]^{+}$$
$$+k_{-2}[Cl^-][Pt(PEt_3)_2(NH_3)_2]^{2+}$$
$$+\frac{k_{1i}[NH_3][Pt(PEt_3)_2Cl_2][Pt(PEt_3)_2(NH_3)_2]^{2+}}{(k_{-1i}/k_{2i}) + [NH_3]}$$

$$\frac{d[Pt(PEt_3)_2(NH_3)_2]^{2+}}{dt} = k_2[NH_3][Pt(PEt_3)_2(NH_3)Cl]^+ - k_{-2}[Cl^-][Pt(PEt_3)_2(NH_3)_2]^{2+}.$$

These latter two equations were used in a numerical integration routine in the same manner as the preceding proposed reaction sequence.

It will be noted that the intermediate in this latter set of reactions involves a five-fold coordinated Pt(II). While such a coordination would not be expected to remain in solution for any great length of time, its existence for the length of time required for further reaction with an NH_3 from the solution is the only requirement.

Both of the two preceding sets of rate equations were found capable of closely approximating the experimental conductances with certain limitations. For example, using the last set of rate equations, a single set of constants could be found which would closely fit a calculated conductance curve to an experimental conductance curve for experiments in which the initial NH_3 and KCl concentrations were varied, just as long as each experiment had the same initial substrate concentration. As soon as the initial coordination compound concentration was changed, the calculated conductance curve would diverge widely from the experimental curve in the region after the induction period.

Given a set of constants which would replicate the experimental data for a certain initial complex concentration with a variety of concentrations for the other components, if the initial complex concentration was increased, then this set of constants would yield too high a calculated reaction rate after the induction period. If this same set of constants were used for an experiment which had a lower initial substrate concentration, then the calculated reaction would proceed at a slower rate than the experimental rate, after the induction period. Because no set of constants could be found which would duplicate the experimental data over the range of experimental conditions, these last two proposed mechanisms were also taken to be inadequate to describe the system. The experimental data can still yield some of the rate constants for the reactions, however, as will be shown below.

While the full rate equations for the reactions could not be found, some assumptions concerning the nature of the ammonation reaction during the induction period and concerning the nature of the second ammonation reaction allows an estimate to be made of the rate constants, k_1, k_2, and k_{-2} for Equations 3.12 and 3.13. The initial treatment of the data for the ammonation of $\underline{t}$-$[Pt(PEt_3)_2Cl_2]$ was the same as the treatment of the $\underline{t}$-$[Pt(NH_3)_2Cl_2]$ data: the linear

portion of the conductance curve corresponding to the leaching out of ions from the glass container was extrapolated back to zero time, and was subtracted from the conductance curve to yield $L(\infty)-L(t)$, where $L(t) \equiv \frac{1}{R(t)}$. Figure 17a shows a conductance *vs.* time plot for one of the experiments, with the extrapolation of the linear portion of the curve back to zero time also indicated. This extrapolated line was used as the $L(\infty)$ values. The values for $L(\infty)-L(t)$ obtained in this way were then plotted as a function of time, as is illustrated in Figure 17b. The assumption was then made that the first ammonation reaction was completed long before the second ammonation reaction reached equilibrium. This assumption was based on the evidence previously cited, as well as on analogy with the other two compounds of this study. This assumption also is in accord with the generalization for aqueous systems that the reaction rate of a Cl^- ligand *trans* to a Cl^- ligand is approximately ten times greater the reaction rate of a Cl^- ligand *trans* to an NH_3 ligand. On the basis of this assumption, an observed pseudo-first-order rate constant for the approach to equilibrium was obtained in the same manner that the observed pseudo-first-order rate constant was determined in the case of the second ammonation reaction of *t*-$[Pt(NH_3)_2Cl_2]$. Figure 17b also shows the extrapolation of the linear portion of the $\log[L(\infty)-L(t)]$ *vs.* t plot which corresponds to the

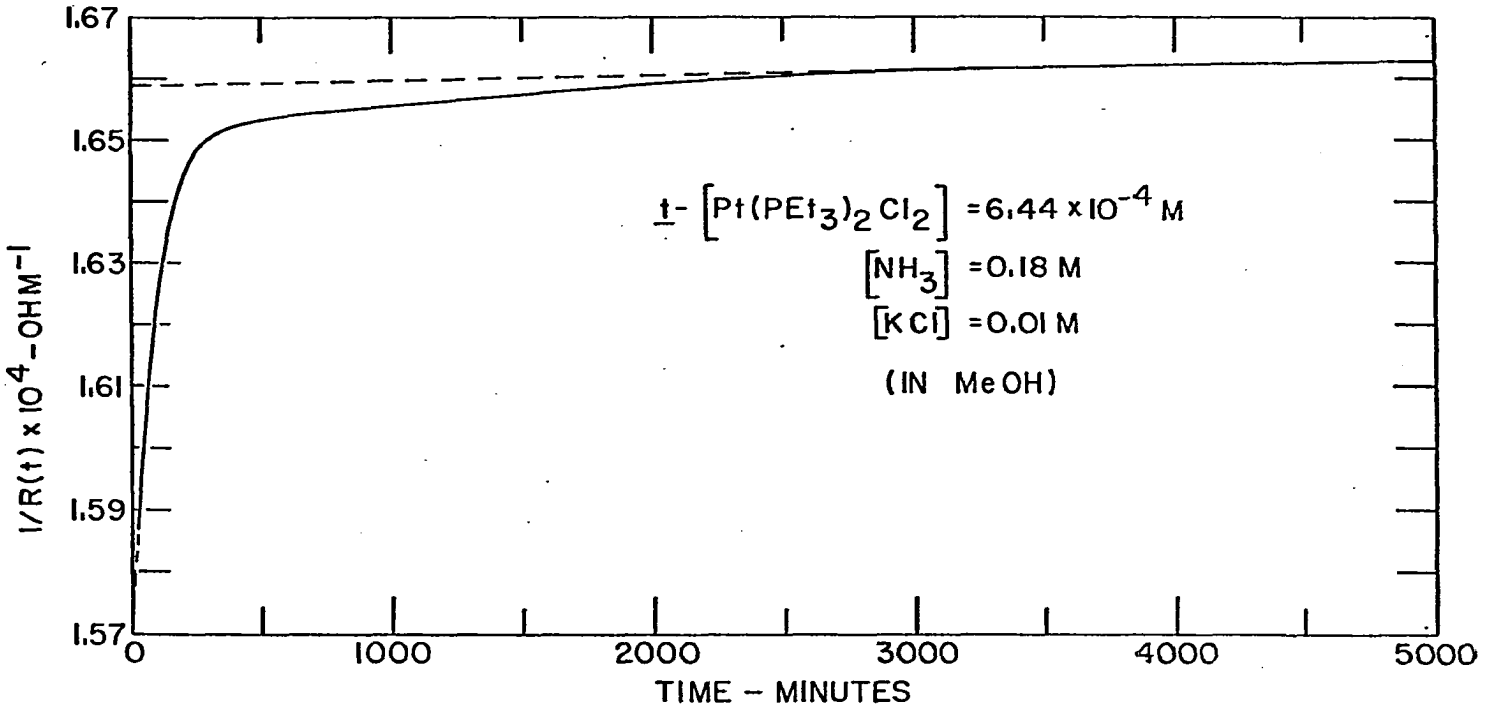

Figure 17a. Conductance plot for a t-$[Pt(PEt_3)_2Cl_2]$ ammonation experiment at 35°C. The extrapolated straight line was used as the conductance values at infinite time in further treatment of the data. The time is the elapsed reaction time

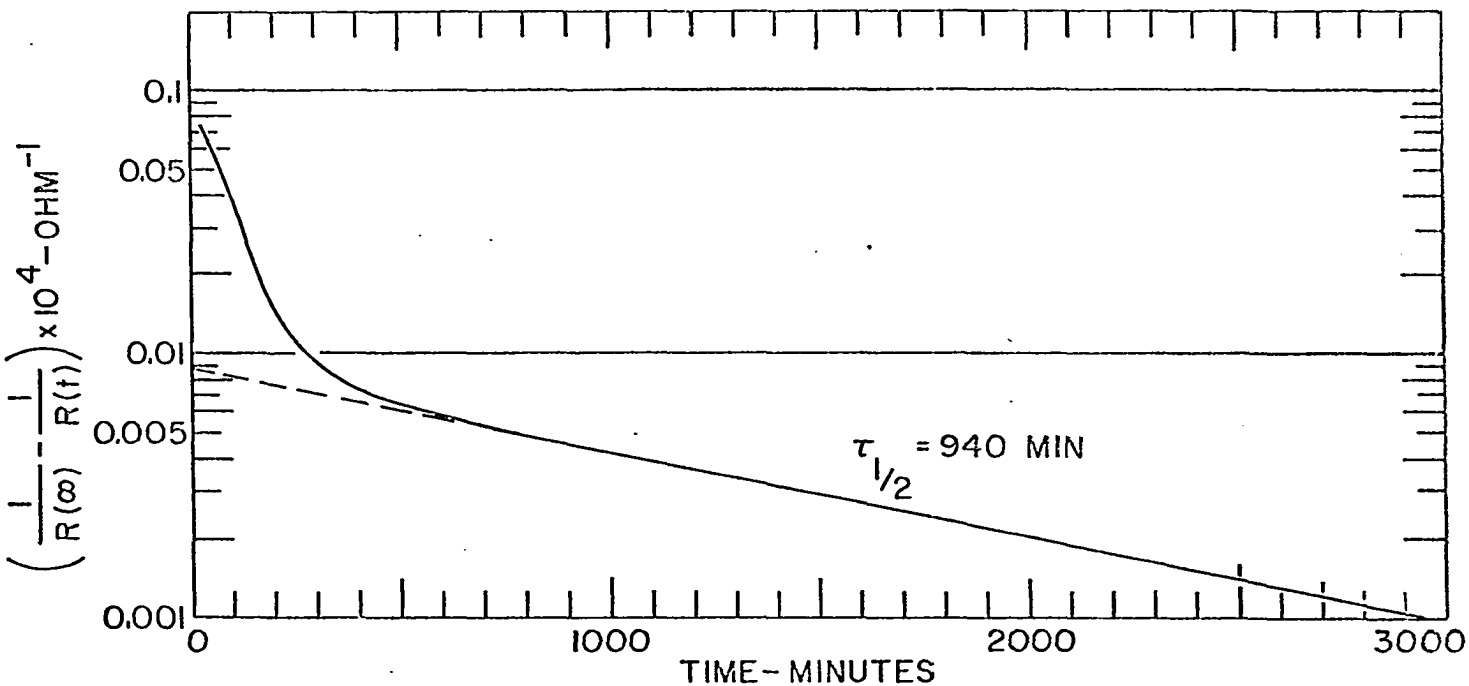

Figure 17b. Semilog plot of the conductance(∞) minus the conductance(t) vs. the elapsed reaction time for the experiment given in Figure 17a. The extrapolated portion is the reversible ammonation reaction at long times. The extrapolation intercept is the value of $((2\Lambda_C - \Lambda_B)[Pt(PEt_3)_2(NH_3)_2]^{2+}_{eq})/1000k$ used in determining the rate constant, k_1

reactions given in Equation 3.13. The interpretation of the slope of this line is not the same as the interpretation for t-$[Pt(NH_3)_2Cl_2]$, however, because an equilibrium reaction is now involved. In terms of the pseudo-first-order rate constants, the rate equation which represents the system during this phase of the reaction is,

$$\frac{d[Pt(PEt_3)_2(NH_3)_2]^{2+}}{dt} = k_2'[Pt(PEt_3)_2(NH_3)Cl]^+ - k_{-2}'[Pt(PEt_3)_2(NH_3)_2]^{2+} .$$

The concentration equation which holds for any time during the reaction is,

$$[Pt(PEt_3)_2Cl_2]_0 = [Pt(PEt_3)_2Cl_2] + [Pt(PEt_3)_2(NH_3)Cl]^+ + [Pt(PEt_3)_2(NH_3)_2]^{2+} .$$

This equation includes the assumption that the concentration of any other Pt(II) species in the solution is negligible. During the phases of the reaction when the first ammonation reaction can be assumed to be completed, this relationship between the complex concentrations becomes,

$$[Pt(PEt_3)_2(NH_3)Cl]^+ = [Pt(PEt_3)_2Cl_2]_0 - [Pt(PEt_3)_2(NH_3)_2]^{2+} . \quad (3.14)$$

When Equation 3.14 is substituted into the differential equation, that equation can be integrated to yield,

$$[Pt(PEt_3)_2(NH_3)_2]^{2+} =$$

$$[Pt(PEt_3)_2Cl_2]_0 \left(\frac{k_2'}{k_2'+k_{-2}'}\right)\{1-\exp[-(k_2'+k_{-2}')t]\} .$$

The equilibrium concentration of this reaction product then becomes,

$$[Pt(PEt_3)_2(NH_3)_2]^{2+}_{eq} = [Pt(PEt_3)_2Cl_2]_0 \left(\frac{k_2'}{k_2'+k_{-2}'}\right) .$$

The form of the conductance equation, Equation 3.2, which applies to the ammonation reactions of $\underline{t}$-$[Pt(PEt_3)_2Cl_2]$ at any time t is,

$$L(t)=L(0) + \frac{1}{1000k}(\Lambda_B[Pt(PEt_3)_2(NH_3)Cl]^+ + 2\Lambda_C[Pt(PEt_3)_2(NH_3)_2]^{2+}) \qquad (3.15)$$

and at equilibrium,

$$L(\infty)=L(0) + \frac{1}{1000k}(\Lambda_B[Pt(PEt_3)_2(NH_3)Cl]^+_{eq} + 2\Lambda_C[Pt(PEt_3)_2(NH_3)_2]^{2+}_{eq}) . \qquad (3.16)$$

Substitution of the relationship given in Equation 3.14, which holds true during the late phases of the reactions and at equilibrium, into Equations 3.15 and 3.16 results in the equation for $L(\infty)-L(t)$ during the late phases of the ammonation reactions,

$$L(\infty)-L(t)= \frac{1}{1000k}(2\Lambda_C-\Lambda_B)([Pt(PEt_3)_2(NH_3)_2]^{2+}_{eq} - [Pt(PEt_3)_2(NH_3)_2]^{2+}) .$$

When the integrated form of the rate equation is introduced along with the equation for the equilibrium concentration this equation becomes,

$$L(\infty)-L(t)=\frac{1}{1000k}\,(2\Lambda_C-\Lambda_B)\,[Pt(PEt_3)_2(NH_3)_2]^{2+}_{eq}$$

$$\exp[-(k'_2+k'_{-2})t]. \qquad (3.17)$$

Thus, a plot of log $[L(\infty)-L(t)]$ *vs.* t during this portion of the reaction system has a slope of $-(k'_2+k'_{-2})$, and an intercept at t=0 of $((2\Lambda_C-\Lambda_B)/1000k)\,[Pt(PEt_3)_2(NH_3)_2]^{2+}_{eq}$. By means of a series of experiments in which $[Cl^-]$ is the same and $[NH_3]$ has been varied, a set of observed rate constants, $k'_2+k'_{-2}$, is obtained which is a function of $[NH_3]$, $k_2[NH_3]+k'_{-2}$, with k'_{-2} remaining constant. A plot of this set of observed rate constants as a function of $[NH_3]$ is a line with a slope k_2, and an intercept of k'_{-2}. Division of the intercept by the $[Cl^-]$ concentration, which was the same for each experiment in the series, yields k_{-2}.

Substitution of the equilibrium form of Equation 3.14 and the general concentration equation into the appropriate places in Equations 3.15 and 3.16 leads to the general equation for L(∞)-L(t), which is valid at any time,

$$L(\infty)-L(t)=\frac{1}{1000k}[\Lambda_B[Pt(PEt_3)_2Cl_2]$$
$$+\,(2\Lambda_C-\Lambda_B)([Pt(PEt_3)_2(NH_3)_2]^{2+}_{eq}$$
$$-[Pt(PEt_3)_2(NH_3)_2]^{2+})]. \qquad (3.18)$$

It will be noted, however, that Equation 3.18 contains the intercept at t=0 of Equation 3.17. If the intercept of Equation 3.17 is subtracted from Equation 3.18, the resultant equation is,

$$\delta[L(\infty)-L(t)] = \frac{1}{1000K}[\Lambda_B[Pt(PEt_3)_2Cl_2]-(2\Lambda_C-\Lambda_B)[Pt(PEt_3)_2(NH_3)_2]^{2+}].$$

The time derivative of the log of this equation is,

$$\frac{d\ \log[\delta(L(\infty)-L(t))]}{dt} =$$

$$\frac{\Lambda_B d[Pt(PEt_3)_2Cl_2]/dt-(2\Lambda_C-\Lambda_B)d[Pt(PEt_3)_2(NH_3)_2]^{2+}/dt}{\Lambda_B[Pt(PEt_3)_2Cl_2]-(2\Lambda_C-\Lambda_B)[Pt(PEt_3)_2(NH_3)_2]^{2+}}$$

As t approaches zero, the concentration and time derivative of $\underline{t}$-$[Pt(PEt_3)_2(NH_3)_2]^{2+}$ both approach zero, so at this limit this equation becomes,

$$\left.\frac{d\ \log[\delta(L(\infty)-L(t))]}{dt}\right|_0 = \frac{\Lambda_B d[Pt(PEt_3)_2Cl_2]/dt|_0}{\Lambda_B[Pt(PEt_3)_2Cl_2]_0} \quad (3.19)$$

The experimental evidence seems to indicate that at t=0 the only reaction taking place is the uncatalyzed first ammonation reaction. If this is assumed to be true, then as t approaches zero,

$$\left.\frac{d[Pt(PEt_3)_2Cl_2]}{dt}\right|_0 = -k_1'[Pt(PEt_3)_2Cl_2]_0 ,$$

where k_1' is the pseudo-first-order rate constant. Substitu-

tion of this equation into Equation 3.19 gives the final relationship,

$$\left.\frac{d \log[\delta(L(\infty)-L(t))]}{dt}\right|_0 = -k_1' \quad . \qquad (3.20)$$

Equation 3.20 can now be used to estimate the rate constant for the initial second-order ammonation reaction, k_1.

The experimental data for the ammonation reactions of $\underline{t}$-$[Pt(PEt_3)_2Cl_2]$ was treated in the manner indicated by the steps leading to Equation 3.20: the linear portion of a $\log[L(\infty)-L(t)]$ *vs.* t plot at long times (*cf.* Figure 17b) was extrapolated back to zero time to give the intercept $\log[(2\Lambda_C-\Lambda_B)[Pt(PEt_3)_2(NH_3)_2]^{2+}_{eq}/1000\ k]$; the antilog of this intercept was subtracted from the $L(\infty)-L(t)$ values, and a $\log[\delta(L(\infty)-L(t))]$ *vs.* t plot was made. Each set of experimental data was subjected to this treatment, and the pseudo-first-order rate constants procured by taking the initial slope of the $\log[\delta(L(\infty)-L(t))]$ *vs.* t plots were plotted as a function of NH_3 concentration. The slope of this k_1' *vs.* $[NH_3]$ plot is the rate constant k_1 for the simple first ammonation reaction which occurs before any catalysis of the reaction begins. There is, perforce, some inherent error in the pseudo-first-order rate constants gained in this manner, because the nature of the handling and measuring technique precluded meaningful measurements during the early minutes of the reactions. At low NH_3

concentrations, however, the errors from this source would be minimized because of the slower reaction rates, so heavier weighting was given to the points at low $[NH_3]$ on the k_1' *vs.* $[NH_3]$ plot.

The observed pseudo-first-order rate constants, k_1' and $k_2'+k_{-2}'$, and the initial concentrations for each experiment are given in Table 6, along with the second-order rate constants, k_1, k_2, and k_{-2} at both 25° and 35°C, and the activation parameters for the reactions at 25°C.

The same assumptions about the nature of the initial ammonation reaction and about the nature of the equilibrium reactions were made in treating the spectrophotometric data. The data was analyzed in the following manner. The equation for the absorbance, A, of the solution at any time t, and at any wavelength when a 1 cm spectrophotometric cell is used is,

$$A=\varepsilon_A[Pt(PEt_3)_2Cl_2]+\varepsilon_B[Pt(PEt_3)_2(NH_3)Cl]^+$$

$$+\varepsilon_C[Pt(PEt_3)_2(NH_3)_2]^{2+}, \qquad (3.21)$$

where the ε's are the extinction coefficient for the complex with which they are associated, and the brackets denote the concentration of the compound at any time t. When the first reaction has gone to completion, and the equilibrium has been established this equation becomes,

Table 5. Ammonation of t-$[Pt(PEt_3)_2Cl_2]$

Temp °C	$[Pt(PEt_3)_2Cl_2]$ mM	$[NH_3]_0$ mM	$[KCl]_0$ mM	$10^5 \times k'_1$ sec^{-1}	$10^5 \times (k'_2 + k'_{-2})$ sec^{-1}
25[a]	0.334	1220	10	30.4[b]	2.18[c]
	0.441	142	10	3.68	0.333
	0.664	1020	10	24.5	2.34
	0.812	1260	10	33.5	2.74
	0.874	814	10	21.1	1.39
	0.899	830	10	18.8	1.84
35	0.282	82	10	5.09[d]	-[e]
	0.297	445	10	30.8	2.18[f]
	0.593	364	10	24.8	1.50
	0.627	604	10	43.3	2.02
	0.642	40.9	10	2.77	0.623
	0.642	83.5	10	5.23	1.18
	0.644	180	10	11.1	1.23

[a]At 25°C: for the first ammonation reaction, $\Delta H^{\ddagger}$ = 18 kcal/mole $\Delta G^{\ddagger}$= 22 kcal/mole, $\Delta S^{\ddagger}$ = -14 cal/mole-deg; the activation parameters for the equilibrium reaction were not calculated because of the uncertainty in the rate constants.

[b]From the computer least-squares fit of these values to the equation $k'_1=[NH_3]k_1$, $k_1(25^0)=2.50 \times 10^{-4} \pm 0.06 \times 10^{-4}$ M^{-1} sec^{-1}.

[c]These values did not lend themselves to a least squares treatment. The graphically estimated values are $k_2(25^0) \approx 2 \times 10^{-5} M^{-1} sec^{-1}$, $k_{-2}(25^0) \approx 3 \times 10^{-4} M^{-1} sec^{-1}$.

[d]From the computer least-squares fit of these values to the equation $k'_1=[NH_3]k_1$, $k_1(35^0)=7.0 \times 10^{-4} \pm 0.3 \times 10^{-4}$ $M^{-1} sec^{-1}$.

[e]A reliable value was not obtained.

[f]From the computer least-squares fit of these values to the equation $k'_2 + k'_{-2}=[NH_3]k_2 + [Cl^-]k_{-2}$, where only experiments with $[Cl^-]$ = 0.01M were used, $k_2(35^0)=2.2 \times 10^{-5} \pm 0.6 \times 10^{-5} M^{-1} sec^{-1}$, $k_{-2}(35^0)=9 \times 10^{-4} \pm 2 \times 10^{-4} M^{-1} sec^{-1}$.

Table 5 (Continued)

Temp °C	$[Pt(PEt_3)_2Cl_2]_0$ mM	$[NH_3]_0$ mM	$[KCl]_0$ mM	$10^5 \times k'_1$ mM	$10^5 \times (k'_2 + k'_{-2})$ mM
	0.893[h]	111	10	6.19	2.33[g]
	0.165[h]	196	10	9.13	1.85
	0.644[i]	320	30	27.8	3.79[g]
	0.632[j]	282	10	19.6	1.30
	0.639[k]	357	10	30.7	1.77
	0.608[l]	201	10	10.4	1.94[g]
	0.627[m]	202	10	9.67	2.08[g]
	0.650[n]	199	10	13.1	2.05[g]
	0.651[n]	218	10	21.6[o]	2.11[g]

[g]This value not included in least-squares determination of k_2 and k_{-2}.

[h]Measurements were made with a spectrophotomer.

[i]Solution aged approximately 12 hours in MeOH-KCl solution prior to addition of NH_3 solution.

[j]Contained 2% by volume of H_2O.

[k]Contained 0.165×10^{-4}M t-$[Pt(PEt_3)_2Cl_4]$ (cf. Table 4).

[l]Contained 0.213×10^{-4}M t-$[Pt(PEt_3)_2(H)Cl]$ (cf. Table 4).

[m]Contained 0.242×10^{-4}M c-$[Pt(PEt_3)_2Cl_2]$ (cf. Table 4).

[n]Contained 0.238×10^{-4}M of an equilibrium mixture of t-$[Pt(PEt_3)_2(NH_3)Cl]^+$ and t-$[Pt(PEt_3)_2(NH_3)_2]^{2+}$ (cf. Table 4).

[o]This value not included in least-squares determination of k_1.

$$A_{eq}=\varepsilon_B[Pt(PEt_3)_2(NH_3)Cl]^+_{eq} + \varepsilon_C[Pt(PEt_3)_2(NH_3)_2]^{2+}_{eq} . \quad (3.22)$$

The concentration of t-$[Pt(PEt_3)_2(NH_3)Cl]^+$ at any t and at equilibrium can be expressed as,

$$[Pt(PEt_3)_2(NH_3)Cl]^+=[Pt(PEt_3)_2Cl_2]_0-[Pt(PEt_3)_2Cl_2] - [Pt(PEt_3)_2(NH_3)_2]^{2+} , \quad (3.23)$$

$$[Pt(PEt_3)_2(NH_3)Cl]^+_{eq}=[Pt(PEt_3)_2Cl_2]_0-[Pt(PEt_3)_2(NH_3)_2]^{2+}_{eq}. \quad (3.24)$$

Substitution of these two equations into Equation 3.21 and 3.22, and the subtraction of Equation 3.22 from Equation 3.21 yields,

$$A-A_{eq} = (\varepsilon_A-\varepsilon_B)\ [Pt(PEt_3)_2Cl_2] + (\varepsilon_C-\varepsilon_B)([Pt(PEt_3)_2(NH_3)_2]^{2+}-[Pt(PEt_3)_2(NH_3)_2]^{2+}_{eq}) \quad (3.25)$$

The slope of the log of Equation 3.25 is

$$\frac{d(A-A_{eq})}{dt} = \frac{(\varepsilon_A-\varepsilon_B)d[Pt(PEt_3)_2Cl_2]/dt+(\varepsilon_C-\varepsilon_B)d[Pt(PEt_3)_2(NH_3)_2]^{2+}/dt}{(A-A_{eq})} \quad (3.26)$$

At t=0, $[Pt(PEt_3)_2(NH_3)_2]^{2+}=0$, $[Pt(PEt_3)_2Cl_2]=[Pt(PEt_3)_2Cl_2]_0$, $d[Pt(PEt_3)_2(NH_3)_2]^{2+}/dt=0$, and $d[Pt(PEt_3)_2Cl_2]/dt = -k_1'[Pt(PEt_3)_2Cl_2]_0$. The equilibrium quotient can be re-

arranged to give,

$$[Pt(PEt_3)_2(NH_3)_2]^{2+}_{eq} = \frac{k_2'}{k_2'+k_{-2}'}[Pt(PEt_3)_2Cl_2]_0 \qquad (3.27)$$

Substitution of Equation 3.27 into Equation 3.26, and imposition of the boundary conditions at t=0 results in,

$$\left.\frac{d(A-A_{eq})}{dt}\right|_0 = \frac{-k_1'}{1 - [(\varepsilon_C-\varepsilon_B)k_2'/(\varepsilon_A-\varepsilon_B)(k_2'+k_{-2}')]} \qquad (3.28)$$

The constants k_2' and k_{-2}' were determined previously, and with these the equilibrium concentrations can be determined from Equations 3.24 and 3.27. The equilibrium concentrations and the absorbance of the solution at equilibrium allowed limits to be placed on the extinction coefficients ε_B and ε_C. The extinction coefficient for ε_A was determined from solutions of $\underline{t}$-$[Pt(PEt_3)_2Cl_2]$. Equation 3.28 was used for the changes in absorbance at 267 mμ. From these calculations it was found that the term in the denominator of Equation 3.26 which is a function of the ε's and k's had a maximum possible value of -0.15, when ε_B=0 at 267 mμ, and a value of +0.02 when ε_C=0 at 267 mμ. The changes in the spectrum at times when the $\underline{t}$-$[Pt(PEt_3)_2Cl_2]$ concentration would have been approximately zero indicated that the value of ε_B is probably larger than ε_C at 267 mμ, so the approximation was made that the function in the denominator of Equation 3.26 was equal to one. Therefore the initial slope

of a $\log(A - A_{eq})$ *vs.* t plot was used for $-k_1'$.

If Equation 3.25 is considered at a time when the first ammonation reaction has approximately gone to completion, the same approximations used to derive Equation 3.17 can be applied. Thus, at reactions times when the first ammonation reaction can be regarded as being completed, Equation 3.25 becomes,

$$A - A_{eq} = (\varepsilon_C - \varepsilon_B)[Pt(PEt_3)_2(NH_3)_2]^{2+}_{eq} \exp[-(k_2' + k_{-2}')t]$$

The time derivative of the log of this equation is,

$$\frac{d \log(A - A_{eq})}{dt} = -(k_2' + k_{-2}'). \qquad (3.29)$$

A plot of $\log(A - A_{eq})$ *vs.* t was made for the spectral changes at 233 mμ for times greater than 500 minutes. The negative of the slope of this plot is the value for $k'_2 + k'_{-2}$ for the spectrophotometric experiment in Table 5.

In the least-squares treatment of the observed rate constant, $k_2' + k_{-2}'$, at 35°C, several of the experimental values were excluded. One of the values was excluded because it was from an experiment which had 0.03 M KCl. Another was rejected because it was not statistically consistent with the other values. The last four entries in Table 5 were also rejected because they were not consistent with the other values, but with the difference that these were from the experiments that had added impurities in them.

The divergence of these values from the values from normal experiments could indicate that the second ammonation reaction may also be more complex than a simple second-order reversible reaction. The k_1' values from the initial slope of the resolved conductance curves for these last four experiments are included in the treatment for finding k_1, however, and are perfectly consistent with the other values. It is noted, in this context, that the initial slope of the resolved conductance plot to which the reaction products was added yielded an observed rate constant, k_1', which is approximately double the value which would be expected on the basis of the other observed rate constants.

The addition of ions to the solution by the reaction of NH_3 with MeOH is illustrated in Figure 18. The extrapolated intercept at t=0 which is plotted in Figure 18 was taken from L(t) *vs.* t plots for several *t*-$[Pt(PEt_3)_2Cl_2]$ ammonation experiments at 35°C, all of which had the same initial KCl concentration, but different initial NH_3 concentrations. The intercepts, L(0), have been plotted in Figure 18 as a function of the initial NH_3 concentration associated with the intercept. These additional ions will have some small effect upon ionic association, as has already been noted.

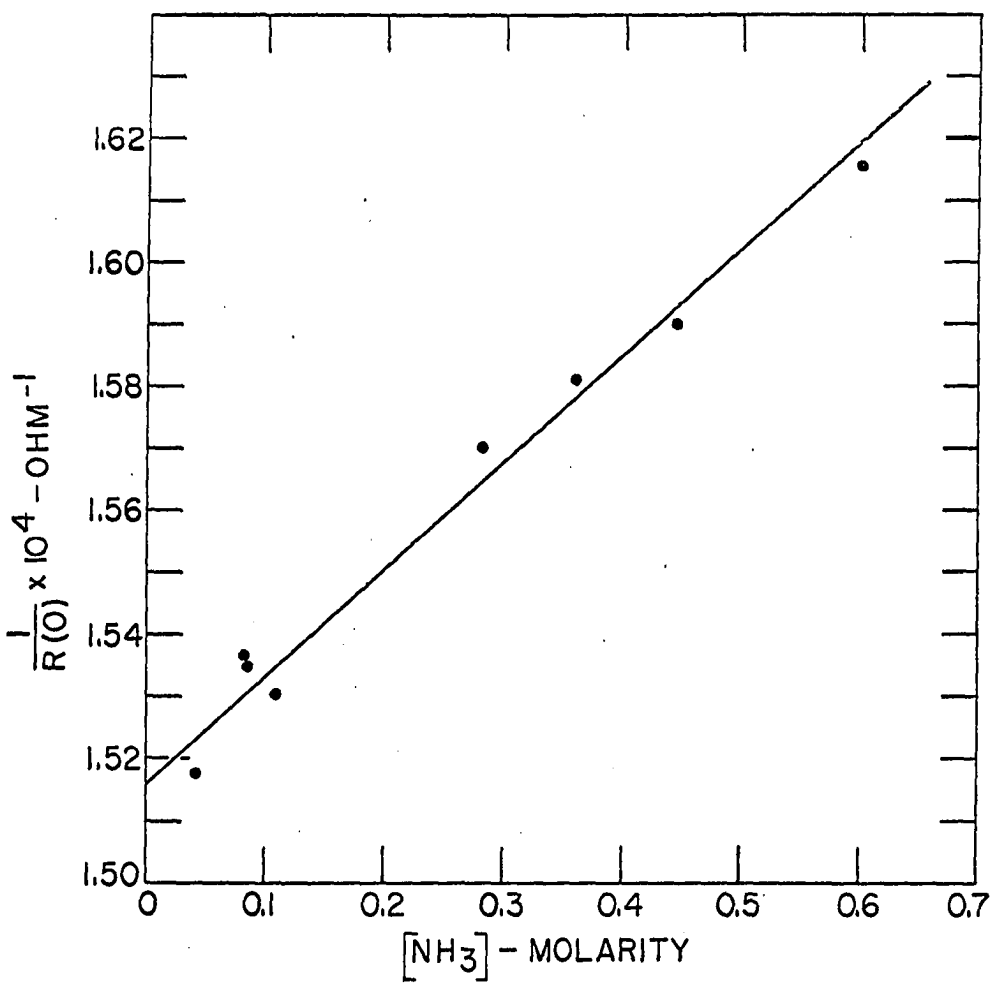

Figure 18. Intercepts of zero time extrapolation for the conductance plots of several t-$[Pt(PEt_3)_2Cl_2]$ ammonation experiments vs. the $[NH_3]$ in each experiment

DISCUSSION

The principal reason for initiating this study was to get further information concerning the influence of the ligands which are cis to the reaction site in the square-planar Pt(II) complexes. In previous studies at this laboratory, a comparison of reaction rates involving complexes with either NH_3 or Cl^- in the cis position indicated that there was a significant increase in rates of reaction when NH_3 was present in the cis position as compared to the same reaction when Cl^- was present in that position (cf. Table 1, for example). One of the objections voiced against comparisons involving complexes with NH_3 and Cl^- in the position cis to the reaction site was that both of these ligands were weak trans labilizing ligands, so that any comparison of their cis labilizing influence would tend to magnify the importance of the cis-effect. Indeed, for comparisons in such systems, the cis-effect could and sometimes did turn out to be more significant than the trans-effect.

The present research established conditions in which the cis influence of a strong trans-labilizing ligand, PEt_3, was compared with that of a weak trans-labilizing ligand, NH_3. According to the generalization of the Russian chemists that a strong trans-director is a weak cis-director, and

vice versa, there should have been a pronounced difference in reaction rates among the compounds in this study. For each of these complex compounds, the entering group, the leaving group, the solvent, the ligand trans to the leaving group, and the temperature were the same. While there were some variations in ionic strength, these variations were small, and a small range of similar ionic strengths was encountered in the reaction conditions for each complex. Therefore, the only significant difference between these compounds was the ligands cis to the reaction site. As can best be seen by comparing the second-order rate constants for the reactions of t-$[Pt(PEt_3)(NH_3)Cl_2]$ and t-$[Pt(NH_3)_2Cl_2]$, a pronounced difference in rate was not found. For the ammonation reactions at 35°C, k_1 = 14.2 x $10^{-4}M^{-1}sec^{-1}$ and k_2 = 1.2 x $10^{-4}M^{-1}sec^{-1}$ for t-$[Pt(PEt_3)(NH_3)Cl_2]$, while k_1 = 11 x $10^{-4}M^{-1}sec^{-1}$ and k_2 = 2.0 x $10^{-4}M^{-1}sec^{-1}$ for t-$[Pt(NH_3)_2Cl_2]$ (the difference in rate between the first and second ammonation reactions reflects the difference in the trans-effect of Cl^- as compared to NH_3). Even the estimated rate constants for t-$Pt(PEt_3)_2Cl_2$, $k_1(35^0)$= 7.0 x $10^{-4}M^{-1}sec^{-1}$ and $k_2(35^0)$ = 2 x $10^{-5}M^{-1}sec^{-1}$, do not differ from those of the other two complexes to the degree that has been observed when comparing the aqueous ammonation reactions for t-$[Pt(NH_3)_2Cl_2]$ with those for the two Cl^- ligands cis to NH_3 in

$[Pt(NH_3)Cl_3]$. Furthermore, the ammonation rates of t-$[Pt(PEt_3)_2Cl_2]$ are probably influenced more by steric considerations than by a cis-effect.

This is not meant to imply that the cis-effect is a chimera, because the solvolysis reaction of t-$[Pt(NH_3)_2Cl_2]$ with MeOH is clearly much larger than the solvolysis reactions of either t-$[Pt(PEt_3)(NH_3)Cl_2]$ or t-$[Pt(PEt_3)_2Cl_2]$, both of which reactions were too slow for detection in the present study. What has been shown is that there is no simple correlation between the trans- and cis-effects based solely on the relative positions of ligands in the trans labilizing series.

Oleari, di Sipio, and de Michelis (73) pointed out that the trans-effect cannot be stated solely in terms of a single ligand, because the group in the position trans to the trans labilizing ligand has an importance which becomes overwhelmingly apparent when the inert behavior of the PEt_3 ligands in t-$[Pt(PEt_3)_2Cl_2]$ is compared with the high trans labilization of PEt_3. This points up the necessity of including the leaving group when comparisons are made in the trans labilization of a ligand. The present research indicates that the nature of the entering group influences the relative position of ligands on a cis-effect scale. A similar finding was reported for the reactions of t-$[Pt(PEt_3)_2Cl_2]$ and t-$[Pt(py)_2Cl_2]$ with a

series of reagents (87). The rate constant for the solvolysis reaction with MeOH of t-$[Pt(py)_2Cl_2]$ was found to be orders of magnitude larger than that for t-$[Pt(PEt_3)_2Cl_2]$, but the rate constant for the reaction of t-$[Pt(PEt_3)_2Cl_2]$ with SCN^- was approximately twice that of t-$[Pt(py)_2Cl_2]$.

A recent trend in theories about the trans-effect coupled with recent thinking on generalized acid-base theory may help to elucidate some of the more important factors which must be taken into account for any ordering of ligands according to their cis-effect. The trend in trans-effect theories is the division into a σ-trans and a Π-trans-effect (26,27,52). The trend in acid-base theory is the hard-soft acid and base concept (43,109).

The division of the trans-effect into the σ- and Π-trans-effects, which was mentioned in the Introduction, has found support in the experimental results of infrared spectra (52) and nuclear magnetic resonance studies (110). Basically, this division of the trans-effect reconciles two diverse theories of the trans-effect by saying that each is correct in its own situation. Once this division has been made, then some progress is possible in sorting out the ligands in a cis-effect series as well. Those ligands which are properly of the Π-trans type reduce charge density in the tetragonal positions of the square-plane, and in this fashion facilitate the approach of the entering group and

cause the trigonal bipyramid intermediate to be stabilized. Such a ligand should produce much the same effect when it is in the position cis to the reaction site, although the less favorable directional characteristics in this cis position would mean that the effect would be much less pronounced.

The σ-trans labilization ligands are thought to cause labilization by partially shifting the electron density on the metal atom towards the ligand which is trans to them, and thus causing a weakening in the bond of the trans-ligand. The directionality of this weakening is explained by the strong σ-bonding of the trans labilizing ligand with the appropriate p orbital of Pt. It is plain that such a directional character in the σ system of the molecule will not be of too much moment when the reaction site is now cis to the strong σ-trans labilizer. The infrared stretching frequencies of ligands in Pt(II) compounds exhibit just such an independence with regard to a strong σ-trans ligand in the cis position (53).

On the basis of the above generalizations concerning the cis-effect of strong σ- and Π-trans labilizing groups, the PEt_3 ligand in the present study would be expected to have a moderate cis-effect because of its Π-bonding characteristics. This effect would not be as great as might be expected, however, because PEt_3 has a strong trans-effect

through a high σ-effect(111) combined with a Π-effect.

The behavior of NH_3 is not as amenable to explanation, however. The thermodynamic stability and the inertness of the Pt-NH_3 bond coupled with its low trans-effect make NH_3 a fairly unique ligand in Pt(II) chemistry. No current theory of the trans-effect or the cis-effect seems adequate to explain the behavior of NH_3.

The variation in the relative reaction rates of Pt(II) compounds as the entering group is changed is a perfect example of the operation of the hard-soft acid and base theory. A ligand such as NH_3 tends to be of the hard base classification, whereas PEt_3 would be more of a soft base. Pt(II) itself is a soft acid. A complex of Pt(II) which has PEt_3 coordinated to it would be a softer acid than a complex with NH_3 coordinated to it. By the principle of soft acids reacting with soft bases, a PEt_3 complex of Pt(II) would be expected to react more readily with a soft base than would an NH_3 complex, and vice versa for a reaction with a hard base. Thus, in comparing the reactions of coordination complexes the relative acid properties of the substrate and the entering group must also be taken into account.

The proposed mechanism for the ammonation reactions of t-$[Pt(PEt_3)(NH_3)Cl_2]$ and t-$[Pt(NH_3)_2Cl_2]$ is given in Figure 19. This mechanism is also proposed for the initial ammona-

tion reaction of t-[$Pt(PEt_3)_2Cl_2$] (i.e. the reaction during the induction period) and for the forward reaction of the equilibrium established in the second ammonation reaction. In Figure 19 both C and C' represent the appropriate PEt_3 or NH_3 ligand in the position cis to the reaction site (e.g. C = PEt_3,C' = NH_3 when the mechanism pictured in Figure 19 is applied to t-[$Pt(PEt_3)(NH_3)Cl_2$]. T is either Cl^- for the first ammonation, or NH_3 when the mechanism is applied to the second ammonation reaction. The MeOH above and below the square-plane are in the outer coordination sphere of the complex, weakly bound to the Pt(II). The weak bond of these outer sphere ligands has been represented by a light solid line in order to maintain a consistent symbolism for the geometry of the projection: a solid line represents a bond in the plane of the paper, a dashed line represents a bond at right angles to and going into the plane of the paper, and a tapering solid line a bond coming out of the plane at righ angles. The rate determining step in this mechanism is the formation of the trigonal-bipyramid coordination. The trigonal-bipyramid formed in this mechanism will be called a transition state herein, with note being made that some researchers tend to believe it is actually an intermediate (27,109).

The mechanism proposed in Figure 19 is in accord with the bimolecularity of the reactions of this study. The

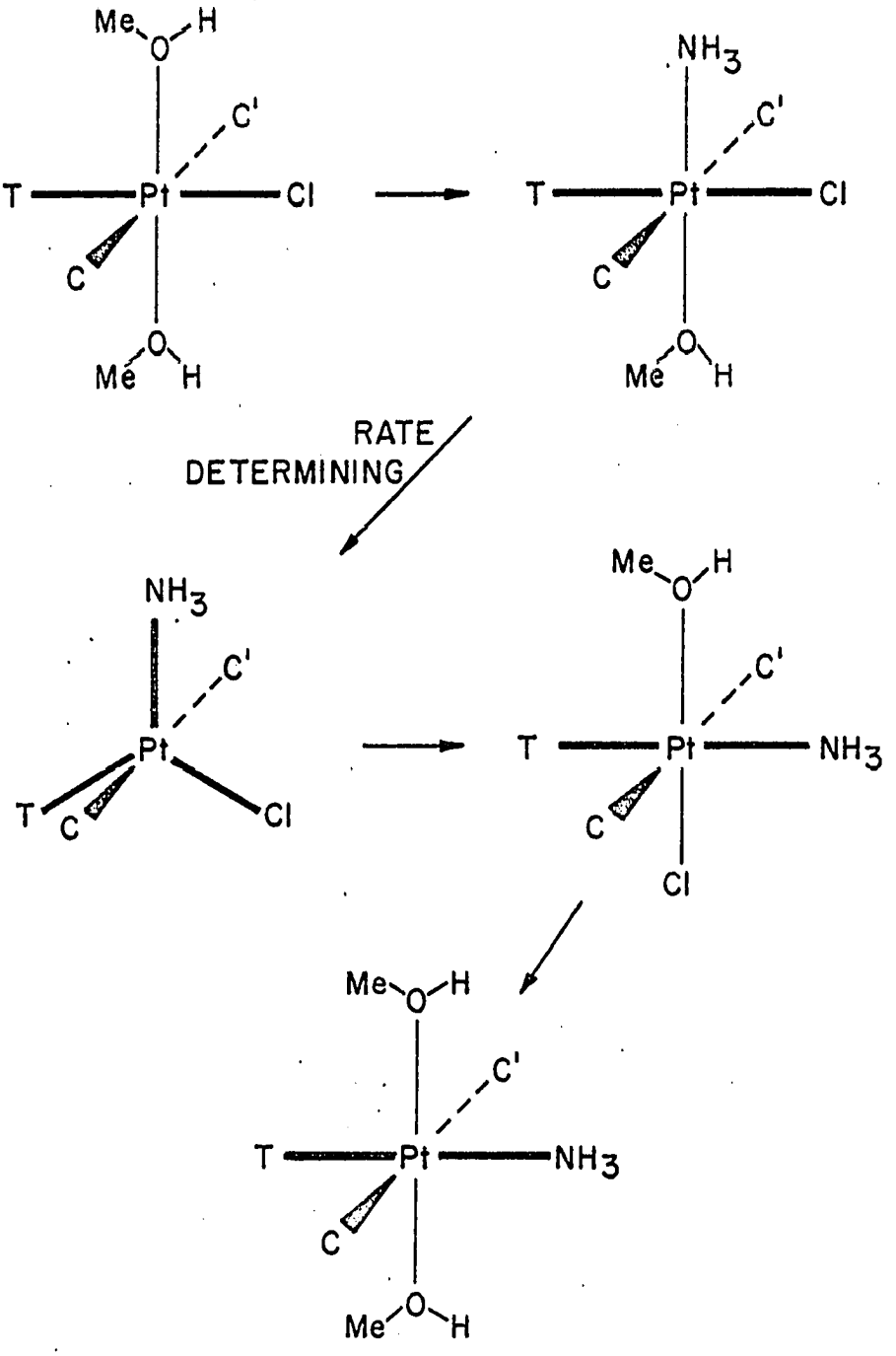

Figure 19. Mechanism for the ammonation reactions of t-$[Pt(NH_3)_2Cl_2]$, t-$[Pt(PEt_3)(NH_3)Cl_2]$, and for the initial second-order and final ammonation reactions of t-$[Pt(PEt_3)_2Cl_2]$

reactions were found to be first-order in both NH_3 and Werner complex concentration. Furthermore, the proposed mechanism will have retention of geometric configuration in going from starting material to product. That the present reactions do retain their configuration is best seen in the ultraviolet spectra of the ammonation reaction of t-$[Pt(PEt_3)_2Cl_2]$ as compared with the spectra for c-$[Pt(PEt_3)_2Cl_2]$ and t-$[Pt(PEt_3)(NH_3)Cl_2]$ ammonation. This comparison indicates that the two PEt_3 ligands remain coordinated to the substrate, and that during the ammonation reactions they remain trans to each other.

Experimental evidence which adds weight to the proposed bimolecular mechanism and also to the formation of a trigonal-bipyramid is gleaned from x-ray diffraction studies of complex compounds. Venanzi studied the compounds formed by several transition metals with a variety of multidentate ligands of P and As (112). He found that compounds formed by the multidentate ligands with transition metals do not always coordinate all of the available sites on the ligand, but that Pt(II) did expand its coordination sphere to form five-coordinate trigonal-bipyramid compounds. The structure of $[Pt(SnCl_3)_5]^{3-}$ has also been found to be a trigonal-bipyramid (51), which is particularly significant because monodentate ligands are involved. These experimental results indicate a propensity of Pt(II) complexes to expand their

coordination sphere under favorable conditions.

The solvolysis reaction of t-$[Pt(NH_3)_2Cl_2]$ is also believed to follow the mechanism proposed in Figure 19, except that in this case the entering group is a MeOH instead of the NH_3 of Figure 19. Once the MeOH has replaced one of the Cl^-, a direct acid-base proton transfer to form t-$[Pt(NH_3)_2(MeO)Cl]$ is expected, if the system is analogous to the one in H_2O. The acid properties of MeOH are such that this would is probably the case. Also, if the system is analogous to the H_2O system, the NH_3 will not replace the MeOH or MeO^- ligands.

The reactions of this study can be approximately compared with reactions of aqueous systems by means of the aqueous ammonation of t-$[Pt(NH_3)_2Cl_2]$. An unpublished study at this laboratory found that at 35°C the aqueous ammonation of t-$[Pt(NH_3)_2Cl_2]$ had a second-order rate constant $k_1 = 120 \times 10^{-4} M^{-1} sec^{-1}$. When compared to the results of this study, $k_1 = 11 \times 10^{-4} M^{-1} sec^{-1}$, it is seen that a tenfold reduction in reaction rate has resulted from the change of solvent. A comparison of the solvolysis reactions at 35°C for this compound, $k_s(H_2O) = 27 \times 10^{-5} sec^{-1}$ (20) and $k_s(MeOH) = 10 \times 10^{-5} sec^{-1}$, reveals that a simple quantitative comparison cannot be made between reactions in the two solvents, however. This difference in the rate constant of the solvolysis reaction in MeOH as compared to that

in H_2O is of the same magnitude as the reported difference in the rate constant of the solvolysis reaction of t-$[Pt(py)_2Cl_2]$ in EtOH as compared to H_2O (109). In comparing the reaction rates of the ammonation reactions and of the solvolysis reactions in two solvents, the importance of including the entering group in descriptions of relative reaction rates is again underscored.

The most obvious extention of the present research is the unraveling of the mechanism for the catalyzed portion of the t-$[Pt(PEt_3)_2Cl_2]$ ammonation. Two sets of experiments which could help to further this end are: the synthesis of t-$[Pt(PEt_3)_2(NH_3)Cl]Cl$ and t-$[Pt(PEt_3)_2(NH_3)_2]Cl_2$ in order to ascertain definitely which of these two is influencing the reaction rate, and what the dependence is of the reaction rate upon the concentration of the compounds; and the addition of the bridged complex t-$[Pt_2(PEt_3)_2Cl_4]$ to a reaction solution, since the possibility exists that a bridged binuclear Pt(II) complex is the catalytic agent itself, rather than only a species formed in one step of the catalysis process as was previously suggested.

Another extension of the present research is a more exhaustive comparison of the cis-effect of ligands which are strong π trans-labilizers with the cis-effect of ligands which are strong σ trans-labilizers in order to further test the proposed generalization made at the beginning of this

chapter that the π-effect should be partially effective in cis as well as in the trans position, whereas the σ-effect should be exclusively operative upon the trans ligand. One of the inherent limitations in any such study is the synthesis of the coordination compounds which would give the most meaningful results. A complex which has been synthesized and which involves a strong σ-effect ligand in the position cis to the reaction site is c-$[Pt(PEt_3)_2(H)Cl]$. Synthesis of c-$[Pt(PEt_3)_2(H)\ I]$ and comparison of its ammonation reaction rate with c-$[Pt(PEt_3)_2I_2]$ should yield some of the desired information.

SUMMARY

As far as could be detected, both ammonation reactions of t-$[Pt(PEt_3)(NH_3)Cl_2]$ went to completion. The rate constants for these reactions at 25°C were $k_1=5.45 \times 10^{-4} M^{-1} sec^{-1}$ and $k_2=0.49 \times 10^{-4} M^{-1} sec^{-1}$; at 35°C, $k_1=14.2 \times 10^{-4} M^{-1} sec^{-1}$ and $k_2=1.2 \times 10^{-4} M^{-1} sec^{-1}$. The activation parameters for the reactions at 25°C were: for the first ammonation reaction, $\Delta H^{\ddagger} = 16.9$ kcal/mole, $\Delta G^{\ddagger} = 21.9$ kcal/mole, $\Delta S^{\ddagger} = -17$ cal/mole-deg; for the second ammonation reaction, $\Delta H^{\ddagger} = 16$ kcal/mole, $\Delta G^{\ddagger} = 23$ kcal/mole, $\Delta S^{\ddagger} = -23$ cal/mole-deg. There was no evidence indicating that a solvolysis path was important for the ammonation reactions of this complex.

The first ammonation reaction of t-$[Pt(NH_3)_2Cl_2]$ did involve a solvolysis reaction, however. The rate constant at 35° for the solvolysis reaction was $k_s=1.3 \times 10^{-4} \pm 0.3 \times 10^{-4}$ sec^{-1}. The rate constant at 35°C for the first ammonation reaction of this complex was $k_1=11.3 \times 10^{-4} \pm 0.8 \times 10^{-4} M^{-1} sec^{-1}$; for the second ammonation reaction, $k_2=1.98 \times 10^{-4} \pm 0.07 \times 10^{-4} M^{-1} sec^{-1}$.

The ammonation reactions of t-$[Pt(PEt_3)_2Cl_2]$ involved an induction period followed by an increase in the reaction rate during the first ammonation reaction. Although the mechanism for the reactions after the induction period could

not be determined, the initial second-order ammonation reaction was estimated to have a rate constant at 25°C of $k_1 = 2.50 \times 10^{-4} \pm 0.06 \times 10^{-4}$ $M^{-1}sec^{-1}$ and at 35° a rate constant of $k_1 = 7.0 \times 10^{-4} \pm 0.3 \times 10^{-4}$ $M^{-1}sec^{-1}$. The second ammonation reaction was a reversible reaction. The approximate rate constant for the forward (ammonation) reaction at 25°C was $k_2 = 0.2 \times 10^{-4}$ $M^{-1}sec^{-1}$. At 35°C the ammonation rate constant was $k_2 = 0.22 \times 10^{-4} \pm 0.06 \times 10^{-4}$ $M^{-1}sec^{-1}$. The rate constants for the reverse reaction were, at 25°C, $k_{-2} = 3 \times 10^{-4}$ $M^{-1}sec^{-1}$ and at 35°C, $k_{-2} = 9 \times 10^{-4} \pm 2 \times 10^{-4}$ $M^{-1}sec^{-1}$. The activation parameters at 25°C for the first ammonation reaction were, $\Delta H^{\ddagger} = 18$ kcal/mole, $\Delta G^{\ddagger} = 22$ kcal/mole, and $\Delta S^{\ddagger} = -14$ cal/mole-deg. Because of the uncertainty in the rate constants for the forward and reverse portions of the second ammonation reaction, the activation parameters were not calculated for these reactions.

The proposal was made that the division of the trans-effect into a π-effect and a σ-effect carries over into the cis-effect. Ligands which have a strong π trans-effect should also manifest a labilizing influence when cis to the reaction site, whereas ligands with a strong σ trans-effect and a weak π-effect should have very little labilizing influence when cis to the reaction site. The similarity in the rate constants of the first and second ammonation reac-

tions of t-$[Pt(PEt_3)(NH_3)Cl_2]$ and t-$[Pt(NH_3)_2Cl_2]$ was cited as an example of the operation of this proposal.

The necessity of including the incoming ligand in comparisons of reaction rates of different complexes was indicated by the presence of the solvolysis path in the first ammonation reaction of t-$[Pt(NH_3)_2Cl_2]$, while the ammonation of t-$[Pt(PEt_3)(NH_3)Cl_2]$ indicated no such path within the limits of the accuracy of the present measurements. The influence of the incoming ligand was cited as a manifestation of the acid-base properties of the incoming ligand and of the substrate in accord with the theory of hard and soft acids and bases.

A bimolecular reaction involving the formation of a trigonal-bypyramid transition state was proposed as the mechanism of the ammonation reactions (exclusive of the fast reaction following the induction period during the first ammonation of t-$[Pt(PEt_3)_2Cl_2]$, for which no satisfactory rate law could be formulated).

LITERATURE CITED

1. Werner, A., Z. anorg. Chem., 3, 267 (1893).
2. Reiset, J., Compt. rend., 10, 870 (1840).
3. Peyrone, M., Ann. Chem. Liebigs, 51, 1 (1844).
4. Reiset, J., Ann. Chim. Phys., 11, 411 (1844).
5. Banerjea, D., Basolo, F., and Pearson, R. G., J. Am. Chem. Soc., 79, 4055 (1957).
6. Hofmann, A. W., Ann. Chem. Liebigs, 103, 357 (1857).
7. Sella, Q., Mem. Accad. Torino, 20, 359 (1863).
8. Cahours, A. and Gal, H., Compt. Rend., 70, 897 (1870).
9. Chatt, J. and Wilkins, R. G., J. Chem. Soc., 1952, 273.
10. Chatt, J. and Wilkins, R. G., J. Chem. Soc., 1952, 4300.
11. Chatt, J. and Wilkins, R. G., J. Chem. Soc., 1956, 525.
12. Chatt, J. and Wilkins, R. G., J. Chem. Soc., 1951, 2532.
13. Haake, P. and Hylton, T. A., J. Am. Chem. Soc., 84, 3774 (1962).
14. Klason, P. and Wanselin, J., J. prakt. Chem., 67, 41 (1903).
15. Grinberg, A. A., Razumova, Z. A., and Troickaja, A. D., Bull. Acad. U.R.S.S., Ser. Chim., 1946, 253.
16. Chatt, J. and Venanzi, L. M., J. Chem. Soc., 1955, 3858.
17. Granthan, L. F., Elleman, T. S., and Martin, D. S., Jr., J. Am. Chem. Soc., 77, 2965 (1955).
18. Tucker, M. A., Colvin, C. B., and Martin, D. S., Jr., Inorg. Chem., 3, 1373 (1964).
19. Reishus, J. W. and Martin, D. S., Jr., J. Am. Chem. Soc., 83, 2457 (1961).

20. Martin, D. S., Jr. and Adams, R. J. Trans-dichlorodiammineplatinum(II). Acid hydrolysis and the isotopic exchange of the chloride ligand. In Kirschner, Stanley, ed. Advances in the chemistry of the coordination compounds. Pp. 579-589. New York, N.Y., Macmillan Company. 1961.

21. Aprile, F. and Martin, D. S., Jr., Inorg. Chem., 1, 551 (1962).

22. Basolo, F., Gray, H. B., and Pearson, R. G., J. Am. Chem. Soc., 82, 4200 (1960).

23. Martelli, M., Orio, A., and Graziani, M., Ric. Sci. (II-A), 8, 361 (1965).

24. Chan, S. C., J. Chem. Soc., A, 1966, 1000.

25. Pearson, R. G., Gray, H. B., and Basolo, F., J. Am. Chem. Soc., 82, 787 (1960).

26. Basolo, F., Chatt, J., Gray, H. B., Pearson, R. G., and Shaw, B. L., J. Chem. Soc., 1961, 2207.

27. Langford, C. H. and Gray, H. B. Ligand substitution processes. New York, N.Y., W. A. Benjamin, Inc. 1965.

28. Basolo, F., Advan. Chem. Ser., 49, 81 (1965).

29. Faraone, G., Cattalini, L., Ricevuto, V., Romeo, R., and Martelli, M., Ann. Chim. (Rome), 55, 506 (1965).

30. Faraone, G., Belluco, U., Ricevuto, V., and Ettorre, R., J. Inorg. Nucl. Chem., 28, 863 (1966).

31. Belluco, U., Martelli, M., and Orio, A., Inorg. Chem., 5, 582 (1966).

32. Faraone, G., Ricevuto, V., Romeo, R., and Trozzo, M., Gazz. Chim. Ital., 96, 590 (1966).

33. Belluco, U., Rigo, P., Graziani, M., and Ettorre, R., Inorg. Chem., 5, 1125 (1966).

34. Belluco, U., Orio, A., and Martelli, M., Inorg. Chem., 5, 1370 (1966).

35. Drago, R. S., Mode, V. A., and Kay, J. G., Inorg. Chem., 5, 2050 (1966).

36. Belluco, U., Ettorre, R., Basolo, F., Pearson, R. G., and Turco, A., Inorg. Chem., 5, 591 (1966).

37. Cattalini, L., Belluco, U., Ettorre, R., and Martelli, M., Gazz. Chim. Ital., 94, 356 (1964).

38. Belluco, U., Cattalini, L., Basolo, F., Pearson, R. G., and Turco, A., J. Am. Chem. Soc., 87, 241 (1965).

39. Orio, A., Belluco, U., and Cattalini, L., Ric. Sci. (II-A), 8, 369 (1965).

40. Belluco, U., Graziani, M., and Rigo, P., Inorg. Chem., 5, 1123 (1966).

41. Edwards, J. O., J. Am. Chem. Soc., 76, 1540 (1954).

42. Edwards, J. O. and Pearson, R. G., J. Am. Chem. Soc., 84, 16 (1962).

43. Pearson, R. G., J. Am. Chem. Soc., 85, 3533 (1963).

44. Gray, H. B., J. Am. Chem. Soc., 84, 1548 (1962).

45. Gray, H. B. and Olcott, R. J., Inorg. Chem., 1, 481 (1962).

46. Basolo, F. and Pearson, R. G., Progr. Inorg. Chem., 4, 381 (1962).

47. Chatt, J., Duncanson, L. A., and Venanzi, L. M., J. Chem. Soc., 1955, 4456.

48. Orgel, L. E., J. Inorg. Nuc. Chem., 2, 137 (1956).

49. Mair, G. A., Powell, H. M., and Venanzi, L. M., Proc. Chem. Soc. (London), 1961, 170.

50. Hartley, J. G., Venanzi, L. N., and Goodall, D. C., J. Chem. Soc., 1963, 3930.

51. Cramer, R. D., Lindsey, R. V., Prewitt, C. T., and Stolberg, U. G., J. Am. Chem. Soc., 87, 658 (1965).

52. Adams, D. M., Chatt, J., Gerratt, J., and Westland, A. D., J. Chem. Soc., 1964, 734.

53. Belluco, U., Cattalini, L., Basolo, F., Pearson, R. G., and Turco, A., Inorg. Chem., 4, 925 (1965).

54. Peshchevitskii, B. I. and Kazakov, V. P., Zh. Neorgan. Khim., 8, 250 (1963).

55. Peshchevitskii, B. I. and Kazakov, V. P., Izv. Sibirsk., Otd. Akad. Nauk S.S.S.R., Ser. Khim. Nauk, 1963, 20.

56. Belyaev, A. V., Kazakov, V. P., and Ptitsyn, B. V., Dokl. Akad. Nauk S.S.S.R., 160, 149 (1965).

57. Jorgenson, S. M., J. prakt. Chem., 33, 489 (1886).

58. Kurnakov, N. W., J. prakt. Chem., 50, 483 (1894).

59. Werner, A. and Miolati, F., Z. physik. Chem., 12, 49 (1893).

60. Drew, H. D. K., Pinkard, F. W., Wardlaw, W., and Cox, E. G., J. Chem. Soc., 1932, 988.

61. Grinberg, A. A. and Ryabchikov, D. I., Acta Physicochem. U.R.S.S., 3, 555 (1935).

62. Grinberg, A. A. and Ryabchikov, D. I., Compt. rend. acad. sci. U.R.S.S., 4, 259 (1935).

63. Jensen, K. A., Z. anorg. Chem., 229, 252 (1936).

64. Jensen, K. A., Z. anorg. Chem., 242, 87 (1939).

65. Grinberg, A. A. and Shagisultanova, G. A., Zh. Neorgan. Khim., 5, 280 (1960).

66. Chernyaev, I. I., Ann. inst. platine U.S.S.R., 4, 261 (1926).

67. Grinberg, A. A., Acta Physicochim. U.R.S.S., 3, 573 (1935).

68. Owston, P. G., Partridge, J. M., and Rowe, J. M., Acta Cryst., 13, 246 (1960).

69. Eisenberg, R. and Ibers, J. A., Inorg. Chem., 4, 773 (1965).

70. Syrkin, Y. K., Bull acad. sci. U.R.S.S., Chem. series, 1948, 69.

71. Baenziger, N. C., Medrud, R. C., and Doyle, J. R., Acta Cryst., 18, 237 (1965).

72. Bersuker, I. B., Zh. Neorgan. Khim., 9, 36 (1964).

73. Oleari, L., di Sipio, L., and de Michelis, G., Ric. Sci. (II-A), 8, 413 (1965).

74. Falk, C. D. and Halpern, J., J. Am. Chem. Soc., 87, 3003 (1965).

75. Grinberg, A. A. and Dobroborskaya, A. I., Zh. Neorgan. Khim., 1, 42 (1956).

76. Grinberg, A. A., Zh. Neorgan. Khim., 4, 1517 (1959).

77. Jowanovitz, L. S., Jr., McNatt, F. B., McCarley, R. E., and Martin, D. S., Jr., Analytical Chem., 32, 1270 (1960).

78. Kharasch, M. S. and Ashford, T. A., J. Am. Chem. Soc., 58, 1736 (1926).

79. Vezes, M., Bull. soc. chim., 19, 897 (1898).

80. Keller, R. N., Inorg. Synth., 2, 247 (1946).

81. Gildengershel, K., Zh. Neorgan. Khim., 1, 400 (1956).

82. Jensen, K. A., Z. anorg. Chem., 229, 225 (1936).

83. Chatt, J., J. Chem. Soc., 1951, 652.

84. Chatt, J., Duncanson, L. A., and Venanzi, L. M., J. Chem. Soc., 1956, 2712.

85. Powell, D. B. and Sheppard, N., J. Chem. Soc., 1956, 3108.

86. Mizushima, S., Nakagawa, I., Schmelz, M. J., Curran, C., and Quagliano, J. V., Spectrochim. Acta, 13, 31 (1958).

87. Goggin, P. L. and Goodfellow, R. J., J. Chem. Soc., A, 1966, 1462.

88. Chatt, J., J. Chem. Soc., 1950, 2301.

89. Chatt, J. and Shaw, B. L., J. Chem. Soc., 1962, 5075.

90. Jones, G. and Bollinger, G. M., J. Am. Chem. Soc., 53, 411 (1931).

91. Evers, E. C. and Knox, A. G., J. Am. Chem. Soc., 73, 1739 (1951).

92. Foster, N. G. and Amis, E. S., Z. phys. Chem. (Frankfurt am Main), 3, 365 (1955).

93. Davies, J. A., Kay, R. L., and Gordon, A. R., J. Chem. Phys., 19, 749 (1951).

94. Long, F. A. and Ballinger, P. Acid ionization constants of alcohols in the solvents water and deuterium oxide. In Pesce, B. ed. Electrolytes. Pp. 152-164. New York, N.Y., Pergamon Press. 1962.

95. Pimentel, George C. and McClellan, A. L. The hydrogen bond. San Francisco, Calif., W. H. Freeman and Co. 1960.

96. Harned, H. S. and Owen, B. B. The physical chemistry of electrolytic solutions. 3rd ed. New York, N.Y., Reinhold Publishing Corporation. 1958.

97. Halverstadt, I. F. and Kumler, W. D., J. Am. Chem. Soc., 64, 2988 (1942).

98. Hasted, J. B., Ritson, D. M., and Collie, C. H., J. Chem. Phys, 16, 1 (1948).

99. Fuoss, R. M., J. Am. Chem. Soc., 80, 5059 (1958).

100. Fuoss, R. M., and Kraus, C. A., J. Am. Chem. Soc., 79, 3304 (1957).

101. Fuoss, R. M., J. Am. Chem. Soc., 79, 3301 (1957).

102. Amis, E. S., J. Chem. Phys., 60, 428 (1956).

103. Hinton, J. F. and Amis, E. S., Chem. Revs., 67, 367 (1967).

104. Teggins, J. E. Gano, D. R., Tucker, M. A., and Martin, D. S., Jr., Inorg. Chem., 6, 69 (1967).

105. Teggins, J. E. and Martin, D. S., Jr., Inorg. Chem., 6, 1003 (1967).

106. Lokken, S. J. and Martin, D. S., Jr., Inorg. Chem., 2, 562 (1963).

107. Chatt, J. and Venanzi, L. M., J. Chem. Soc., 1955, 2787.

108. Mossmer, G. G. and Amma, E. L., Inorg. Chem., 5, 1775 (1966).

109. Basolo, F. and Pearson, R. G. Mechanisms of inorganic reactions. 2nd ed. New York, N.Y., John Wiley and Sons, Inc. 1967.

110. Parshall, G. W., J. Am. Chem. Soc., 86, 5367 (1964).

111. Pidcock, A., Richards, R. E., and Venanzi, L. M., J. Chem. Soc., A, 1966, 1707.

112. Venanzi, L. M., Angew. Chem. Intern. Ed. Eng., 3, 453 (1964).

113. Roginskii, S. A., Dokl. Akad. Nauk S.S.S.R. 130, 366 (1960).

114. Lebedev, Ya. S., Tavetkov, Yu. D. and Voevodskii, V. V., Kinetika i Kataliz, 1, 496 (1960).

115. Peshchevitskii, B. I. and Kazakov, V. P., Zh. Neorgan. Khim., 8, 2816 (1963).

116. Leffler, J. E., J. Org. Chem., 20, 1202 (1955).

117. Leffler, J. E. and Grunwald, E. Rates and equilibria of organic reactions. New York, N.Y., John Wiley and Sons, Inc. 1963.

ACKNOWLEDGEMENTS AND DEDICATION

The author wishes to thank Evelyn E. Conrad of the Spectrochemistry Group, who obtained the infrared spectrum used in this dissertation; Gregor A. Junk of the Mass Spectroscopy Group, who obtained the mass spectrum; and Wayne Stensland of the Radiochemistry Group, who obtained the neutron activation analysis. The Instrumentation Group, which designed and constructed many of the components of the conductance apparatus, the glass shop, which constructed the conductance cells, the Graphic Arts Group, which prepared the figures in this dissertation, and the research shop, which provided assistance in the construction of the conductance apparatus, are also thanked for their contributions.

In particular, the author wishes to acknowledge a debt of gratitude to Dr. D. S. Martin for his counsel and guidance throughout the course of the research and preparation of this manuscript.

This dissertation is dedicated to the author's wife, Marilyn, without whom it may never have existed.

APPENDIX A

In recent years, a great deal of interest has centered on the correlation of Pt(II) kinetics data through the use of Equation 1.2 of the Introduction:

$$\log k_y = sn_{Pt} + \log k_s, \qquad (1.2)$$

the meaning of the symbols having been defined in the Introduction.

While this approach to correlating kinetics data has received attention in what is politically called the western world, the Russian experimenters have concentrated on the two following equations as a vehicle for correlating a broad spectrum of kinetics data:

$$\ln A = \ln \underline{a} + \nu E, \qquad (6.1)$$

where A is the Arrhenius pre-exponential factor, E is the Arrhenius activation energy, and $\underline{a}$ and ν are constants which are characteristic of the system under consideration (54,55, 113,114); and,

$$\Delta S^{\ddagger} = \nu^{\ddagger}\Delta H^{\ddagger} + C, \qquad (6.2)$$

where $\Delta S^{\ddagger}$ and $\Delta H^{\ddagger}$ are the entropy and enthalpy of activation, $\nu^{\ddagger}$ is the compensation coefficient, and C is a constant (these latter two quantities are constants which are characteristic of the system under consideration) (56,115). Equation 6.2 has also been called the isokinetic relationship (116). The application of Equations 6.1 and 6.2 have

been quite extensive, both in organic and inorganic chemistry. Equation 1.2 has thus far been applied mostly to reactions of Pt(II) complexes, although analogous linear-free-energy relationships are well known in organic chemistry (notably the Hammett and Taft equations).

As we stated in the Introduction, Equation 1.2 has been applied to series of reactions involving the same substrate and reaction conditions, but different entering groups. Equations 6.1 and 6.2, however, have been used to show linear relationships involving any one variable in the system (solvent, substrate composition, oxidation state, charge), while holding the other variable constant.

A series of reactions which conforms to Equation 6.2, using a particular value of $\nu^{\ddagger}$ and of C to describe the series, possesses unique properties which become evident when an inversion temperature is defined, $T_i = 1/\nu^{\ddagger}$ ($\nu^{\ddagger}$ has the units of the reciprocal of absolute temperature), Equation 6.2 is redefined in terms of the difference, δ, between the thermodynamic properties of individual members of the series,

$$\delta\Delta S^{\ddagger} = \nu^{\ddagger}\delta\Delta H^{\ddagger} , \qquad (6.3)$$

and both of these are combined with the equation for the difference in free energy of activation,

$$\delta\Delta G^{\ddagger} = \delta\Delta H^{\ddagger} - T\delta\Delta S^{\ddagger} .$$

The resultant equations,

$$\delta\Delta G^{\ddagger} = (T_i - T)\,\delta\Delta S^{\ddagger} \qquad (6.4)$$

$$\delta\Delta G^{\ddagger} = (1 - \frac{T}{T_i})\,\delta\Delta H^{\ddagger} \qquad (6.5)$$

reveal the reasons for calling Equations 6.2 and 6.3 an isokinetic relationship, and T_i an inversion temperature (117). When $T = T_i$, $\delta\Delta G^{\ddagger} = 0$, so that all the reactions in the series are proceeding with the same reaction rate: they are isokinetic. In going from temperatures below T_i to temperatures above T_i, Equations 6.4 and 6.5 change sign, which means that there is an inversion of the relationship between individual members in the series - thus the reasons for calling T_i an inversion temperature. It should be pointed out that all of the above holds true precisely only for a series in which only one mechanism exist for each reaction in the series. In actual practice, Equation 6.2 will have a small degree of dispersion about the straight line, and at $T = T_i$, there will be small differences in the reaction rates (117). These small variations are caused by the presence of minor competing mechanisms which contribute in part to the observed reaction rates, and the associated thermodynamic quantities.

An extension of Equation 6.1 has been the formulation of a scale for the <u>trans</u> influence, TI, of any ligand. By taking a series of reactions which have a single compensation

effect (i.e. a series which conforms to Equation 6.1 or 6.2, using a single value of ν or $\nu^{\ddagger}$ and of $\ln a$ or C to describe the series), such as any one of those given in Table 6, and selecting as a reference the activation energy for the reactions involving Cl as the ligand trans to the reaction site, the trans influence for any other ligand (X) in the series can be defined as $TI = E_{Cl}/E_X$ (54). The virtue claimed for this manner of defining TI is a uniform scale for the trans effect which has equally valid application to any series of Pt(II) and Pt(IV) reactions. In Table 6, the compensation effect series are given for the reactions,

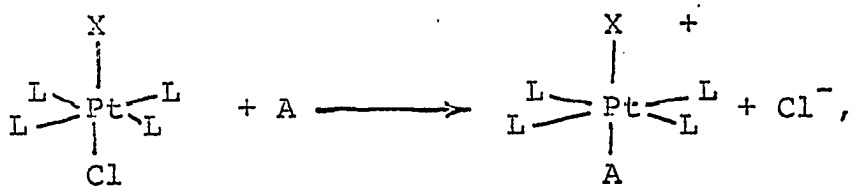

for Pt(IV), with the nature of the L ligands indicated in the first column of the table, the A group in the second, and the trans ligand (X) in the next four columns. The last four columns indicate the TI values for the X ligands calculated from the activation energies for each series. The last row of the table contains data for the reaction,

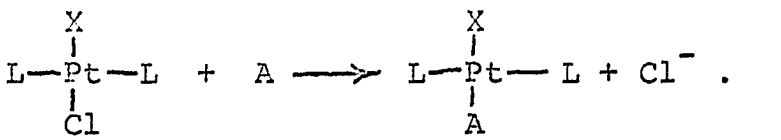

Table 6. Trans influence in the replacement of chlorine on the X-Pt-Cl axis[a]

L ligands	A	Activation energy[b] X =				TI X =			
		Cl	Br	I	NO_2	Cl	Br	I	NO_2
Pt(IV)[c]									
En-NH_3-Cl[d]	py[e]	20.8	18.9	--	--	1.00	1.11	--	--
En-py-Cl	py	21.1	19.0	--	--	1.00	1.11	--	--
En-NH_2CH_3-NO_2	py	21.13	19.0	--	--	1.00	1.11	--	--
En-NH_3-NO_2	py	21.26	19.27	--	--	1.00	1.11	--	--
NH_3-NH_3-NH_3-NH_3	py	19.2	17.3	15.4	--	1.00	1.11	1.25	--
NH_3-NH_3-NH_3-NH_3	NH_3	19.5	17.4	15.45	--	1.00	1.12	1.26	--
NH_3-NH_3-NO_2-NO_2	py	21.1	19.2	--	--	1.00	1.10	--	--
NH_3-NH_3-NH_3-Cl	py	21.25	19.3	--	--	1.00	1.10	--	--
Pt(II)									
NH_3,Cl	py	19.0	17.0	--	--	1.00	1.12	--	1.73

[a](54).

[b]In kcal/mole.

[c]The ligands, L, are arranged in the order shown around the equator of the Pt(IV) octahedron.

[d]En = ethylenediamine.

[e]Py = pyridine.

APPENDIX B

```
C     THE FOLLOWING IS A RUNGE- KUTTA NUMERICAL INTEGRATION
C     ROUTINE FOR A SET OF DIFFERENTIAL EQUATIONS REPRESENTING
C     AN IRREVERSIBLE REACTION FOLLOWED BY A REVERSIBLE
C     REACTION.  THE CONCENTRATIONS OF THE PRODUCTS ARE
C     CALCULATED AS A FUNCTION OF TIME, AND THE CONDUCTANCE OF
C     A SOLUTION CONTAINING THESE CONCENTRATIONS IS
C     CALCULATED.  A PLOT IS THEN MADE OF THIS CALCULATED
C     CONDUCTANCE AS A FUNCTION OF TIME, AND THE
C     EXPERIMENTAL CONDUCTANCE VALUES ARE SUPERIMPOSED ON
C     THIS PLOT.  WITH SLIGHT MODIFICATION, THE PROGRAM CAN
C     HANDLE ANY REACTIONS WHICH CAN ADEQUATELY BE
C     REPRESENTED BY TWO INDEPENDENT DIFFERENTIAL EQUATIONS,
C     USING ANY EXPERIMENTAL TECHNIQUE.
C     N.B. THIS LISTING WAS MADE BY AN IBM 1401, WHICH DOES
C     NOT CONTAIN ALL THE CHARACTERS USED BY THE IBM 360/50.
C     CONSEQUENTLY, THE SYMBOL @ WILL APPEAR IN THIS LISTING
C     WHERE EVER A SINGLE QUOTATION MARK APPEARS IN THE
C     OPERATIONAL PROGRAM.
      DIMENSION ALPHA(11,6),EXR(200),R(200),TIME(200),WHEN(7),
     1 XLAB(5),YLAB(5),GLAB1(5),GLAB2(5),EXNO(3),TPLT(200),
     2 X(2000),Y(2000),T(2000),RTIME(2000),XCORD(6),YCORD(6)
      REAL K1,K2,K2R
    1 FORMAT (@1@///4X,@PT(P)(N)CL2 + NH3   KINETICS@,28X,
     1 3A4,30X,7A4/)
    2 FORMAT (2I4, I3, F10.8)
    3 FORMAT (8F10.7)
    4 FORMAT (@0@,5X,@PT(P)2CL2 = @,F10.7,4X,@AM = @,F8.5,
     1 4X,@CL = @,F8.5,4X,@XLMBDA = @,F6.2,4X,@YLMBDA = @,
     2 F6.2,4X,@CELLK = @,F6.4)
    5 FORMAT (@0@,5X,@K1 = @,F10.7,6X,@K2 = @,F10.7,6X,
     1 @K2R = @,F10.7,6X,@1/R(0) = @,F11.9//)
    6 FORMAT (@0@,11X,@T-HRS.@,6X,@PT(P)2CL2@,6X,@PTP2NH3CL@,
     1 5X,@PTP2(NH3)2@,10X,@CL@,11X,@LAMBDA@,10X,@1/R(T)@)
    8 FORMAT (20A4)
    9 FORMAT (3F5.2,I3)
   11 FORMAT (2F6.3,11A4)
   12 FORMAT (2I3,7A4)
   14 FORMAT (I1//5X,@AM(FINAL) = @, F9.7)
   15 FORMAT(T11,2F10.0)
C     NORUNS = NUMBER OF SEPARATE EXPERIMENTS TO BE TREATED
      READ (1,12) NORUNS
C     FROM THIS POINT ON, ALL OF THE QUANTITIES DEFINED APPLY
C     TO THE INDIVIDUAL EXPERIMENTS.  EACH EXPERIMENT TREATED
C     MUST HAVE ITS OWN SET OF THESE QUANTITIES.
   20 DO 34  M=1, NORUNS
C     NIC = NUMBER OF SETS OF INTEGRATION LIMITS AND TIME
C     INCREMENTS - ONE LOWER LIMIT, UPPER LIMIT, PRINTING
C     CONTROL AND TIME INCREMENT PER SET.
C     NCL = NUMBER OF LINES OF LABELLING ON THE GRAPHS
C     EXNO = IDENTIFICATION NUMBER FOR THE EXPERIMENT
      READ (1,12) NIC, NCL, EXNO
```

```
C       A = INITIAL COMPLEX CONCENTRATION
C       AM = INITIAL AMMONIA CONCENTRATION
C       B = INITIAL CHLORIDE CONCENTRATION
C       RZERO = INITIAL CONDUCTANCE VALUE (1/R(0))
C       CELLK = CELL CONSTANT
C       X(1) = INITIAL CONCENTRATION OF FIRST REACTION PRODUCT
C       Y(1) = INITIAL CONCENTRATION OF SECOND REACTION PRODUCT
        READ (1,3) A, AM, B, RZERO, CELLK, X(1), Y(1)
C       K1 = RATE CONSTANT FOR FIRST (IRREVERSIBLE) REACTION
C       K2 = RATE CONSTANT FOR FORWARD REACTION OF EQUILIBRIUM
C       K2R = RATE CONSTANT FOR REVERSE REACTION OF EQUILIBRIUM
C       XLMBDA = EQUIVALENT CONDUCTANCE OF FIRST REACTION
C       PRODUCT
C       YLMBDA = EQUIVALENT CONDUCTANCE OF SECOND REACTION
C       PRODUCT
        READ(1,3) K1,K2,K2R,XLMBDA,YLMBDA
C       DATE IS AN IBM SUPPLIED SUBROUTINE WHICH GIVES THE TIME
C       WHEN THE PROGRAM RAN.
        CALL  DATE(WHEN)
C       THE NEXT THREE STATEMENTS PRINT OUT THE VALUES FOR THE
C       VARIOUS CONSTANTS AND THE INITIAL CONDITIONS.
        WRITE (3,1) EXNO, WHEN
        WRITE (3,4) A, AM, B, XLMBDA, YLMBDA, CELLK
        WRITE(3,5) K1,K2,K2R,RZERO
C       THE FOLLOWING STATEMENT PLACES THE LABELS AT THE HEAD
C       OF EACH COLUMN OF OUTPUT.
        WRITE (3,6)
C       THE FOLLOWING STATEMENTS INITIALIZE THE QUANTITIES
C       INDICATED.
        NLINE = 6
        J = 0
        T(1) = 0.0
C       RUNGEK IS THE SUBROUTINE CONTAINING THE RUNGE-KUTTA
C       INTEGRATION ROUTINE.
        CALL RUNGEK(NIC,EXNO,K1,K2,K2R,A,B,AM,XLMBDA,YLMBDA,
     1  CELLK,RZERO,X,Y,NLINE,T,RTIME)
C       N3 = LOWER LIMIT ON FIRST PAIR OF INTEGRATION LIMITS
C       N4 = UPPER LIMIT ON THE LAST PAIR OF INTEGRATION LIMITS
C       N5 = EVERY N5-TH CONDUCTANCE VALUE FROM N3 UP TO N4
C       WILL BE PLOTTED
C       TIME2 = UPPER LIMIT ON T(N) FOR THE PLOT CONTAINING
C       THE EARLY PORTION OF THE REACTIONS (THE SECOND PLOT)
  280 READ (1,2) N3, N4, N5, TIME2
C       THE CALCULATED CONDUCTANCE VALUES ARE PREPARED FOR
C       PLOTTING ON TWO GRAPHS - ONE FOR THE TOTAL TIME OF THE
C       REACTIONS, AND ONE FOR THE THE EARLY PORTION OF THE
C       REACTIONS.
        DO 29 N = N3, N4, N5
C       J = NUMBER OF CALCULATED CONDUCTANCE VALUES TO BE
C       PLOTTED
        J= J + 1
```

```
C     TPLT = TIME COORDINATES OF CALCULATED CONDUCTANCE VALUES
C     WHICH WILL BE PLOTTED
      TPLT(J) = T(N)
C     R = CALCULATED CONDUCTANCE VALUES WHICH WILL BE
C     PLOTTED - IN SCIENTIFIC NOTATION
      R(J) = 10000.0 * RTIME(N)
      IF ( TPLT(J) - TIME2 ) 281, 281, 29
C     J2 = NUMBER OF CALCULATED CONDUCTANCE VALUES TO BE
C     PLOTTED ON THE SECOND PLOT
  281 J2 = J
   29 CONTINUE
C     AMF = FINAL CONCENTRATION OF AMMONIA
      AMF = AM - X(N4) - 2.0*Y(N4)
C     THE FOLLOWING 4 STATEMENTS CONTROL THE PRINTING OF AMF
      KCON = 0
      IF(26-NLINE) 291, 291, 292
  291 KCON = 1
  292 WRITE(3,14) KCON, AMF
C     XLAB = LABEL ON X-AXIS
C     YLAB = LABEL ON Y-AXIS
C     GLAB1 AND GLAB2 = TWO LINES IN WHICH ANY IDENTIFYING
C     LABELS CAN BE PLACED - THEY ARE PRINTED IN THE CORNER
C     OF THE PLOTS
      READ (1,8 ) XLAB, YLAB, GLAB1, GLAB2
C     XSF = SCALE FACTOR ALONG THE X-AXIS (XSF UNITS/INCH)
C     YMIN = VALUE OF Y AT ORIGIN OF Y-AXIS ON FIRST PLOT
C     YSF = SCALE FACTOR ALONG THE Y-AXIS (YSF UNITS/INCH)
C     NEXPT = NUMBER OF EXPERIMENTAL POINTS TO BE
C     SUPERIMPOSED ON THE PLOT
      READ (1, 9) XSF, YMIN, YSF, NEXPT
C     GRAPH = A USER SUBROUTINE ON DISC AT THE LOCAL
C     COMPUTATION CENTER
C     THE NUMBERS IN THE CALL LIST FOR GRAPH INDICATE WHICH
C     OF THE OPTIONS IN THAT SUBROUTINE ARE BEING USED.
      CALL GRAPH (J, TPLT, R, 0, 2, 12.0,  8.5 , XSF, 0,
     1 YSF,YMIN,XLAB,YLAB,GLAB1,GLAB2)
  294 DO 295 I=1,NEXPT
C     EXR = EXPERIMENTAL CONDUCTANCE VALUES
C     TIME = TIME OF REACTION AT WHICH EXR WAS MEASURED
      READ(1,15)EXR(I),TIME(I)
C     CONVERSION OF TIME TO HOURS - CALCULATED VALUES WERE
C     IN HOURS.
      TIME(I)=TIME(I)/60.0
C     CONVERSION OF EXPERIMENTAL CONDUCTANCES TO SCIENTIFIC
C     NOTATION.
  295 EXR(I)=10000.0*EXR(I)
C     SUPERPOSITION OF EXPERIMENTAL CONDUCTANCES ON THE PLOT
C     OF THE CALCULATED CONDUCTANCES.
   31 CALL GRAPH (NEXPT, TIME, EXR, 3, 7, 0,0,0,0,0,0,0,0,0,0)
C     XCORD = X-COORDINATE OF THE BEGINNING OF EACH LINE OF
C     GRAPH LABELLING (THERE ARE NCL LINES)
```

```
C      YCORD = Y-COORDINATE OF THE ABOVE LINE OF LABELLING
C      ALPHA = ACTUAL INFORMATION IN EACH LINE OF LABELLING
       READ(1,11)(XCORD(NL),YCORD(NL),(ALPHA(NL1,NL),
      1 NL1=1,11),NL=1,NCL)
       DO 33   NL = 1, NCL
C      LETTER = USER SUBROUTINE FOR LABELLING THE PLOTS
C      FROM SUBROUTINE GRAPH
   33 CALL LETTER (XCORD(NL),YCORD(NL),.15,ALPHA(1,NL),0,44,
     1  0,0,0,0,0,0,0,0,0,0)
C      XSCA = SCALE FACTOR FOR X-AXIS ON SECOND PLOT (THE PLOT
C      OF THE SHORT REACTION TIMES)
C      YLST = VALUE OF Y AT ORIGIN OF Y-AXIS ON SECOND PLOT
C      YSCA = SCALE FACTOR FOR Y-AXIS ON SECOND PLOT
C      N2ND = NUMBER OF EXPERIMENTAL POINTS TO BE PLOTTED ON
C      SECOND PLOT
       READ (1, 9 ) XSCA, YLST, YSCA, N2ND
C      THE SECOND PLOT IS MADE, THE EXPERIMENTAL POINTS ARE
C      SUPERIMPOSED, AND THE LABELLING IS WRITTEN ON THE PLOT.
   40 CALL GRAPH (J2,TPLT, R, 0, 2, 12.0,  8.5 , XSCA, 0,
     1 YSCA,YLST,XLAB,YLAB,GLAB1,GLAB2)
   41 CALL GRAPH(N2ND,TIME,EXR,3,7,0,0,0,0,0,0,0,0,0,0)
      DO 50 NL = 1, NCL
   50 CALL LETTER(XCORD(NL),YCORD(NL),0.15,ALPHA(1,NL),0,44,
     1   0,0,0,0,0,0,0,0,0,0)
   34 CONTINUE
      STOP
      END
```

```
      SUBROUTINE RUNGEK(NIC,EXNO,K1,K2,K2R,A,B,AM,XLMBDA,
     1 YLMBDA,CELLK,RZERO,X,Y,NLINE,RTIME)
      DIMENSION X(1),Y(1),COND(2000),EXNO(3),T(1),RTIME(1)
      REAL K1,K2,K2R
C     DXDT = THE DIFFERENTIAL EQUATION FOR THE RATE OF
C     CHANGE OF THE CONCENTRATION OF THE FIRST REACTION
C     PRODUCT, WRITTEN IN THE FORM OF AN ARITHEMTIC STATEMENT
C     FUNCTION.
      DXDT(U,V) = K1*(AM-U-2.0*V)*(A-U-V) - K2*(AM-U-2.0*V)*U
     1  + K2R*(B+U+2.0*V)*V
C     DYDT = A SIMILAR FUNCTION FOR THE SECOND REACTION
C     PRODUCT.
      DYDT(U,V) = K2*(AM-U-2.0*V)*U - K2R*(B+U+2.0*V)*V
    2 FORMAT (2I4, I3, F10.8)
    7 FORMAT (@0@,7X,F10.4,5X,F10.8,5X,F10.8,5X,F10.8,6X,F9.7,
     1     6X,F9.5,6X,F11.9)
   13 FORMAT(@1@//12X,@T-HRS.@,6X,@PT(P)2CL2@,6X,@PTP2NH3CL@,
     1 5X,@PTP2(NH3)2@,10X,@CL@,11X,@LAMBDA@,10X,@1/R(T)@,
     2 11X,3A4)
   21 DO 28  K = 1, NIC
C     N1 = LOWER LIMIT OF THE INTEGRATION
C     N2 = UPPER LIMIT OF THE INTEGRATION
C     N3 = ORDINAL NUMBER OF THE CALCULATED VALUES TO BE
C     PRINTED OUT (I.E. EVERY N3-RD VALUE WILL BE PRINTED )
C     DT = TIME INCREMENT FOR THE INTEGRATION
      READ (1,2) N1, N2, N3, DT
   22 DO 23 N = N1, N2
C     THE NEXT 11 STATEMENTS ARE THE NUMERICAL INTEGRATION
C     OPERATIONS.
      DX1 = X(N-1) + 0.5 * DT * DXDT(X(N-1), Y(N-1))
      DY1 = Y(N-1) + 0.5 * DT * DYDT(X(N-1), Y(N-1))
      DX2 = X(N-1) + 0.5 * DT * DXDT(DX1, DY1)
      DY2 = Y(N-1) + 0.5 * DT * DYDT(DX1, DY1)
      DX3 = X(N-1) + DT * DXDT(DX2, DY2)
      DY3 = Y(N-1) + DT * DYDT(DX2, DY2)
      DX4 = DT * DXDT(DX3, DY3)
      DY4 = DT * DYDT(DX3, DY3)
C     X(N) = CONCENTRATION OF FIRST REACTION PRODUCT AT T(N)
      X(N) = (2.0*DX1 + 4.0*DX2 + 2.0*DX3 + DX4
     1 - 2.0*X(N-1))/6.0
C     Y(N) = CONCENTRATION OF SECOND REACTION PRODUCT AT T(N)
      Y(N) = (2.0*DY1 + 4.0*DY2 + 2.0*DY3 + DY4
     1 - 2.0*Y(N-1))/6.0
C     T(N) = TIME SINCE BEGINNING OF REACTION
      T(N) = T(N-1) + DT
C     COND = SPECIFIC CONDUCTANCE PER LITER OF THE IONS FORMED
C     BY THE FIRST AND SECOND REACTIONS AT TIME T(N)
      COND(N) = XLMBDA * X(N) + 2.0 * YLMBDA * Y(N)
C     RTIME = TOTAL CONDUCTANCE OF THE SOLUTION AT TIME T(N)
   23 RTIME(N) = RZERO + (1.0/(1000.0*CELLK)) * COND(N)
C     THE REMAINING STATEMENTS IN THE SUBROUTINE CONTROL
```

```
C     THE PRINTING OF THE RESULTS OF THE CALCULATIONS.
   24 DO 28 N= N1, N2, N3
C     NLINE = NUMBER OF LINES OF OUTPUT WHICH HAVE BEEN
C     PRINTED ON EACH PAGE.  THIS IS USED IN ORDER TO PLACE
C     THE COLUMN HEADINGS ON EACH PAGE OF PRINTED OUTPUT.
      IF( 27 - NLINE ) 241, 241, 251
  241 NLINE = 1
   25 WRITE (3,13) EXNO
C     PTCL2 = CONCENTRATION AT T(N) OF THE INITIAL COMPLEX
  251 PTCL2 = A - X(N) - Y(N)
C     CL = CHLORIDE CONCENTRATION AT T(N)
      CL = B + X(N) + 2.0*Y(N)
   26 WRITE (3,7) T(N), PTCL2, X(N), Y(N), CL, COND(N),
     1 RTIME(N)
   28 NLINE = NLINE + 1
      RETURN
      END
```

APPENDIX C

The following figures are reproductions of the computer generated plots for the ammonation reactions of $\underline{t}$-$[Pt(PEt_3)(NH_3)Cl_2]$. Figure 20 contains the ammonation experiments at 25°C and Figure 21 contains the 35°C experiments. For each of these figures, one experiment is contained on each page, with two plots for each experiment. The two plots for each experiment are on a different time scale. The upper plot on the page is the experiment over long times. The lower plot is a repeat of the early portion of the upper plot, on an expanded time scale.

The line on each graph is the calculated conductance curve. The individual points which are plotted are all of the experimentally determined conductances, with the exception of the points at early times. The reason for the exclusion of these points was given in the main body of the text.

The scale on the ordinate of the plots was always adjusted by the computer to maintain two figures to the right of the decimal. When reading the plots, therefore, the values along the ordinate should be adjusted by the isolated exponential which appears near the top of that axis. When this is done, the numbers will be in proper scientific notation. The scale factor on each axis was chosen such that the plot would fill out the graph.

Figure 20. Reproductions of the computer generated conductance plots for the ammonation reactions of t-$[Pt(PEt_3)(NH_3)Cl_2]$ at 25°C. $X\lambda$ is the value of the equivalent conductance for c-$[Pt(PEt_3)(NH_3)_2Cl]Cl$ which was used in the calculations. $^{3}Y\lambda$ is the value for $[Pt(PEt_3)(NH_3)_3]Cl_2$. The rate constants used in the calculations for each plot were, $k_1 = 1.96M^{-1}hr^{-1}$ and $k_2 = 0.177M^{-1}hr^{-1}$

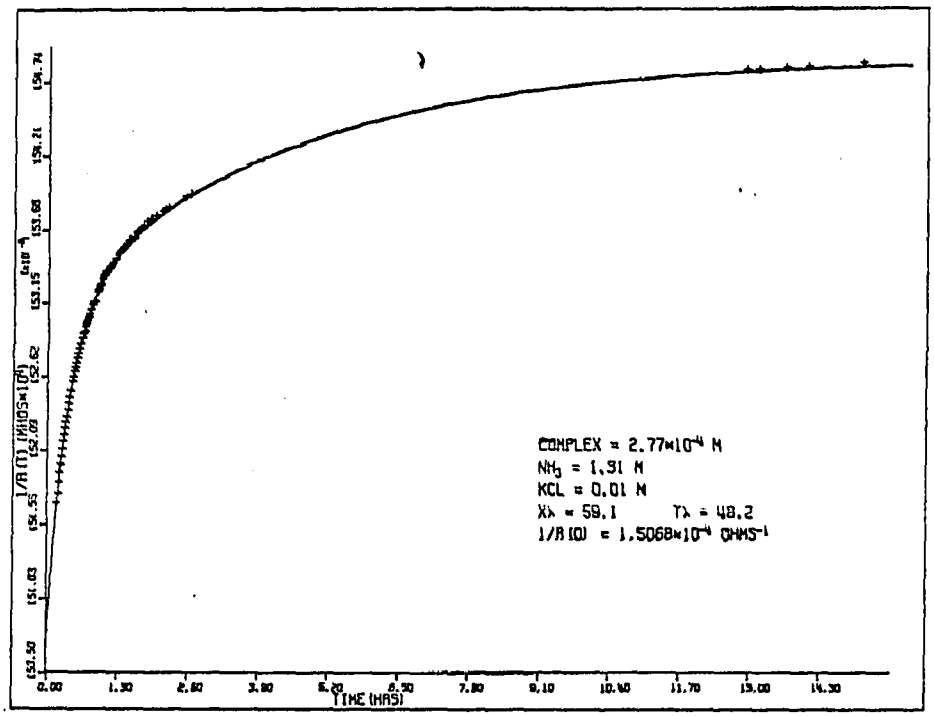
COMPLEX = 2.77×10⁻⁴ M
NH₃ = 1.31 M
KCL = 0.01 M
Xλ = 59.1 Yλ = 48.2
1/R(0) = 1.5068×10⁻⁴ OHMS⁻¹
TIME (HRS)

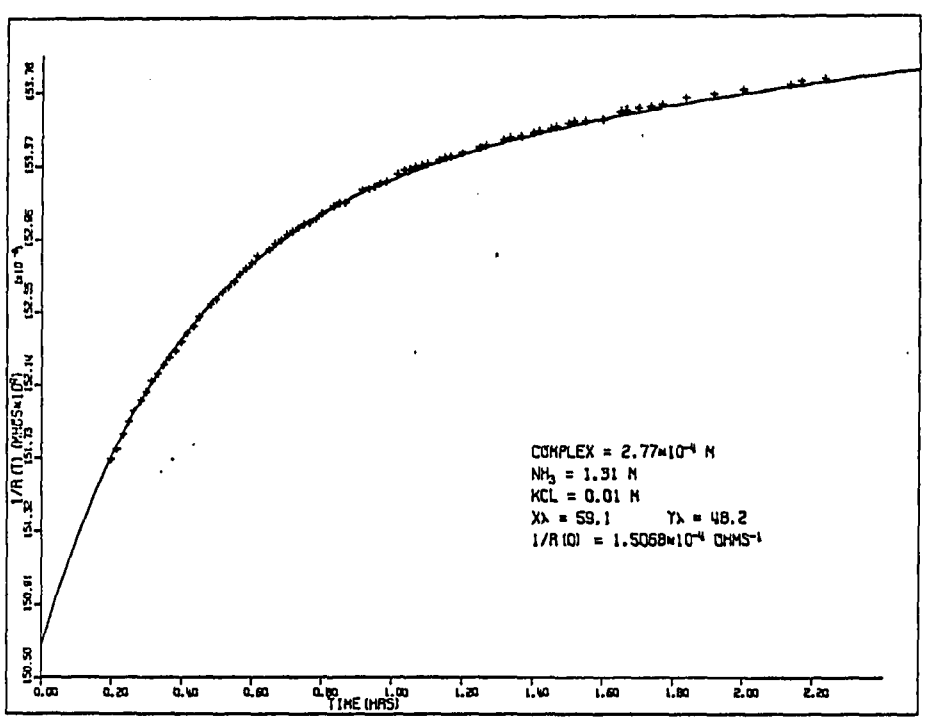
COMPLEX = 2.77×10⁻⁴ M
NH₃ = 1.31 M
KCL = 0.01 M
Xλ = 59.1 Yλ = 48.2
1/R(0) = 1.5068×10⁻⁴ OHMS⁻¹
TIME (HRS)

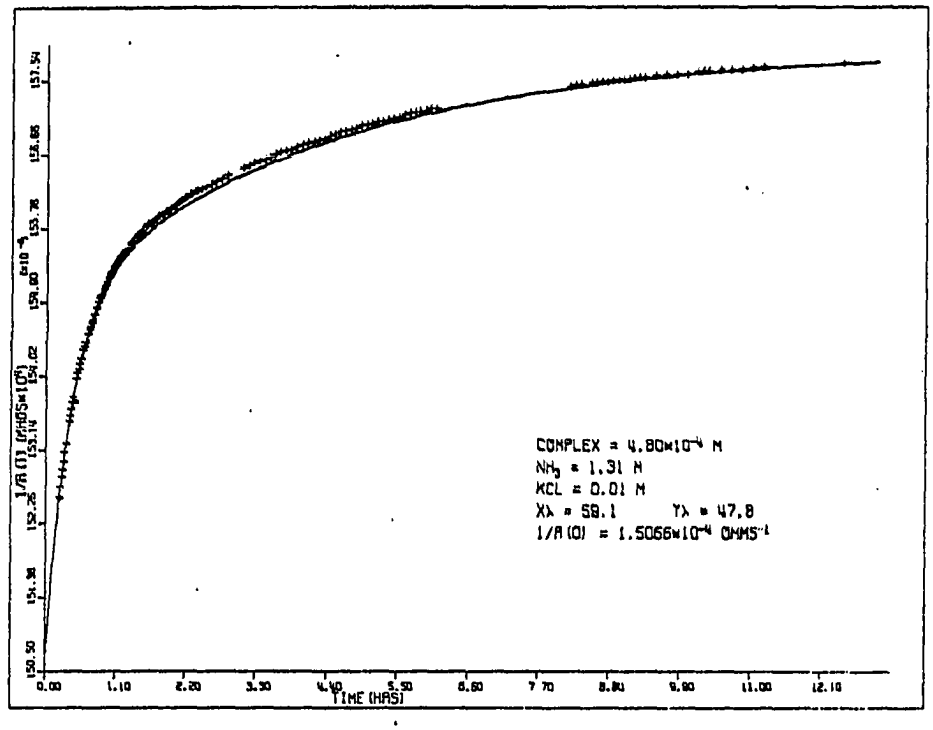

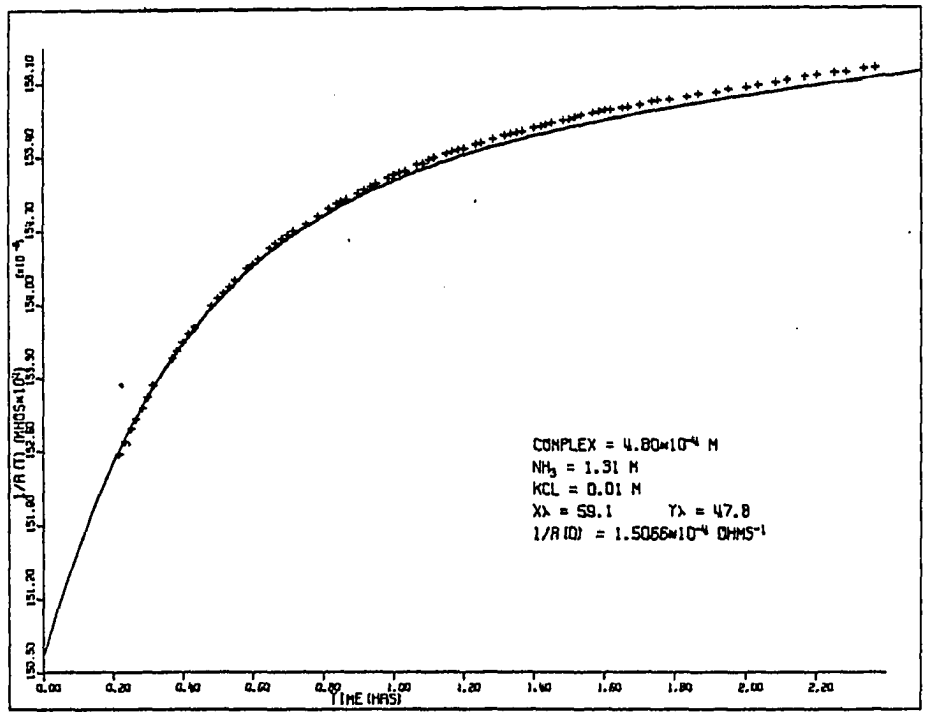

Figure 20 (Continued)

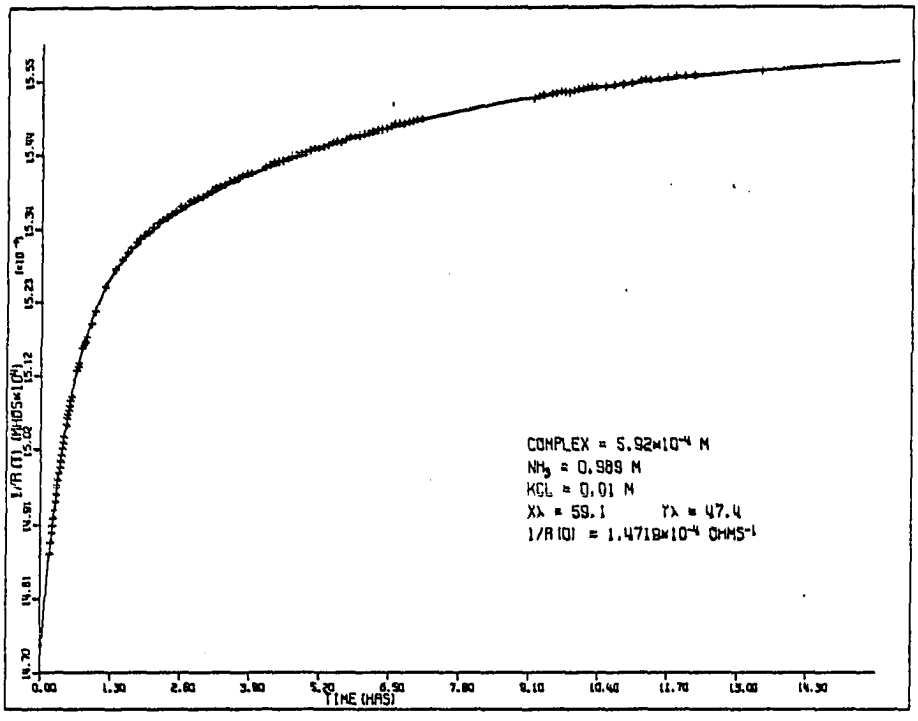

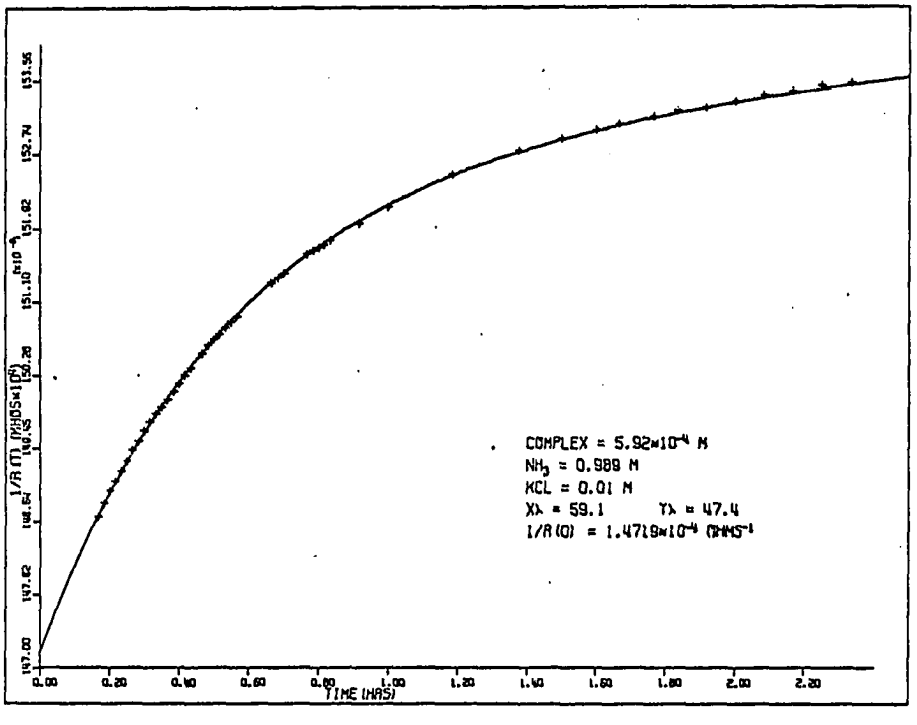

Figure 20 (Continued)

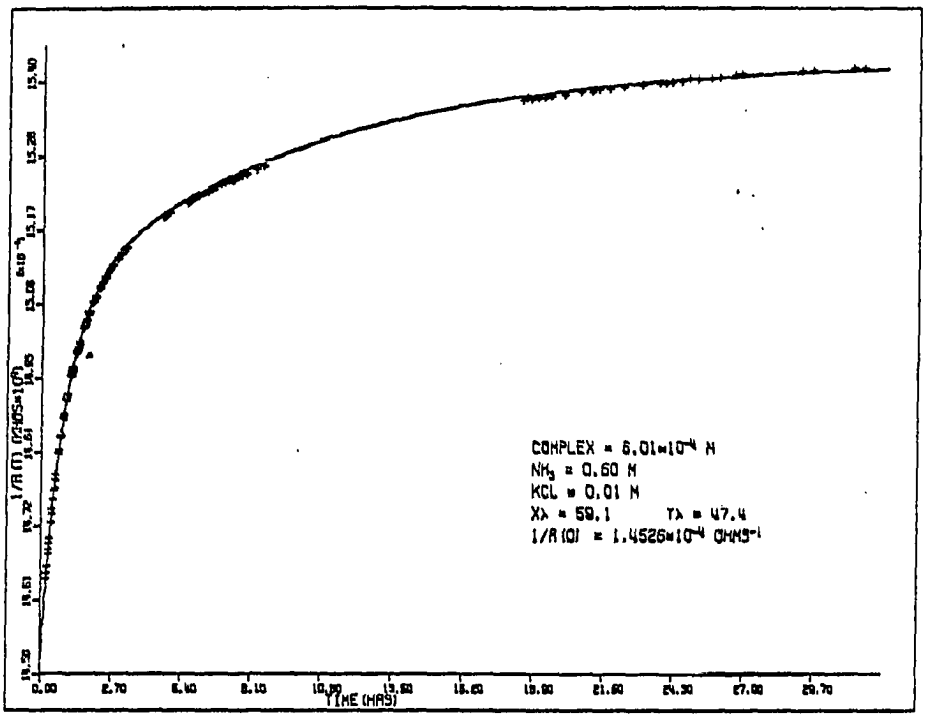

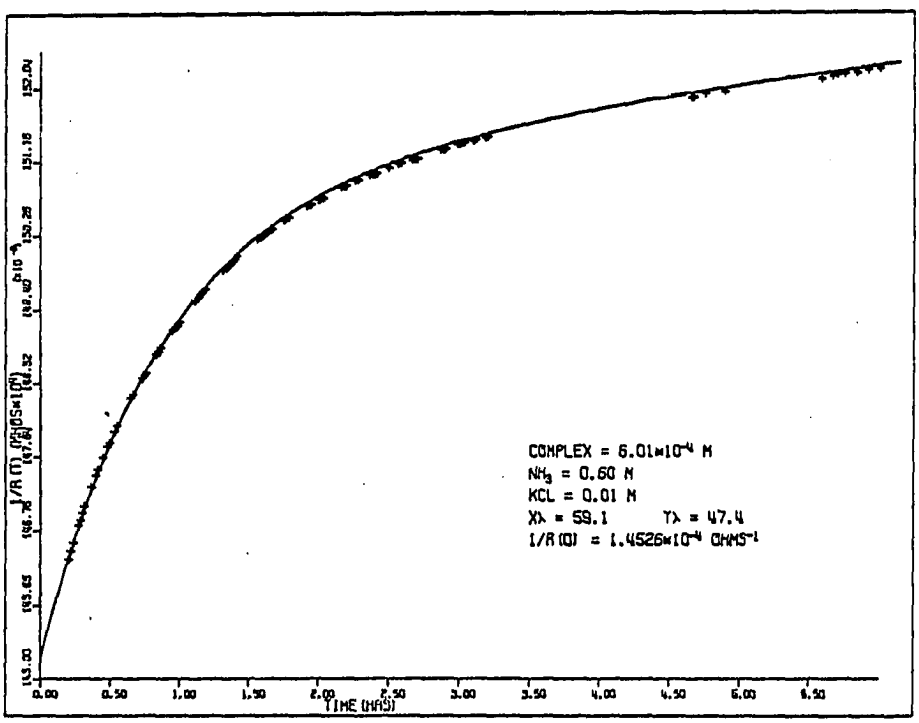

Figure 20 (Continued)

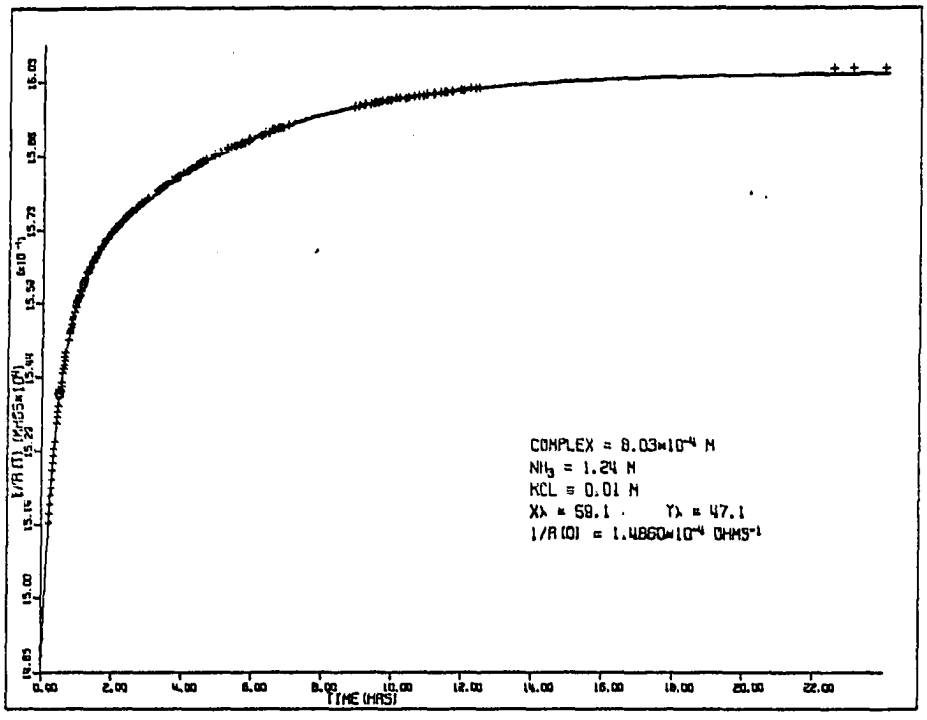

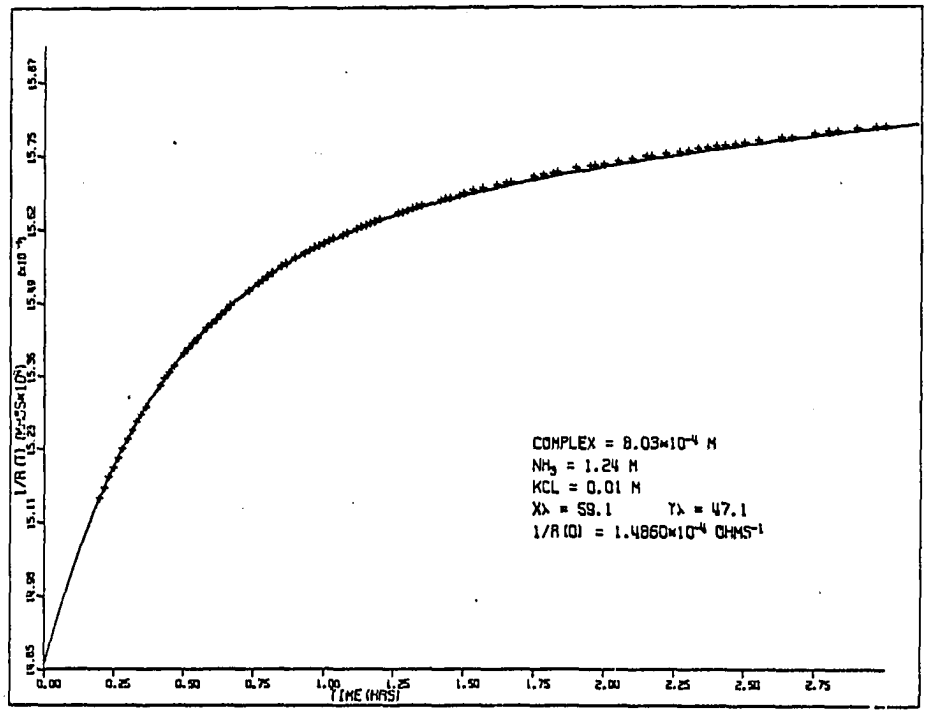

Figure 20 (Continued)

Figure 21. Reproduction of the computer generated conductance plots for the ammonation reactions of t-$[Pt(PEt_3)(NH_3)Cl_2]$ at 35°C. $X\lambda$ is the value of the equivalent conductance for c-$[Pt(PEt_3)(NH_3)_2Cl]Cl$ which was used in the calculations. $^3Y\lambda$ is the value for $[Pt(PEt_3)(NH_3)_3]Cl_2$. The rate constants used in the calculations for each plot were, k_1 = 5.11 $M^{-1}hr^{-1}$ and k_2 = 0.44 $M^{-1}hr^{-1}$

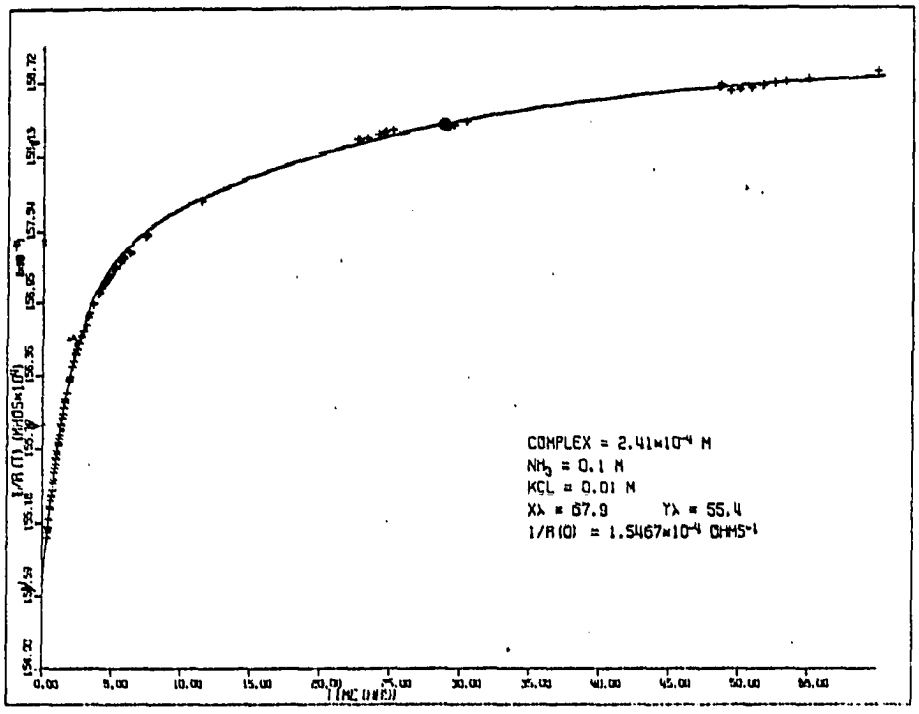
COMPLEX = 2.41×10⁻⁴ M
NH₃ = 0.1 M
KCL = 0.01 M
Xλ = 67.9 Yλ = 55.4
1/R(0) = 1.5467×10⁻⁴ OHMS⁻¹
TIME (HRS)

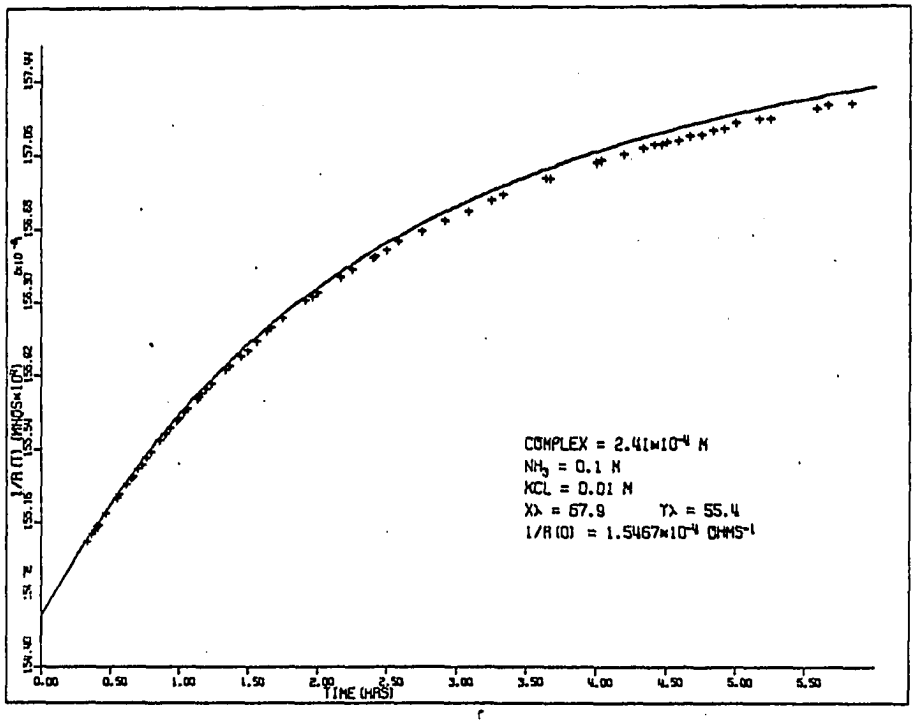
COMPLEX = 2.41×10⁻⁴ M
NH₃ = 0.1 M
KCL = 0.01 M
Xλ = 67.9 Yλ = 55.4
1/R(0) = 1.5467×10⁻⁴ OHMS⁻¹
TIME (HRS)

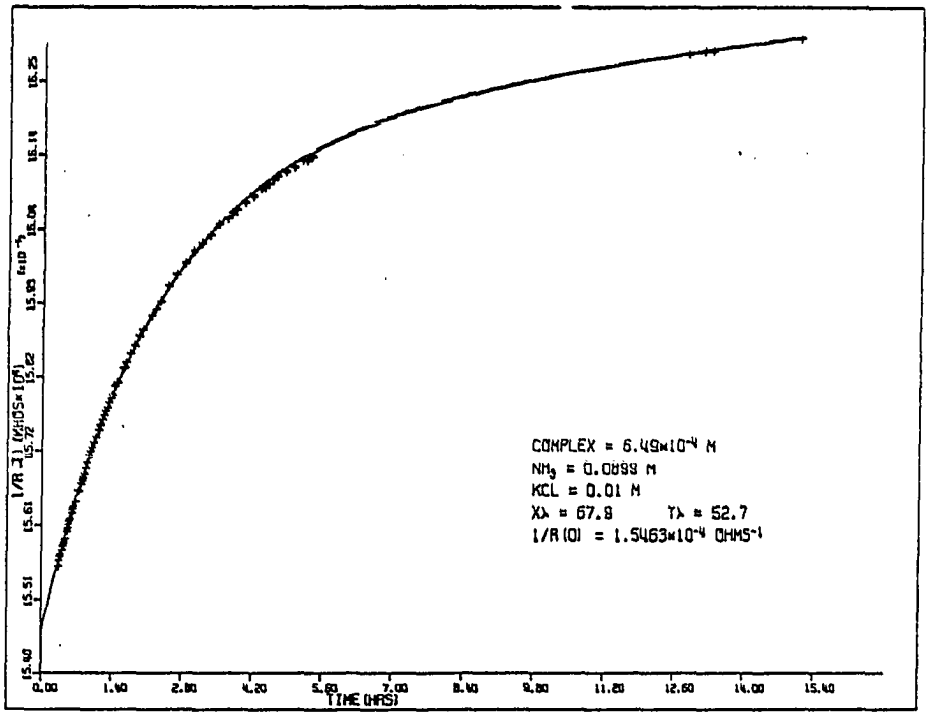

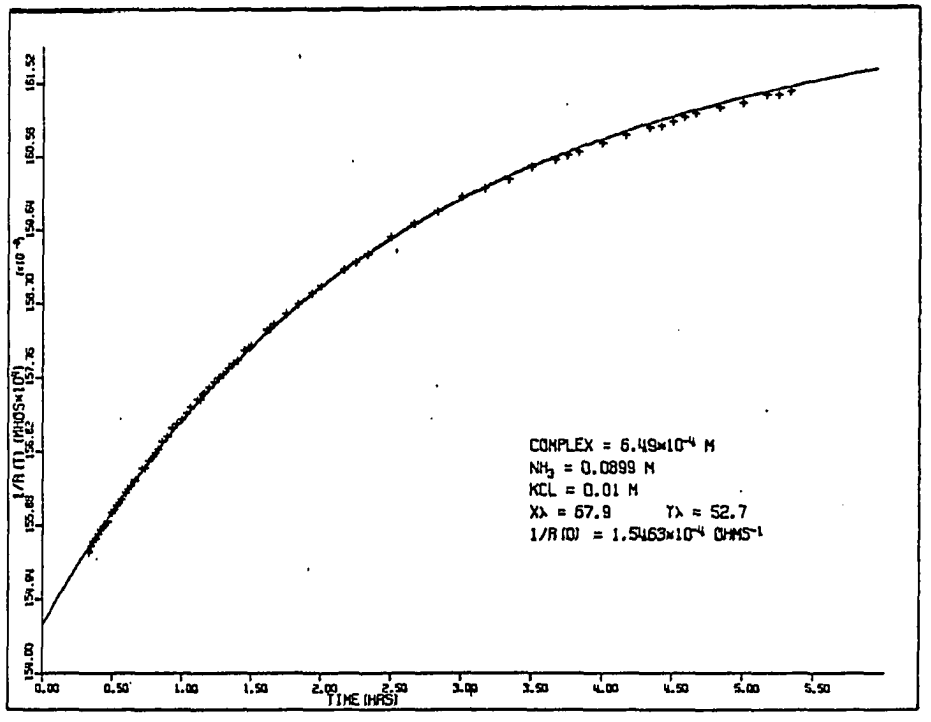

Figure 21 (Continued)

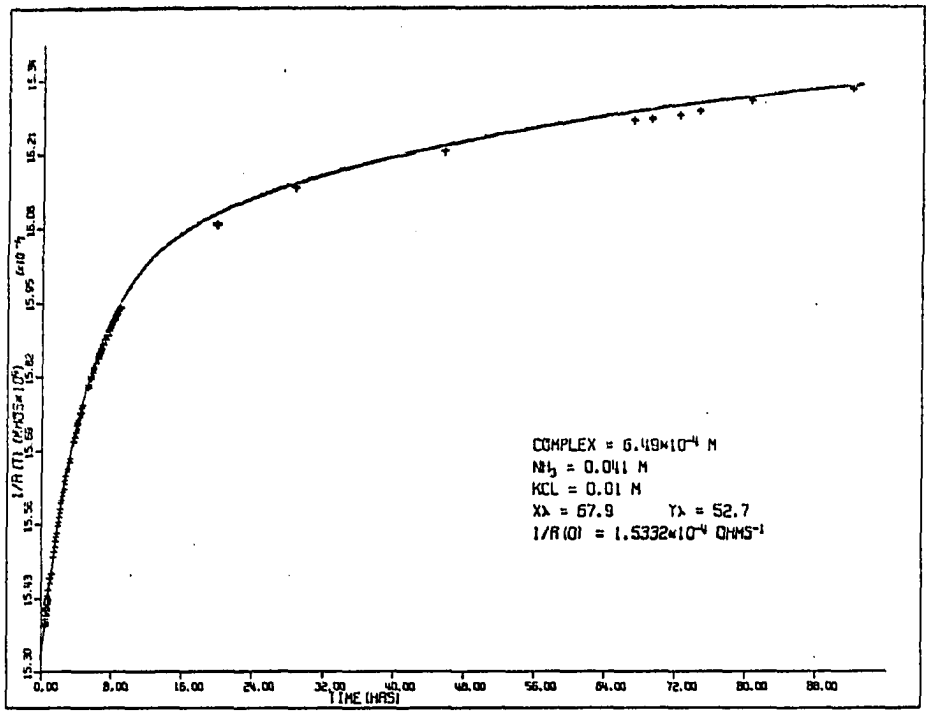

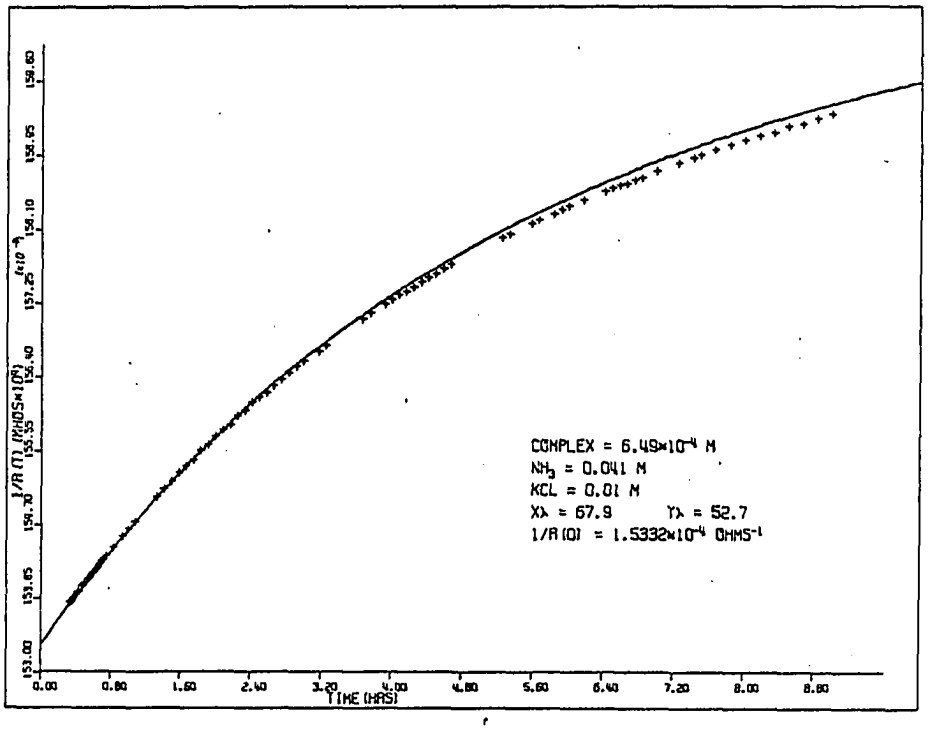

Figure 21 (Continued)

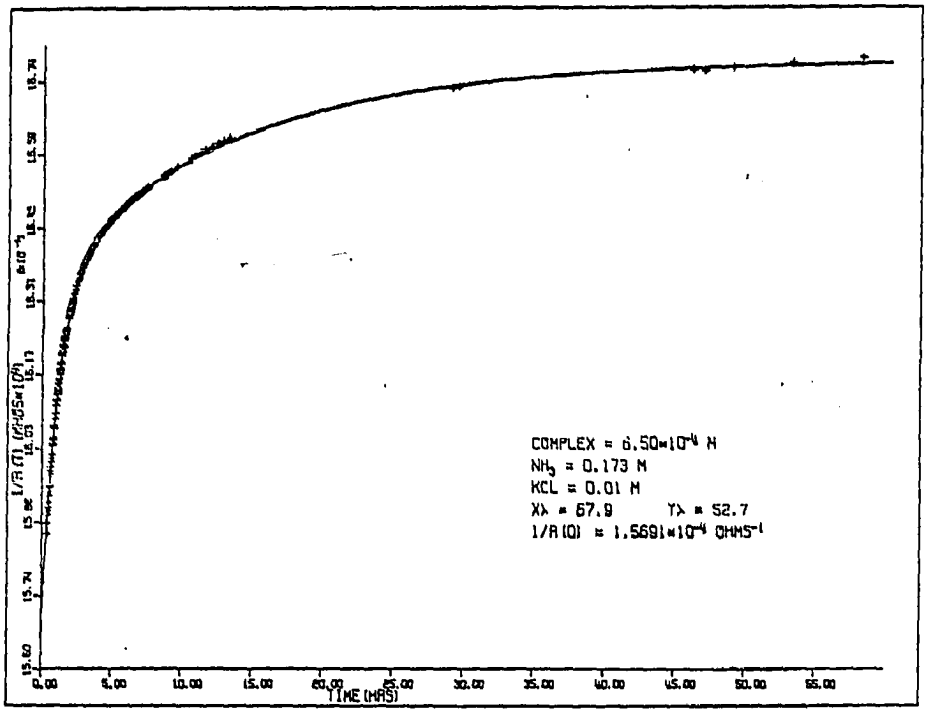

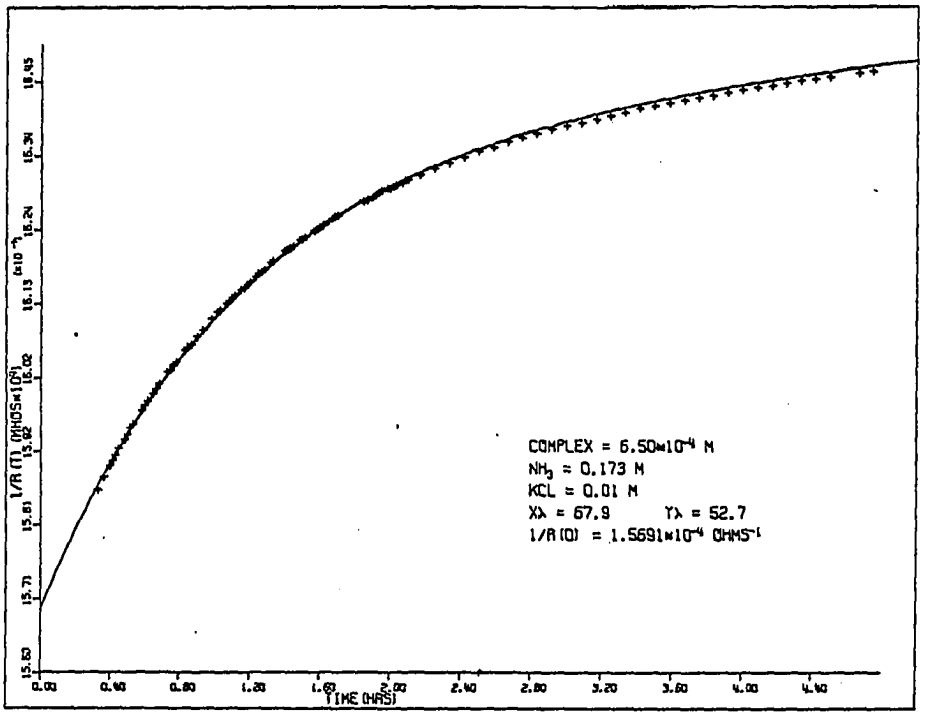

Figure 21 (Continued)

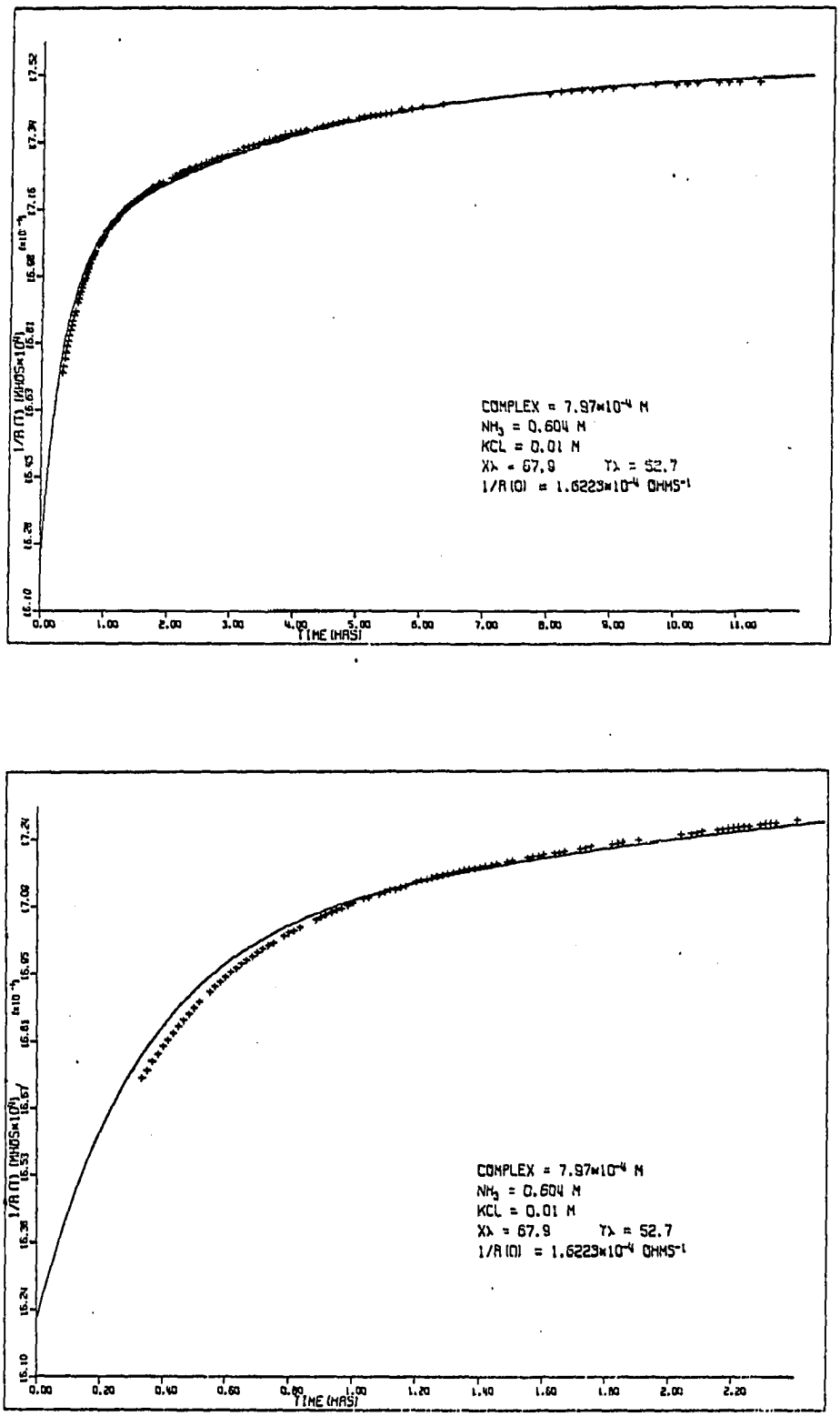

Figure 21 (Continued)

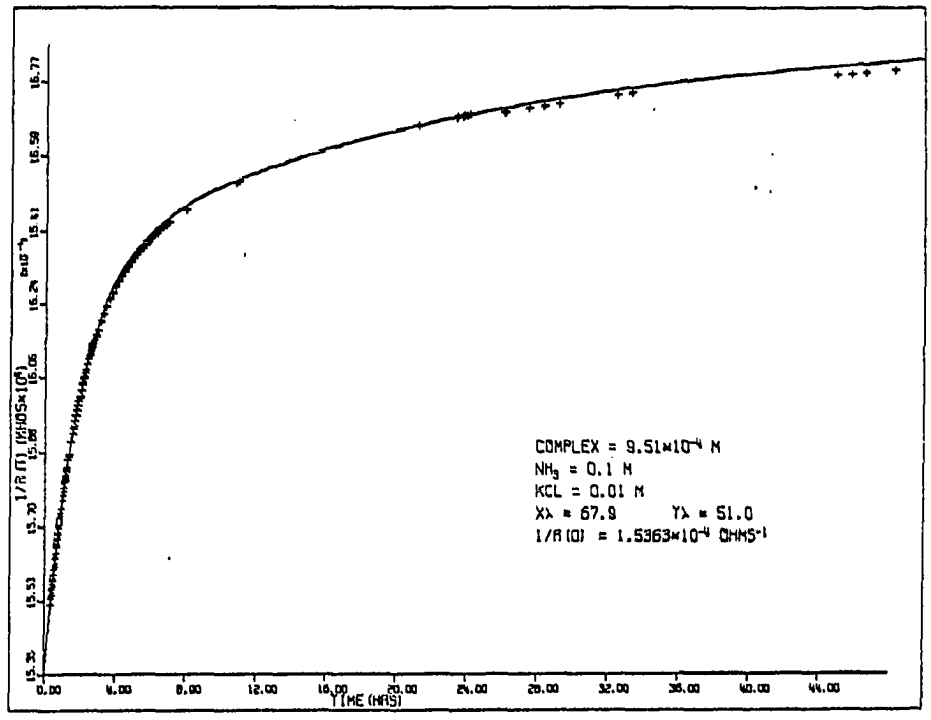

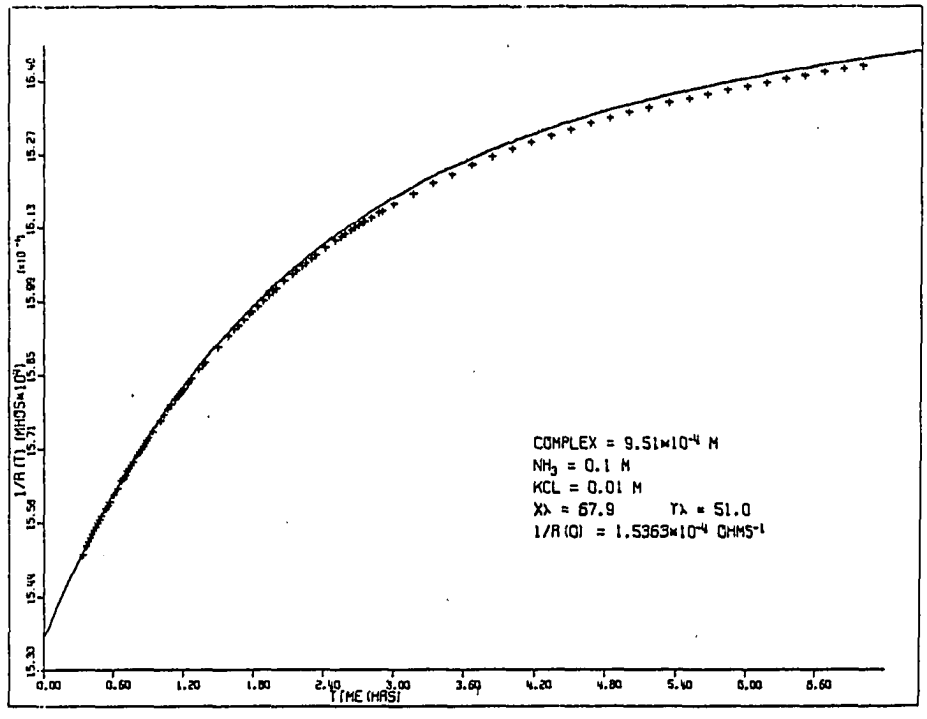

Figure 21 (Continued)

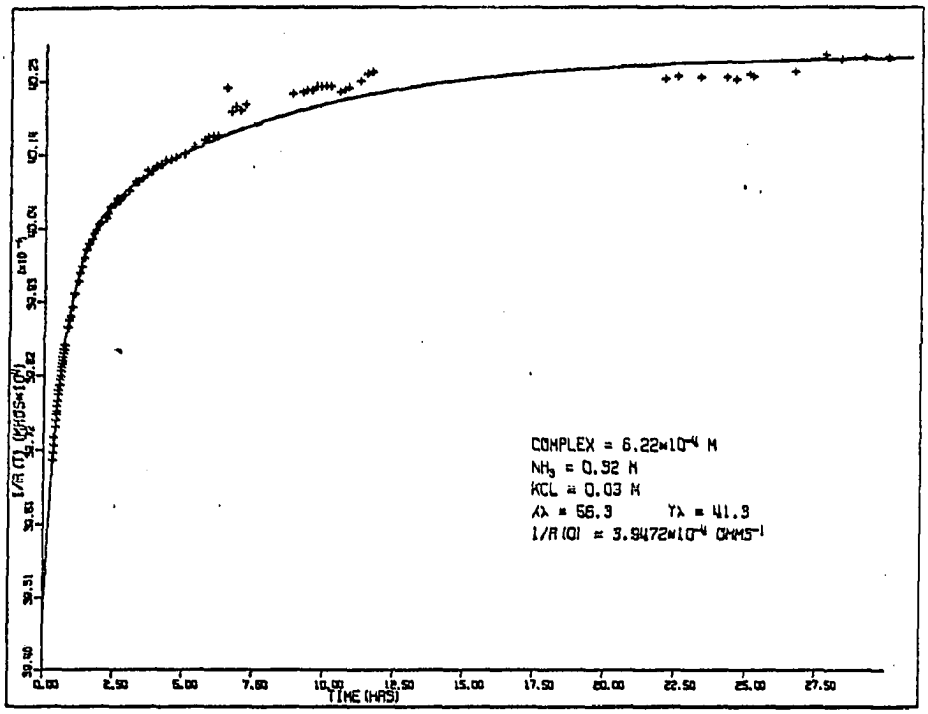

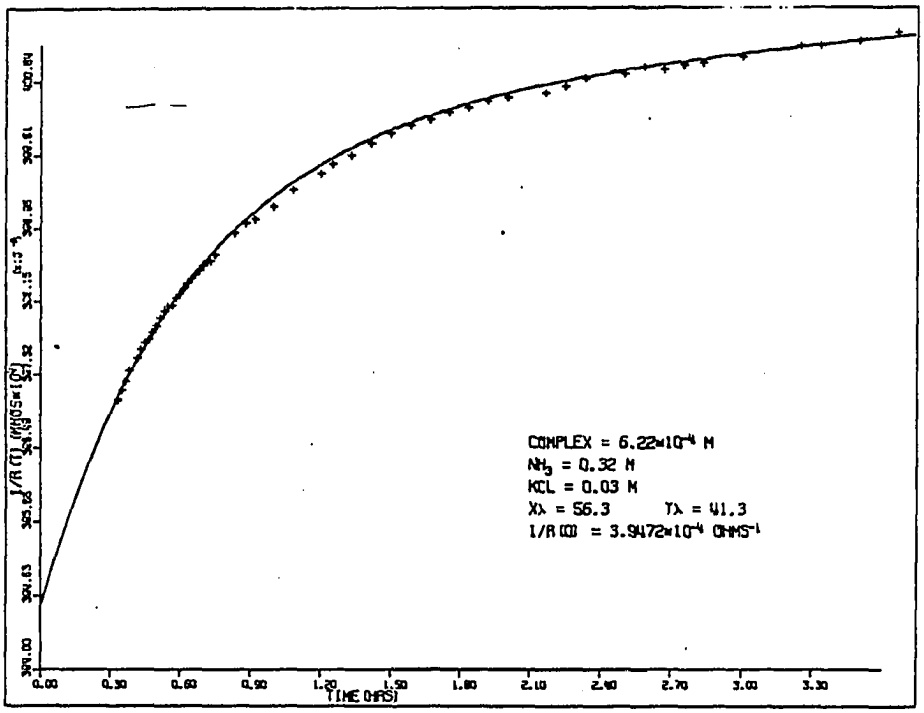

Figure 21 (Continued)

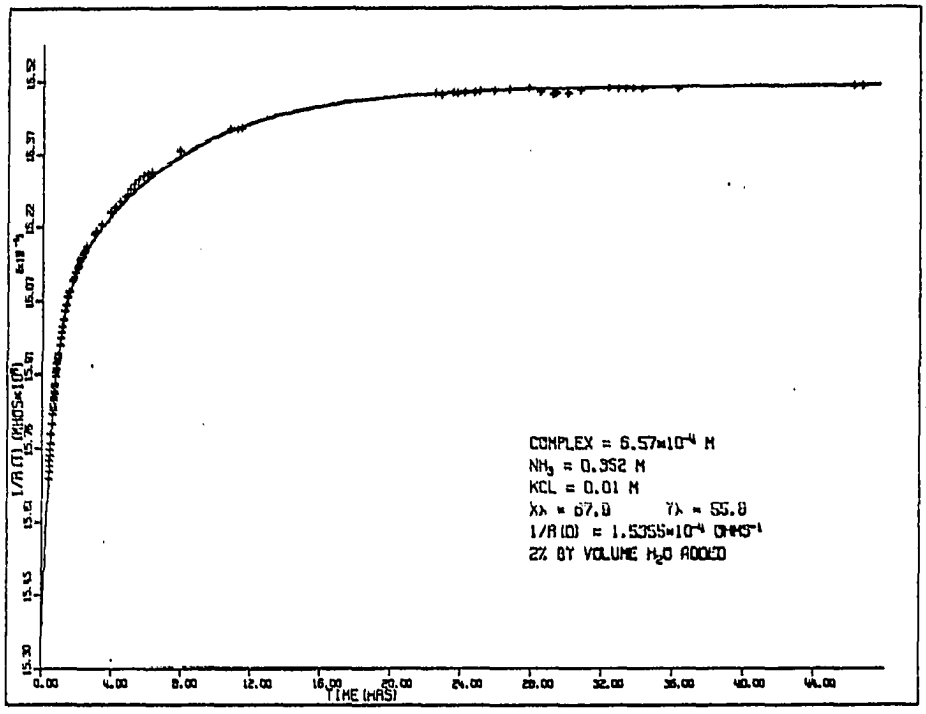

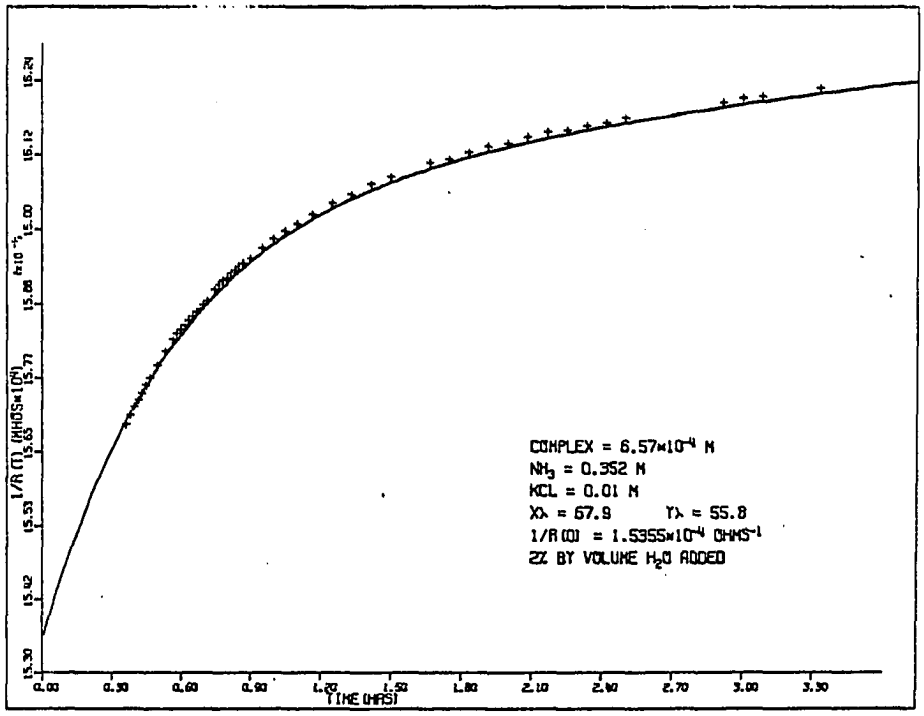

Figure 21 (Continued)